Aus der Neurochirurgischen Klinik und Poliklinik
Ludwig-Maximilians-Universität München
Direktor: Prof. Dr. med. Jörg-Christian Tonn

und dem Laser-Forschungslabor am Klinikum Großhadern
Ludwig-Maximilians-Universität München
Wissenschaftlicher Leiter: Dr. Reinhold Baumgartner

Novel Concepts of Light Application for ALA-PDT of Malignant Gliomas

Dissertation
zum Erwerb des Doktorgrades der Humanbiologie
an der Medizinischen Fakultät der
Ludwig-Maximilians-Universität zu München

vorgelegt von
Tobias J. Beck
aus
Hechingen
2010

Mit Genehmigung der Medizinischen Fakultät
der Universität München

Berichterstatter:	Prof. Dr. med. Jörg-Christian Tonn
Mitberichterstatter:	Prof. Dr. med. Claus Belka Prof. Dr. med. Peter Grafe
Mitbetreuung durch den promovierten Mitarbeiter:	Dr. rer. nat. Wolfgang Beyer
Dekan:	Prof. Dr. med. Dr. h.c. M. Reiser, FACR, FRCR
Tag der mündlichen Prüfung:	05.07.2010

Für Valerie, Leander und Bine

Table of Contents

Abstract

Malignant gliomas are the most common and most malignant tumors of the central nervous system in humans. Median survival of the patients lies between 12 and 14 months in spite of various available therapy options. Tumor recurrences mostly occur at the margin of the original tumor volume caused by residual tumor cells. Even better and more effective resection techniques, which were implemented into the clinic could not help to improve this situation. A therapy with focus on local effects could help to reduce residual tumor cells and possibly improve the therapeutic outcome. Since the treatment of brain tumors is a very difficult intervention and no healthy brain tissue should be damaged, the therapy should meet also safety aspects.

Photodynamic therapy (PDT) with aminolevulinic acid (ALA) induced protoporphyrin IX (PpIX) could comply with the requirements of such a therapy, since several experimental and clinical studies showed only few side effects occurred performing ALA-PDT. ALA-PDT is a light-based therapy, in which PpIX, a so called photosensitizer, accumulates in the target cells and is irradiated with red light. This irradiation activates the photosensitizer and in the presence of oxygen, this induces a cell toxic effect within the treated cells. Since in ALA-PDT this phototoxic effect can be limited to tumor cells, this effect could be the basis of a new and safe therapeutic intervention in neurosurgery. The effectiveness of the photodynamic effect depends on one hand on the intracellular concentration of PpIX and oxygen and on the other hand on the intensity and dose of the irradiated light. When treating humans, it is difficult to increase the intratumoral concentrations of oxygen or PpIX. Therefore, it seems to be more promising to investigate and improve the light irradiation within the target volume in order to improve the therapeutic outcome of ALA-PDT.

In the present work, two new concepts of light application in ALA-PDT are presented. The first concept investigates the so called interstitial light application, where thin light emitting fibers are placed directly into the tumor volume. The therapeutic light is emitted at the distal end of the fibers and the active length is up to several centimeters. Before initiating a first clinical feasibility study, *in vivo* measurements were performed to determine the optical tissue properties of brain tumors. Based on the results, comprehensive optical and thermal calculations were performed. The aim of these calculations was to understand the light and heat distribution within the tissue under irradiation. From the results of the calculations, the optimum distances in between the fibers and between fibers and tumor margin could be deduced. This was done with respect to the fact that a too short distance could result in unwanted local tissue heating and too long distances could result in insufficient light intensities in between the fibers or at the tumor margin. A modified commercial software tool was used to transfer the target positions of the fibers to updated CT and MRT images. Thus, the absolute positions of the fibers within the tumor volume were determined and the fibers were placed accordingly with a stereotactic equipment. The distance in between the fibers was determined to be 9 mm and it

could be shown that at this distance the tissue temperature did not increase above 42 °C. With this approach, 10 patients were treated within a feasibility study. The tumors of all patients could be irradiated completely by illuminating the tumor with up 6 fibers simultaneously. The median tumor volume was 5.9 cm^3 and the total applied light dose was between 4320 J and 11529 J. No side effects were observed and median survival was 15 months. Four patients survived longer than 24 months.

The second concept, which was investigated within the present work, had the intention to irradiate the photosensitizer with a different wavelength compared to the usually used red light. The idea was to increase the effectiveness of the PDT by using infrared light, since light with a longer wavelength has a higher penetration depth in tissue. In principle, PpIX can be activated also with infrared light, however, the applied light intensities have to be much higher compared to normal red light PDT. The reason is due to a non linear effect which is utilized, i.e. two-photon absorption. In two-photon absorption, the photosensitizers is excited via absorption of two photons with lower energy quasi simultaneously instead of absorbing one single photon with higher energy and initiates the phototoxic effect. This approach could be investigated only in cell experiments, since it is still in a very experimental stage. Cell experiments were done with C6 cells, which is a rat glioma cell line. Irradiation was performed with pulsed laser light of a titanium-sapphire laser with a wavelength of 800 nm. Since two-photon absorption needs very high light intensities, the laser light was focused on the sample surface via several optics. Cells were incubated with ALA before the irradiation. Cell survival was investigated with ethium bromide/acrydine orange staining after the treatment. Non incubated cells showed necrotic areas when light intensity increased $10.9 \cdot 10^{10}$ W/cm^2. Since these cells were not incubated with ALA, this seems to be the lower limit were thermal effects start taking place. ALA-incubated cells showed necrotic effects already with lower light intensities ($> 6.1 \cdot 10^{10}$ W/cm^2). It seems that with these light intensities a phototoxic effect related with the ALA incubation could be initiated since non incubated cells showed no damage.

The present work intended to investigate new concepts of light application in ALA-PDT. One of the concepts was still in a very experimental stage and cell experiments with promising results were performed. The other concept could be implemented into the clinic and the safety of this treatment modality could be shown in a feasibility study. The further investigation of both concepts could result in improving ALA-PDT as a treatment option in neurosurgery.

Zusammenfassung

Maligne Gliome sind die häufigsten und bösartigsten Tumore des Zentralen Nervensystems beim Menschen. Trotz vielfältiger therapeutischer Möglichkeiten liegt das mediane Überleben der Patienten derzeit bei 12-14 Monaten. Tumorrezidive treten häufig lokal an den Rändern des ursprünglichen Tumorvolumens auf und das trotz verbesserter Resektionsmethoden. Ursache hierfür sind wohl residuale Tumorzellnester, die nicht ausreichend reseziert werden konnten. Mit verbesserten lokalen Therapien könnte eine Reduktion dieser restlichen Tumorzellen erreicht und dadurch der Therapieerfolg verbessert werden. Da es sich bei der Behandlung von Gehirntumoren um sehr diffizile Eingriffe handelt und eine Schädigung des umliegenden gesunden Gewebes verhindert werden soll, muss eine solche Therapieform nicht nur besonders effizient, sondern auch besonders sicher sein.

Die Photodynamische Therapie (PDT) mit Aminolävulinsäure (ALA) -induziertem Protoporphyrin IX (PpIX) könnte eine solche Therapieform darstellen. Bei der PDT handelt es sich um eine Lichttherapie, bei der ein sogenannter Photosensibilisator durch die Bestrahlung mit Licht aktiviert wird und unter Mitwirkung von Sauerstoff einen toxischen Prozess in den zu behandelnden Zellen einleitet. Die Sicherheit des Verfahrens hängt davon ab, inwieweit es gelingt, den zelltoxischen Effekt auf die Tumorzellen zu begrenzen. Dabei spielen sowohl die Wahl geeigneter Photosensibilisatoren als auch die Applikation des Therapielichts eine Rolle. Mehrere experimentelle und klinische Untersuchungen konnten zeigen, dass es bei der Verwendung von ALA-induziertem PpIX als Photosensibilisator zu weniger Nebenwirkungen kommt als bei anderen Sensibilisatoren. Daher scheint dieser Photosensibilisator in Bezug auf Sicherheitsaspekte besonders interessant für die Anwendung in der Neurochirurgie zu sein. Die Effizienz des Verfahrens hängt zum einen von der Verfügbarkeit von Sauerstoff in den Zellen ab und zum anderen von der Lichtintensität mit der PPIX angeregt wird. Da es durch Streu- und Absorptionsprozesse im Gewebe zu einer Dämpfung der Lichtintensität kommt, liegt die Eindringtiefe von rotem Therapielicht nur bei wenigen Millimetern. Dies führt dazu, dass die in der Tiefe verfügbare Lichtintensität mit zunehmender Gewebedicke stark abnimmt. Dadurch kommt es insbesondere bei der oberflächlichen Bestrahlung von massiven Tumoren zu einem Therapieeffekt, der auf wenige Millimeter begrenzt bleibt. Neue Konzepte zur Applikation des Therapielichts könnten den Therapieerfolg der ALA-PDT trotz dieses Phänomens verbessern.

In den vorliegenden Arbeiten werden zwei neu entwickelte Konzepte zur Lichtapplikation bei ALA-PDT vorgestellt. Das erste Konzept befasst sich mit der sogenannten interstitiellen Lichtapplikation. Dabei werden dünne radial abstrahlende Lichtapplikatoren direkt in einen massiven Tumor eingeführt und das Therapielicht intratumoral über eine Länge von einigen Zentimetern abgegeben. Vor der Durchführung einer ersten klinischen Machbarkeitsstudie wurden *in vivo*-Messungen optischer Gewebeparameter sowie optische und thermische Simulationsrechnungen durchgeführt. Diese Simulationen hatten zum Ziel, den optimalen Abstand zwischen den einzelnen Fasern und zwischen Fasern und Tumorrand zu bestimmen. Dabei musste zum einen darauf geachtet werden, dass

der Abstand nicht zu gering war, da dies möglicherweise zu einer unerwünschten lokalen Temperaturerhöhung geführt hätte. Zum anderen durfte der Abstand auch nicht zu groß ausfallen, da sonst die Lichtintensität zwischen den Applikatoren bzw. am Tumorrand zu gering gewesen wäre und man somit die benötigte Photodynamische Dosis nicht erreicht hätte. Die theoretisch ermittelten Positionen der Lichtapplikatoren konnten mittels einer modifizierten Software auf die aktuellen CT- und MRT-Bilder der Patienten übertragen werden. Daraus konnten die exakten Positionen der Applikatoren bestimmt werden und mittels eines stereotaktischen Verfahrens wurden die Fasern dann entsprechend gesetzt. Der aus den Simulationen abgeleitete optimale Abstand betrug 9 mm. Es zeigte sich, dass bei Einhaltung dieser Distanz die Gewebetemperatur nicht über 42 °C anstieg. Insgesamt wurden in der so durchgeführten klinischen Machbarkeitsstudie zehn Patienten behandelt. Durch Verwendung von bis zu sechs Applikatoren, die zeitgleich Licht an den Tumor abgaben, konnten die Tumore aller Patienten komplett bestrahlt werden. Das mittlere Tumorvolumen betrug 5,9 cm^3 und die gesamte abgegebene Bestrahlung betrug zwischen 4320 J und 11529 J. Es konnten keine Nebenwirkungen festgestellt werden. Das mittlere Überleben der Patienten betrug 15 Monate und es gab vier Patienten, die länger lebten als 24 Monate.

Das zweite Konzept, dass im Rahmen der vorliegenden Arbeit entwickelt wurde, sollte untersuchen, ob eine Steigerung der Effektivität der ALA-PDT durch Bestrahlung mit infrarotem Licht erreicht werden kann, da diese Wellenlänge eine höhere Eindringtiefe in Gewebe besitzt. Bei Bestrahlung von PPIX mit infrarotem Licht kommt es bei Verwendung von Bestrahlungsstärken, wie sie in der PDT üblich sind, zwar zu keiner signifikanten Anregung des Photosensibilisators. Wenn man aber das Anregungslicht bündelt und PPIX somit einer erhöten Lichtintensität aussetzt, kommt es zu dem nicht-linearen Phänomen der Zwei-Photonen-Absorption. Dabei wird das Molekühl durch die Absorption zweier Photonen in einen angeregten Zustand gebracht und kann damit den phototoxischen Prozess in der Zelle in die Wege leiten. Da es sich hierbei um einen sehr experimentellen Ansatz handelt, konnten Untersuchungen zu dem Konzept nur an Zellen durchgeführt werden. Bei den bestrahlten Zellen handelte es sich um Gliomzellen der Ratte (C6). Die Bestrahlung erfolgte mit gepulstem Laserlicht der Wellenlänge 800 nm, das in einem Titan:Saphir-Laser erzeugt und über mehrere Optiken gebündelt wurde. Dadurch konnten die für den Zwei-Photonen-Effekt benötigten Lichtintensitäten erzeugt werden. Die Zellen wurden vor der Bestrahlung mit ALA inkubiert. Nach der Behandlung wurde das Überleben der Zellen mit einer Färbung untersucht (Ethidium-Bromid/Acridin Orange). Nicht inkubierte Zellen zeigten einen nekrotischen Effekt bei Bestrahlungsstärke $> 10{,}9 \cdot 10^{10}$ W/cm^2. Da diese Zellen nicht inkubiert wurden, ist bei diesen Bestrahlungsstärken von einem thermischen Effekt auszugehen. ALA-inkubierte Zellen zeigten einen nekrotischen Effekt bereits bei deutlich kleineren Bestrahlungsstärken ($> 6{,}1 \cdot 10^{10}$ W/cm^2). Da nicht inkubierte Zellen bei dieser Bestrahlungsstärke keinerlei toxischen Effekt zeigten, ist davon auszugehen, dass bei den ALA-inkubierten Zellen einen phototoxischer Prozess induziert werden konnte.

Mit der vorliegenden Arbeit sollten neue Wege der Lichtapplikation bei der ALA-PDT untersucht werden. Mit der klinischen Umsetzung des Konzepts der interstitiellen PDT konnte die Sicherheit und Wirksamkeit dieser Methode gezeigt werden. Da das Konzept der Zwei-Photonen-PDT noch nicht so weit entwickelt ist, konnten hier nur *in-vitro* Experimente durchgeführt werden. Die Weiterentwicklung beider Konzepte könnte die PDT als Therapieoption zur Behandlung des Malignen Glioms qualifizieren.

Chapter 1

Introduction

The present doctoral thesis is a cumulative thesis and consists of four original manuscripts ((Stepp et al., 2007), (Beck et al., 2007b), (Stummer et al., 2008), and (Beck et al., 2007a)). The common objectives of these manuscripts are the investigation of novel light application concepts for Photodynamic Therapy of malignant gliomas with aminolevulinic acid induced protoporphyrin IX. Two new concepts were developed and evaluated in experimental and clinical studies. The description of the concepts and the results of the studies are published in the above mentioned manuscripts.

Malignant Gliomas

Malignant gliomas are the most common and most malignant primary tumors of the central nervous system (CNS). Gliomas arise from glial cells and are classified by a four point scale of the World Health Organization (WHO) depending on the histologic grade of the tumor as determined by pathologic evaluation (Louis et al., 2007). WHO grade I and II are low grade tumors, which are well-differentiated, slowly growing, biologically less aggressive, with a good prognosis for the patient. WHO grade III and IV are high-grade gliomas (malignant gliomas), which are undifferentiated or anaplastic, fast growing, invading adjacent tissues, and carrying a poor prognosis. Malignant gliomas are highly vascular tumors and have a tendency to infiltrate. They have extensive volumes of necrosis and hypoxia. Often tumor growth causes a breakdown of the blood-brain barrier in the vicinity of the tumor. High-grade gliomas almost always recur even after complete surgical excision.

Another classification of gliomas can be done according to the specific type of cell they most resemble. Ependymomas derive from ependymal cells and emerge in grade II and III. Oligodendrogliomas derive from oligodendrocytes and occur in grade II and III. Astrocytomas are the most common gliomas and derive from astrocytes cells of the brain. This glioma type can be found in all four grades: Pilocytic astrocytoma (grade I), diffuse astrocytoma (grade II), anaplastic astrocytoma (grade III), and glioblastoma multiforme (grade IV). Finally, mixed gliomas occur, such as oligoastrocytoma, which is a combination of astrocytomas and oligodendrocytes.

In Germany, the number of newly diagnosed primary intracranial tumors is about 8,000 per year (Hirntumorhilfe, 2009). More than 70% of all primary brain tumors are gliomas (Ohgaki, 2009). About half of all gliomas are glioblastoma multiforme (GBM). GBM occurs at 2-3 cases per 100,000 people in Germany and is the most common and aggressive type of primary brain tumor. Most patients are between 50 and 70 years old and about 1/3 is female and 2/3 is male.

Diagnosis and Therapy

The overall prognosis for patients suffering from a malignant glioma continues to be dismal. The median survival of patients suffering from a glioblastoma multiforme (WHO grade IV) after tumor resection, external beam irradiation, and various forms of chemotherapy still lies in the range of 12-14 months (Shapiro et al., 1989; Jemal et al., 2004; Stupp et al., 2009).

Two reviews about diagnosis and treatment of high-grade astrocytomas (Sathornsumetee et al., 2007) and recurrent high-grade astrocytomas (Butowski et al., 2006) have been published lately. Diagnosis is mostly performed with modern imaging techniques such as Computed Tomography (CT), Magnetic Resonance Imaging (MRI) (Cha, 2004), Magnetic Resonance Spectroscopy (MRS) (Meyerand et al., 1999), and Positron Emission Tomography (PET)(Chao et al., 2001; Rachinger et al., 2005). These techniques are well established and associated with minimal side effects. The most accurate diagnosis, however, requires histopathological investigation of excised tissue, taken either as a stereotactic biopsy or during tumor resection, since tumor grading can be determined only histologically.

There are several approaches to treat malignant gliomas. Generally, tumor resection is performed as a first therapeutic measure. The strategy to reduce tumor mass seems to have a benefit to patient's survival, as could be shown by retrospective analysis of residual tumor after resection and its influence on prognosis (Albert et al., 1994; Lacroix et al., 2001). Stummer et al. could show by analysis of postoperative MRI findings, that patients without residual contrast-enhancing tumor had higher overall median survival than those with residual-enhancing tumor (17.9 months vs. 12.9 months) (Stummer et al., 2006). Decreasing tumor mass seems therefore to be helpful in order to improve the efficacy of adjuvant therapies. One of the results of a study investigating the effectiveness of temozolomid seems to confirm this approch, since patients with a complete tumor had showed a better therapeutic outcome after radiochemotherapy with temozolomid (den Bent et al., 2006).

Although a complete resection seems to be advantageous, the radicality of resection has its limits due to tumor locations close to eloquent areas (Albert et al., 1994). A widely used concomitant therapy is radiation therapy, which can be performed with several techniques. Clinical trials have been performed for conventional radiotherapy (Veninga et al., 2001), intensity-modulated radiotherapy (IMRT) (Voynov et al., 2002), temporary (Sneed et al., 1997) or permanent (Gaspar et al., 1999) brachytherapy, single- or multifraction radiosurgery (Hall et al., 1995; Cho et al., 1999).

Until some years ago, chemotherapy as a further treatment approach had limited therapeutic outcome when malignant gliomas were treated, which may be associated with the blood-brain-barrier. However, some years ago, a trial of the European Organisation for Research and Treatment of Cancer could show that treating malignant gliomas with a combination of surgery, radiotherapy, and chemotherapy seems to be a promising approach (Stupp et al., 2005; Hegi et al., 2005). One of the findings of this study was that overall survival was 2 months higher with concomitant adjuvant radiochemotherapy with temozolomide followed by adjuvant temozolomide than with radiotherapy alone.

Besides all these efforts, median survival of patients suffering from malignant gliomas is still restricted to 15 months. Tumor recurrences usually occur locally at the margin of previously treated tumor volumes (Bashir et al., 1988; Albert et al., 1994). Thus, the

improvement and further development of local treatment concepts could offer new perspectives in the treatment of brain tumors. One of these concepts could be Photodynamic Therapy (PDT) and its principle and clinical applications are discussed in the following.

Basic Principle of Photodynamic Therapy

Photodynamic therapy (PDT) is a light activated therapy and its basics have been discovered about 100 years ago. In 1898, the medical student Oscar Raab performed cell culture experiments in order to investigate potential anti-malarial agents and found that certain substances increased their toxicity when illuminated with light (Raab, 1898). Some years later, in 1903, Hermann von Tappeiner and Albert Jesionek implemented this 'light effective' phenomenon to the clinic and treated the first patient suffering from skin cancer (v. Tappeiner and Jesionek, 1903). From then on, further research was performed and several clinical applications of the new form of therapy were investigated, but the clinical outcome was limited. Until, due to advances in the development of the light absorbing molecules, also called photosensitizer, PDT started its comeback about 40 years ago.

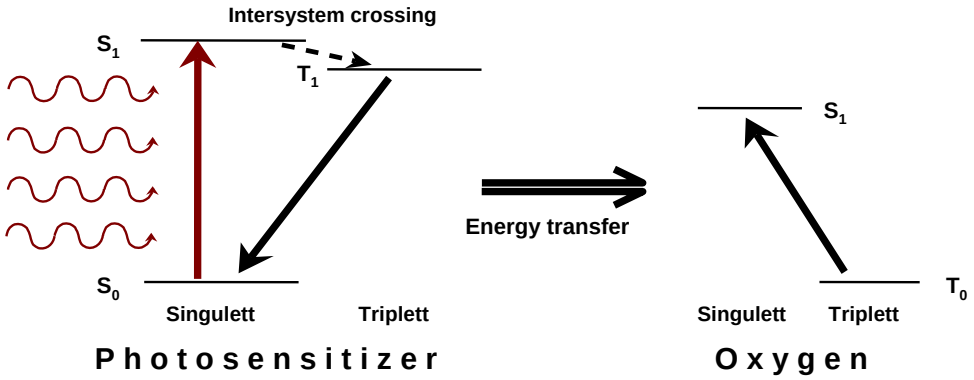

Figure 1.1: Energy level for a photosensitizer activated by red light.

The toxicity of the photodynamic effect is based on the interaction of light with the photosensitizer located in the target tissue. The photosensitizer is excited from a ground singlet state to an excited singlet state. It then undergoes intersystem crossing to a longer-lived triplet state. When the photosensitizer and an intracellular oxygen molecule are in proximity, an energy transfer can take place that allows the photosensitizer to relax to its ground singlet state, and create an excited singlet state oxygen molecule (see Fig. 1.1). Singlet oxygen is a very aggressive chemical species and will very rapidly react with any nearby biomolecules. Ultimately, these destructive reactions will result in cell killing through apoptosis or necrosis.

At first glance, the need of the three components oxygen, photosensitizer, and light seems to make this therapy concept complicated. However, this complex system offers also the perspective to limit the toxic effect to a target volume or area, which could be advantageous regarding safety aspects of a new therapy. This selectivity can in principle be obtained either by a selective accumulation of the photosensitizer or by applying the therapeutic light only to selected tissue regions. Both, a highly selective photosensitizer and a selective light application are discussed below.

Due to this promising properties, photodynamic therapy (PDT) has received increased attention as a treatment modality for tumors and other diseases in several clinical areas, e.g. dermatology, urology, ophthalmology, and otorhinolaryngology. In neurosurgery, PDT was implemented as a new treatment modality some decades ago.

Photodynamic Therapy in Neurosurgery

The treatment of recurrent glioblastomas with PDT was reported for the first time by Perria in 1980 (Perria et al., 1980) after Diamond had suggested in 1972 the use of PDT for the treatment of brain tumors (Diamond et al., 1972). Since then, many small clinical trials were performed to investigate the safety and efficacy of this treatment modality. Mostly, the photosensitizers used were porphyrin based such as hematoporphyrin derivative (HpD), a mixture of ether and ester linked porphyrins, or its purified forms Photofrin® (porfimer sodium) and Photofrin II® (dihematoporphyrin ether/ester). A review has been published by Madsen and Hirschberg (Madsen and Hirschberg, 2006).

The technical and clinical setups of the studies were various. However, most studies applied PDT as adjuvant therapy after tumor resection and light irradiation was done intracavitarily. One approach was to place a balloon device within the resection cavity as light source. Muller and Wilson treated recurrent (Muller and Wilson, 1995) and newly diagnosed (Muller and Wilson, 1996) supratentorial gliomas by inserting a balloon irradiator (described in (Wilson et al., 1986)) into the resection cavity and expanded it with a light dispersion medium. Other groups used the same or a modified balloon applicator to treat recurrent brain tumors after resection (Origitano and Reichman, 1993; Schmidt et al., 2004) or suggested to implant a permanent balloon catheter, which could help to perform a long term photodynamic therapy (Madsen et al., 2001).

Another approach to illuminate the resection cavity is to position a simple light guiding fiber in the center of the cavity (Perria et al., 1980; Kostron et al., 1996; Rosenthal et al., 2001; Stylli et al., 2005). Usually, the illumination involves the use of a light dispersing medium which is placed within the resection cavity in order to uniformly distribute the light within the resected tumor cavity (Stylli and Kaye, 2006). The influence of a scattering medium on the light distribution of the surface was investigated for hollow organs (Star et al., 1987; Beyer, 2003). From these studies it can be deduced, that when the geometry of the resection cavity deviates from the ideal shape of a sphere or when the position of the light guiding fiber is not in the center of the sphere, then the use of a scattering medium results in a less homogeneous light distribution on the tissue surface compared to the use of a transparent medium. Thus, using a light-scattering medium is not of advantage to achieve a uniform light distribution across the entire surface.

For deep seated or non-resectable tumors a possibly minimally invasive way to apply the light to the sensitized tumor is to place light guiding fibers directly within the treatment volume. This treatment modality is referred to as interstitial photodynamic therapy (iPDT). Its feasibility and effectiveness has been investigated in brain tumor models (Cheng et al., 1984; Lilge et al., 1996; Hebeda et al., 1998a) and in first clinical applications with HpD (E. R. Laws et al., 1981; Lajat and Patrice, 1987) and Photofrin or Photofrin II (Powers et al., 1991; Origitano and Reichman, 1993; Kaneko, 1999; Krishnamurthy et al., 2000; Schmidt et al., 2004).

Some of these studies have shown that Photofrin-mediated PDT may prolong survival (Muller and Wilson, 1987; Muller and Wilson, 1996). Despite, PDT is not included in the

standard treatment procedure of malignant gliomas up to now. On one hand, this is due to the lack of proof of efficacy by prospective, randomized clinical trials. The other reason may be due to the severe treatment related adverse effects reported by several authors. The use of hematoporphyrin derivative and Photofrin leads to a photosensitization also of the skin, which forces patients to avoid direct or diffuse sun light for about 2 months (Muller and Wilson, 1996; Popovic et al., 1996). An even more severe side effect is the unspecific damage to normal brain tissue associated with the therapy. It seems that there is a leakage across the blood-brain barrier within malignant glioma, which leads to an unspecific sensitization of peritumoral tissue due to transport of the photosensitizer with edema bulk flow (Dereski et al., 1989; Stummer et al., 1993; Chen et al., 1996; Stummer et al., 1996; Goetz et al., 2002).

All these experiences lead to the assumption, that a photosensitizer, which would accumulate more selectively in tumor tissue could reduce side effects associated with PDT treatment. Aminolevulinic acid induced protoporphyrin IX seem to be such a tumor selective photosensitizer and could have the potential to reanimate PDT as a therapy modality in neurosurgery.

ALA-based PDT

In most photosensitizing drugs, which have obtained regulatory approval in the last years, e.g. Photofrin, Visudyne, Foscan, the photosensitizer, i.e. the light absorbing molecule, is applied directly to the patient. In contrast to this, in ALA-PDT, the photosensitizer protoporphyrin IX (PpIX) is not applied directly, but the precursor aminolevulinic acid (ALA) is given and PpIX is synthesized *in situ* from ALA. ALA is naturally occurring in cells as part of the heme synthesis. The synthesis of endogenous ALA is controlled by the presence of unused heme via a feedback mechanism. The administration of exogenous ALA bypasses the rate-limiting step in the synthesis of heme and every step in the biosynthetic pathway tries to operate at its maximum capacity. Since PpIX is the direct precursor of heme, a cell, in which the rate of PpIX synthesis is greater than the rate of its conversion into heme, accumulates PpIX. This mechanism of PpIX accumulation is illustrated in Fig. 1.2. Usually, malignant tissue accumulates significantly more PpIX compared to normal tissue of similar origin, which can lead to a high tumor selectivity of ALA-PDT. The activities of two enzymes in the heme biosynthetic pathway play a major role in PpIX generation and accumulation: ferrochelatase (FC) is responsibe for the conversion of PpIX into heme and porphobilinogen deaminase(PBGD), which is responsible for the synthesis of the precursor uroporphyrinogen.

PpIX is produced primarily in the mitochondria, but can be redistributed into the cytosol and perinuclear region after longer incubation times. The action radius of generated singlet oxygen is only about 10-20 nm. Cell death can be caused either by apoptotic or necrotic pathway. Apoptosis is a physiological and controlled cell death. Necrosis is a passive cell death, mainly caused by plasma membrane destruction.

Beyond these direct phototoxic effects, activation of the immune response after PDT has been reported (e.g. increased expression of heat shock proteins) (van Duijnhoven et al., 2003; Jalili et al., 2004; Korbelik et al., 2005). These effects are under ongoing experimental investigation and clinical evaluation.

Many clinical applications using ALA-PDT were investigated in the last years (Pottier et al., 2006).

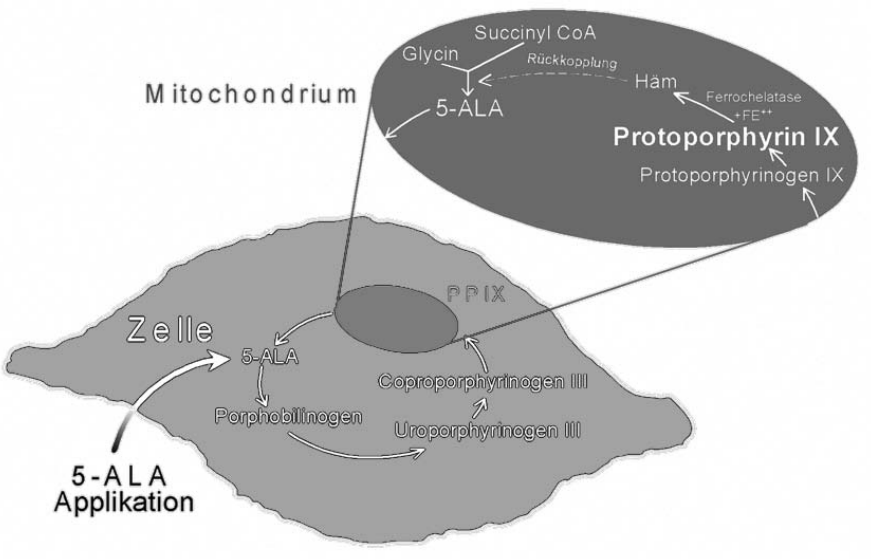

Figure 1.2: Protoporphyrin IX is produced during the heme biosynthesis.

ALA in Neurosurgery

Several experimental studies examining the usability of ALA as a fluorescence marker in brain tumor models have been performed in the last 10 years (Stummer et al., 1998b; Hebeda et al., 1998b; Tsai et al., 1999). The results encouraged Stummer et al. to use ALA for the first time in patients and they found a highly selective tumor uptake and only minimal skin sensitization (Stummer et al., 1998c; Stummer et al., 1998a; Stummer et al., 2000; Stummer et al., 2003). A prospectively-randomized phase III study investigated the usefulness of fluorescence-guided surgery with ALA from 1999 to 2004 (Stummer et al., 2006) and resulted in the European approval of aminolevulinic acid (generic name: Gliolan®) with the indication of intraoperative photodynamic diagnosis of residual glioma (Krammer and Plaetzer, 2008). Fig. 1.3 shows the impressive tumor demarcation of a malignant glioma under fluorescence excitation light.

The successful establishment of ALA in the intraoperative diagnosis of malignant gliomas is due to a high tumor selectivity of the photosensitizer accumulation. Mainly, this effect can be ascribed to the fact, that the synthesis and accumulation of PpIX occurs directly within the tumor cells in contrast to HpD and Photofrin. However, a key prerequisite for PpIX accumulation in brain tumors is a disruption in the blood-brain barrier, since ALA is a polar molecule and could not pass an intact blood-brain barrier (Novotny et al., 2000; Ennis et al., 2003). Additionally, it is presumed that tumor proliferation plays another important role for the intratumoral PpIX synthesis (Novotny et al., 2000).

As described before, such tumor selective properties are one of the prerequisites of a safe photodynamic tumor therapy and thus, one would expect ALA-PpIX to be a potential and safe photosensitizer for PDT. Therefore, the potential of ALA-PpIX as a PS for PDT of malignant gliomas has been investigated in several experimental studies *in vitro* (Madsen et al., 2000; Hirschberg et al., 2002; Madsen et al., 2003; Hirschberg et al., 2006; Zelenkov et al., 2007; Inoue et al., 2007; Madsen et al., 2009) and *in vivo* (Olzowy

et al., 2002; Hirschberg et al., 2002; Angell-Petersen et al., 2006; Madsen et al., 2006).

Both, the *in vitro* and the *in vivo* studies were very promising and it seemed that using ALA induced PpIX as a tumor selective photosensitizer could solve the safety problem, which occurred when using other sensitizers. These results encouraged the first clinical ALA-PDT studies in the brain. In 2001, Hochstetter (Hochstetter, 2001) treated the first patients suffering from glioblastoma. In this preliminary investigation, 5 patients received ALA prior to surgery. After tumor resection, PpIX fluorescence was detected and the tumor cavity was irradiated with a cylindrical diffuser. No side-effects were observed and MR images showed an effective zone of 2 cm diameter without sign of brain edema.

Based on these promising results, in 2002 a multi-center study started at the Departments of Neurosurgery in Munich and Dusseldorf, Germany. The aim was to apply ALA-PDT as an adjuvant therapy after tumor resection. The experiences obtained during this trial were partly published by Stepp et al. (Stepp et al., 2007). The study could show the safety and effectiveness of this therapy.

The contribution of Tobias J. Beck to this study was to implement the irradiation in the clinic, to measure the fluorescence of the photosensitizer before, during and after the irradiation, to analyze the fluorescence spectra, and to determine the photobleaching effect.

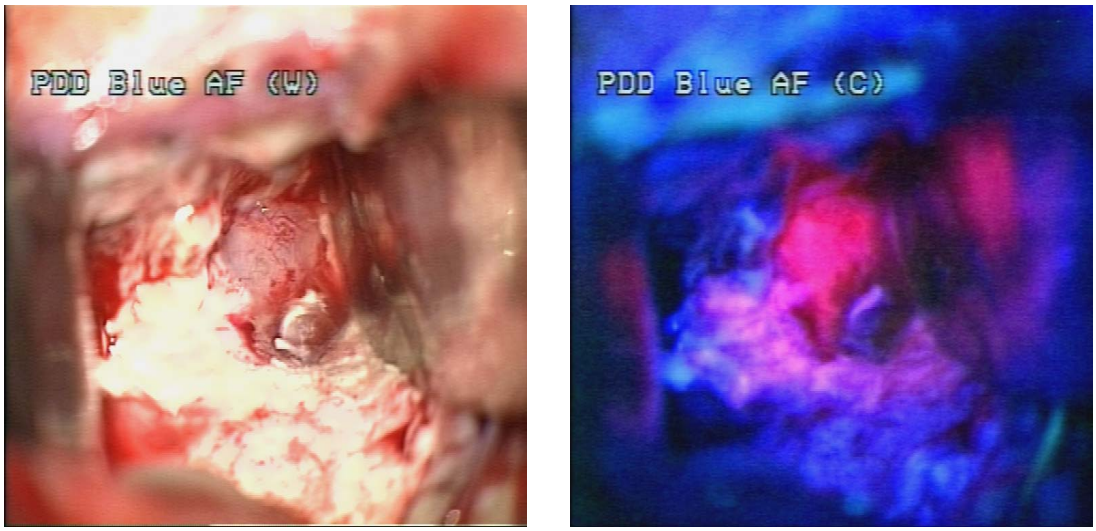

Figure 1.3: Image of a malignant glioma through an operation microscope under white light illumination (left image) and under illumination with fluorescence excitation light (right image).

Novel irradiation concept I

As discussed above, there is still a limited effectiveness of ALA-PDT. One of the reasons seems to be a limited light intensity within the target tissue. When irradiating the surface of the tumor, the light intensity decreases rapidly in deeper tissue layers, which is mainly due to light scattering and absorption. Therefore, the objective of the present work was to develop and evaluate novel concepts of light application in order to increase the effectiveness of ALA-PDT as a treatment modality for malignant gliomas.

Within the first concept, the tumor was supposed to be irradiated from inside, instead of illuminating the tumor surface. This therapy concept has been referred to as *interstitial Photodynamic Therapy (iPDT)*. The study focused on the development and the clinical implementation of an accurate and reproducible irradiation scheme for iPDT with the aim to overcome the limited penetration depth of therapeutic light and to illuminate the entire bulk tumor. In order to obtain an effective and homogeneous therapeutic effect within the treatment volume, it is important to know the light distribution within the tissue. This light distribution is determined by the interaction of photons with tissue structures. Monte Carlo simulations of fluence rate and heat transport simulations were performed using the optical properties of normal brain tissue infiltrated by tumor cells. The optimum distance between the inserted light diffusers was determined to be 9 mm with regard to both fluence rate and temperature distribution. For this distance a temperature increase above 42 °C was not expected to occur. For the clinical implementation of the simulated data, a modified 3D-treatment-planning software was used to calculate both, the treatment-volume and the exact position of the light diffusers within the lesion. Up to six cylindrical light diffusers were stereotactically implanted to achieve a complete irradiation of the tumor volume, which was possible in every single patient. The feasibility and the risk of iPDT were tested in 10 patients with small and circumscribed recurrent malignant gliomas. Side effects of iPDT were not observed during the study and the median survival was 15 months. The technical setup and the first clinical results of the iPDT study were published by Beck et al. (Beck et al., 2007b). Stummer et al. published a case report of one patient treated with iPDT, which focused on the clinical impact of this treatment modality (Stummer et al., 2008). The patient suffered from a prior left frontal glioblastoma multiforme treated by surgery, radiation and chemotherapy, and developed a remote lesion in the left insula, which was refractory to secondary treatments. After treating the patient as described above, the contrast uptake in the lesion had disappeared in the MRI images 24 h after therapy. Circumferential contrast enhancement was observed at 72 h, which disappeared in the course of subsequential months. Edema resolved completely. The patient was free of recurrence 56 months after treatment.

The contribution of Tobias J. Beck to these two manuscripts was to investigate the basics of light application with optical and thermal simulations, modeling the light distribution within the irradiated tissue, helping to implement the theoretical data in the clinical setup, developing technical equipment used for the treatment, supporting the stereotactical procedure, and preparing the manuscript (Beck et al., 2007b) together with Prof. Kreth.

Two-Photon Excitation induced Photodynamic Therapy

The other concept investigated the usability of another type of light source in order to induce the phototoxic effect in ALA-incubated cells: infrared (IR) laser light, which in general has a higher penetration depth compared to red light. Unfortunately, light intensities usually used in red light PDT (200 mW/cm^2) are not effective at all when irradiating with IR light, since PpIX does not absorb light within this wavelength region very effectively. However, when PpIX is exposed to very high light intensities of IR light, then there is a chance to induce a PDT effect by exciting the sensitizer via two-photon absorption. In this process an atom or molecule absorbs two photons at approximately the same time and achieves an excited state that corresponds to the sum of the energy of the incident photons (see Fig. 1.4). There need not be an intermediate state for the molecule to reach before arriving at the final excited state. Instead, the atom is excited to a "virtual state" which need not correspond to any electronic or vibrational energy eigenstate. The theory of this phenomena was first developed by Göppert-Meyer in 1931 (Göppert-Mayer, 1931). In 1961, the first lasers came up and the theory could be verified with experiments.

The resulting excited state after two-photon excitation (TPE) offers an identical behavior compared to molecules undergoing an ordinary single photon absorption. Thus, TPE excited molecules can also relax by emitting fluorescent light or by interacting with oxygen resulting in reactive oxygen species.

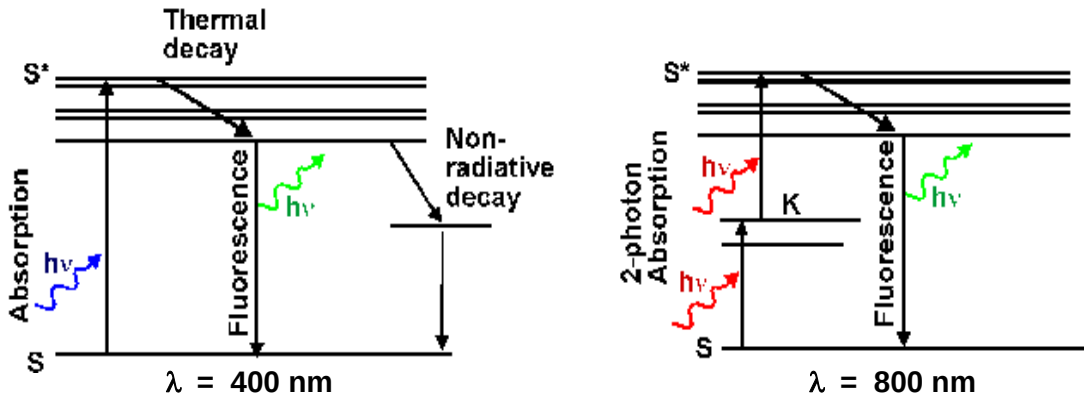

Figure 1.4: Term scheme for single photon excitation (SPE) and for two photon excitation (TPE).

The effect of two-photon or multiphoton excitation has already found diagnostic applications in life science: near infrared (NIR) multiphoton microscopy is a novel optical tool for fluorescence imaging based on non-resonant two-photon fluorophore excitation (König, 2000). This technique allows to obtain morphological and functional fluorescence images of endogenous fluorophores. However, also exogenous fluorophores can be imaged with high spatial resolution. Madsen et al. (Madsen et al., 2000) reported about two-photon fluorescence microscopy in human glioma spheroids in order to show the conversion of 5-ALA to PpIX throughout the entire spheroid volume.

Besides fluorescence effects, two-photon excited PDT has also gained interest, mainly due to the expected higher therapeutic penetration depth in tissue compared to VIS-

single-photon excitation. In addition to the higher penetration depth, the two-photon photodynamic therapy has the potential of improving the therapeutic outcome due to a highly localized photodynamic effect, since the tissue volume, where the light intensity is high enough, is only some μm^3.

About ten years ago, first experimental studies were published (Fisher et al., 1997; Bhawalkar et al., 1997). Since then, reports have been published investigating basic pathways of TPE (Goyan and Cramb, 2000; Frederiksen et al., 2001; Dittrich and Schwille, 2001; Frederiksen et al., 2005; Samkoe et al., 2006), how to enhance two-photon absorption by using novel effective two-photon phototherapeutic agents (Drobizhev et al., 2002; Liu et al., 2002; Ogawa et al., 2006), and about the treatment of cells in vitro (König et al., 1999; Karotki et al., 2006). Furthermore, the application of TPE-PDT in clinical therapies, such as treatment of age-related macular degeneration (AMD), were investigated in model systems (Samkoe and Cramb, 2003).

Novel irradiation concept II

The approach of the present study was to investigate TPE-PDT in cell culture experiments. Monolayers of C6 rat glioma cells were irradiated with a pulsed and focused fs Ti:Sapphire laser emitting light at 800 nm. The beam profile of the laser beam was carefully analyzed before the experiment and the applied irradiance was known for each position within the irradiated cell layer. Cells were divided into four groups, three control groups (no drug and no light, drug but no light, light but no drug) and one group, that was incubated with 5-ALA and irradiated 4 to 5 hours later. The survival of this group was tested after irradiation by means of ethidium bromide and acridine orange staining and compared to a control group, which was irradiated under the same conditions, but not incubated with 5-ALA before. Both groups showed necrotic areas depending on the applied irradiance. Cells of both groups became necrotic when treated with an irradiance above $10.9 \cdot 10^{10}$ W/cm^2. 5-ALA incubated cells became necrotic also after irradiation with a mean irradiance down to $6.1 \cdot 10^{10}$ W/cm^2, while non-incubated cells remained viable below $10.9 \cdot 10^{10}$ W/cm^2. Therefore it seemed, that below a mean power density of $10.9 \cdot 10^{10}$ W/cm^2 no thermal damage was induced in the cells and necrosis of the 5-ALA incubated cells can be ascribed to the photodynamic effect induced by two-photon excitation. The results of this experimental study were published by Beck et al. (Beck et al., 2007a).

The contribution of Tobias J. Beck to this study was to measure and calculate the applied light intensities, modeling the light distribution within the monolayer of cells, performing the light irradiation, evaluating the data of the area of necrotic cells, measuring the PpIX fluorescence of the incubated cells before the treatment and preparing the manuscript.

References

Albert, F. K., Forsting, M., Sartor, K., Adams, H. P., and Kunze, S. (1994). Early postoperative magnetic resonance imaging after resection of malignant glioma: objective evaluation of residual tumor and its influence on regrowth and prognosis. *Neurosurgery*, 34(1):45–60.

Angell-Petersen, E., Spetalen, S., Madsen, S. J., Sun, C. H., Peng, Q., Carper, S. W., Sioud, M., and Hirschberg, H. (2006). Influence of light fluence rate on the effects of photodynamic therapy in an orthotopic rat glioma model. *J. Neurosurg.*, 104(1):109–117.

Bashir, R., Hochberg, F., and Oot, R. (1988). Regrowth patterns of glioblastoma multiforme related to planning of interstitial brachytherapy radiation fields. *Neurosurgery*, 23(1):27–30.

Beck, T. J., Burkanas, M., Bagdonas, S., Krivickiene, Z., Beyer, W., Sroka, R., Baumgartner, R., and Rotomskis, R. (2007a). Two-photon photodynamic therapy of C6 cells by means of 5-aminolevulinic acid induced protoporphyrin IX. *J. Photochem. Photobiol. B*, 87(3):174–182.

Beck, T. J., Kreth, F. W., Beyer, W., Mehrkens, J. H., Obermeier, A., Stepp, H., Stummer, W., and Baumgartner, R. (2007b). Interstitial photodynamic therapy of nonresectable malignant glioma recurrences using 5-aminolevulinic acid induced protoporphyrin IX. *Lasers Surg. Med.*, 39(5):386–393.

Beyer, W. (2003). Light delivery systems and consequences for dosimetry. Abstract: 5nd Int.Symp.on Photodynamic Diagnosis and Therapy in Clinical Practice, Brixen, Italy, Okt.2003, 7.-11., Abstract Nr.5.

Bhawalkar, J. D., Kumar, N. D., Zhao, C. F., and Prasad, P. N. (1997). Two-photon photodynamic therapy. *J. Clin. Laser Med. Surg.*, 15(5):201–204.

Butowski, N. A., Sneed, P. K., and Chang, S. M. (2006). Diagnosis and treatment of recurrent high-grade astrocytoma. *J. Clin. Oncol.*, 24(8):1273–1280.

Cha, S. (2004). Perfusion MR imaging of brain tumors. *Top. Magn Reson. Imaging*, 15(5):279–289.

Chao, S. T., Suh, J. H., Raja, S., Lee, S. Y., and Barnett, G. (2001). The sensitivity and specificity of FDG PET in distinguishing recurrent brain tumor from radionecrosis in patients treated with stereotactic radiosurgery. *Int. J. Cancer*, 96(3):191–197.

Chen, Q., Chopp, M., Madigan, L., Dereski, M. O., and Hetzel, F. W. (1996). Damage threshold of normal rat brain in photodynamic therapy. *Photochemistry and Photobiology*, 64(1):163–167.

Cheng, M. K., McKean, J., Boisvert, D., Tulip, J., and Mielke, B. W. (1984). Effects of photoradiation therapy on normal rat brain. *Neurosurgery*, 15(6):804–810.

Cho, K. H., Hall, W. A., Gerbi, B. J., Higgins, P. D., McGuire, W. A., and Clark, H. B. (1999). Single dose versus fractionated stereotactic radiotherapy for recurrent high-grade gliomas. *Int. J. Radiat. Oncol. Biol. Phys.*, 45(5):1133–1141.

den Bent, M. J. V., Hegi, M. E., and Stupp, R. (2006). Recent developments in the use of chemotherapy in brain tumours. *Eur. J. Cancer*, 42(5):582–588.

Dereski, M. O., Chopp, M., Chen, Q., and Hetzel, F. W. (1989). Normal brain-tissue response to photodynamic therapy - histology, vascular-permeability and specific-gravity. *Photochemistry and Photobiology*, 50(5):653–657.

Diamond, I., Granelli, S. G., McDonagh, A. F., Nielsen, S., Wilson, C. B., and Jaenicke, R. (1972). Photodynamic therapy of malignant tumours. *Lancet*, 2(7788):1175–1177.

Dittrich, P. S. and Schwille, P. (2001). Photobleaching and stabilization of fluorophores used for single-molecule analysis with one- and two-photon excitation. *Appl. Phys. B*, 73(8):829–837.

Drobizhev, M., Karotki, A., Kruk, M., Mamardashvili, N. Z., and Rebane, A. (2002). Drastic enhancement of two-photon absorption in porphyrins associated with symmetrical electron-accepting substitution. *Chem. Phys. Lett.*, 361(5-6):504–512.

E. R. Laws, J., Cortese, D. A., Kinsey, J. H., Eagan, R. T., and Anderson, R. E. (1981). Photoradiation therapy in the treatment of malignant brain tumors: a phase I (feasibility) study. *Neurosurgery*, 9(6):672–678.

Ennis, S. R., Novotny, A., Xiang, J., Shakui, P., Masada, T., Stummer, W., Smith, D. E., and Keep, R. F. (2003). Transport of 5-aminolevulinic acid between blood and brain. *Brain Res.*, 959(2):226–234.

Fisher, W. G., Partridge, W. P., Dees, C., and Wachter, E. A. (1997). Simultaneous two-photon activation of type-I photodynamic therapy agents. *Photochem. Photobiol.*, 66(2):141–155.

Frederiksen, P. K., Jorgensen, M., and Ogilby, P. R. (2001). Two-photon photosensitized production of singlet oxygen. *J. Am. Chem. Soc.*, 123(6):1215–1221.

Frederiksen, P. K., McIlroy, S. P., Nielsen, C. B., Nikolajsen, L., Skovsen, E., Jorgensen, M., Mikkelsen, K. V., and Ogilby, P. R. (2005). Two-photon photosensitized production of singlet oxygen in water. *J. Am. Chem. Soc.*, 127(1):255–269.

Gaspar, L. E., Zamorano, L. J., Shamsa, F., Fontanesi, J., Ezzell, G. E., and Yakar, D. A. (1999). Permanent 125iodine implants for recurrent malignant gliomas. *Int. J. Radiat. Oncol. Biol. Phys.*, 43(5):977–982.

Goetz, C., Hasan, A., Stummer, W., Heimann, A., and Kempski, O. (2002). Photodynamic effects in perifocal, oedematous brain tissue. *Acta Neurochirurgica*, 144(2):173–179.

Goyan, R. L. and Cramb, D. T. (2000). Near-infrared two-photon excitation of protoporphyrin IX: Photodynamics and photoproduct generation. *Photochem. Photobiol.*, 72(6):821–827.

Göppert-Mayer, M. (1931). Über Elementarakte mit zwei Quantensprüngen. *Ann. Phys.*, 9(273).

Hall, W. A., Djalilian, H. R., Sperduto, P. W., Cho, K. H., Gerbi, B. J., Gibbons, J. P., Rohr, M., and Clark, H. B. (1995). Stereotactic radiosurgery for recurrent malignant gliomas. *J. Clin. Oncol.*, 13(7):1642–1648.

Hebeda, K. M., Kamphorst, W., Sterenborg, H. J. C. M., and Wolbers, J. G. (1998a). Damage to tumour and brain by interstitial photodynamic therapy in the 9L rat tumour model comparing intravenous and intratumoral administration of the photosensitiser. *Acta Neurochirurgica*, 140(5):495–501.

Hebeda, K. M., Saarnak, A. E., Olivo, M., Sterenborg, H. J. C. M., and Wolbers, J. G. (1998b). 5-aminolevulinic acid induced endogenous porphyrin fluorescence in 9L and C6 brain tumours in the normal rat brain. *Acta Neurochirurgica*, 140(8):503–512.

Hegi, M. E., Diserens, A. C., Gorlia, T., Hamou, M. F., de Tribolet, N., Weller, M., Kros, J. M., Hainfellner, J. A., Mason, W., Mariani, L., Bromberg, J. E., Hau, P., Mirimanoff, R. O., Cairncross, J. G., Janzer, R. C., and Stupp, R. (2005). MGMT gene silencing and benefit from temozolomide in glioblastoma. *N. Engl. J. Med.*, 352(10):997–1003.

Hirntumorhilfe (2009). Electronic Citation: http://www.hirntumorhilfe.de/.

Hirschberg, H., Sun, C. H., Krasieva, T., and Madsen, S. J. (2006). Effects of ALA-mediated photodynamic therapy on the invasiveness of human glioma cells. *Lasers Surg. Med.*, 38(10):939–945.

Hirschberg, H., Sun, C. H., Tromberg, B. J., and Madsen, S. J. (2002). ALA- and ALA-ester-mediated photodynamic therapy of human glioma spheroids. *J. Neurooncol.*, 57(1):1–7.

Hochstetter, A. (2001). High-Dose Laser Irradiation and 5-Aminolevulinic Acid (5-ALA) for Photodynamic Therapy of Glioblastomas. *IPA 8th World Congress of Photodynamic Medicine, Vancouver, Canada.*

Inoue, H., Kajimoto, Y., Shibata, M. A., Miyoshi, N., Ogawa, N., Miyatake, S., Otsuki, Y., and Kuroiwa, T. (2007). Massive apoptotic cell death of human glioma cells via a mitochondrial pathway following 5-aminolevulinic acid-mediated photodynamic therapy. *J. Neurooncol.*, 83(3):223–231.

Jalili, A., Makowski, M., Switaj, T., Nowis, D., Wilczynski, G. M., Wilczek, E., Chorazy-Massalska, M., Radzikowska, A., Maslinski, W., Bialy, L., Sienko, J., Sieron, A., Adamek, M., Basak, G., Mroz, P., Krasnodebski, I. W., Jakobisiak, M., and Golab, J. (2004). Effective photoimmunotherapy of murine colon carcinoma induced by the combination of photodynamic therapy and dendritic cells. *Clin. Cancer Res.*, 10(13):4498–4508.

Jemal, A., Tiwari, R. C., Murray, T., Ghafoor, A., Samuels, A., Ward, E., Feuer, E. J., and Thun, M. J. (2004). Cancer statistics, 2004. *CA Cancer J. Clin.*, 54(1):8–29.

Kaneko, S. (1999). Stereotactic intratumoral PDT for malignant brain tumours. *Photodynamic News*, 2(3):8–10.

Karotki, A., Khurana, M., Lepock, J. R., and Wilson, B. C. (2006). Simultaneous Two-photon Excitation of Photofrin in Relation to Photodynamic Therapy. *Photochem. Photobiol.*, 82(2):443–452.

König, K. (2000). Invited Review: Multiphoton microscopy in life sciences. *J. Microsc.*, 200:83–104.

König, K., Riemann, I., and Fischer, P. (1999). Photodynamic therapy by nonresonant two-photon excitation. *Proc. SPIE, Optical Methods for Tumor Treatment and Detection: Mechanisms and Techniques in Photodynamic Therapy VIII; Thomas J. Dougherty; Ed.*, 3592:43–49.

Korbelik, M., Sun, J., and Cecic, I. (2005). Photodynamic therapy-induced cell surface expression and release of heat shock proteins: relevance for tumor response. *Cancer Res.*, 65(3):1018–1026.

Kostron, H., Obwegeser, A., and Jakober, R. (1996). Photodynamic therapy in neurosurgery: a review. *J. Photochem. Photobiol. B*, 36(2):157–168.

Krammer, B. and Plaetzer, K. (2008). ALA and its clinical impact, from bench to bedside. *Photochem. Photobiol. Sci.*, 7(3):283–289.

Krishnamurthy, S., Powers, S. K., Witmer, P., and Brown, T. (2000). Optimal light dose for interstitial photodynamic therapy in treatment for malignant brain tumors. *Lasers in Surgery and Medicine*, 27(3):224–234.

Lacroix, M., Abi-Said, D., Fourney, D. R., Gokaslan, Z. L., Shi, W., DeMonte, F., Lang, F. F., McCutcheon, I. E., Hassenbusch, S. J., Holland, E., Hess, K., Michael, C., Miller, D., and Sawaya, R. (2001). A multivariate analysis of 416 patients with glioblastoma multiforme: prognosis, extent of resection, and survival. *J. Neurosurg.*, 95(2):190–198.

Lajat, Y. and Patrice, T. (1987). Photochemotherapy applied stereotactically to brain tumors. *Surgical Neurology*, 27(4):403–404.

Lilge, L., Olivo, M. C., Schatz, S. W., MaGuire, J. A., Patterson, M. S., and Wilson, B. C. (1996). The sensitivity of normal brain and intracranially implanted VX2 tumour to interstitial photodynamic therapy. *British Journal of Cancer*, 73(3):332–343.

Liu, J., Zhao, Y. W., Zhao, J. Q., Xia, A. D., Jiang, L. J., Wu, S., Ma, L., and Dong, Y. Q. (2002). Two-photon excitation studies of hypocrellins for photodynamic therapy. *J. Photochem. Photobiol. B: Biol.*, 68(2-3):156–164.

Louis, D. N., Ohgaki, H., Wiestler, O. D., Cavenee, W. K., Burger, P. C., Jouvet, A., Scheithauer, B. W., and Kleihues, P. (2007). The 2007 WHO classification of tumours of the central nervous system. *Acta Neuropathol.*, 114(2):97–109.

Madsen, S. and Hirschberg, H. (2006). Photodynamic Therapy and Detection of High-Grade Gliomas. *J. Environ. Pathol. Toxicol. Oncol.*, 25(1-2):453–466.

Madsen, S. J., Angell-Petersen, E., Spetalen, S., Carper, S. W., Ziegler, S. A., and Hirschberg, H. (2006). Photodynamic therapy of newly implanted glioma cells in the rat brain. *Lasers Surg. Med.*, 38(5):540–548.

Madsen, S. J., Mathews, M. S., Angell-Petersen, E., Sun, C. H., Vo, V., Sanchez, R., and Hirschberg, H. (2009). Motexafin gadolinium enhances the efficacy of aminolevulinic acid mediated-photodynamic therapy in human glioma spheroids. *J. Neurooncol.*, 91(2):141–149.

Madsen, S. J., Sun, C. H., Tromberg, B. J., and Hirschberg, H. (2001). Development of a novel indwelling balloon applicator for optimizing light delivery in photodynamic therapy. *Lasers Surg. Med.*, 29(5):406–412.

Madsen, S. J., Sun, C. H., Tromberg, B. J., and Hirschberg, H. (2003). Repetitive 5-aminolevulinic acid-mediated photodynamic therapy on human glioma spheroids. *Journal of Neuro-Oncology*, 62(3):243–250.

Madsen, S. J., Sun, C. H., Tromberg, B. J., Wallace, V. P., and Hirschberg, H. (2000). Photodynamic therapy of human glioma spheroids using 5- aminolevulinic acid. *Photochem. Photobiol.*, 72(1):128–134.

Meyerand, M. E., Pipas, J. M., Mamourian, A., Tosteson, T. D., and Dunn, J. F. (1999). Classification of biopsy-confirmed brain tumors using single-voxel MR spectroscopy. *AJNR Am. J. Neuroradiol.*, 20(1):117–123.

Muller, P. J. and Wilson, B. C. (1987). Photodynamic therapy of malignant primary brain tumours: clinical effects, post-operative ICP, and light penetration of the brain. *Photochem. Photobiol.*, 46(5):929–935.

Muller, P. J. and Wilson, B. C. (1995). Photodynamic therapy for recurrent supratentorial gliomas. *Semin. Surg. Oncol.*, 11(5):346–354.

Muller, P. J. and Wilson, B. C. (1996). Photodynamic therapy for malignant newly diagnosed supratentorial gliomas. *J Clin. Laser Med. Surg.*, 14(5):263–270.

Novotny, A., Xiang, J., Stummer, W., Teuscher, N. S., Smith, D. E., and Keep, R. F. (2000). Mechanisms of 5-aminolevulinic acid uptake at the choroid plexus. *J. Neurochem.*, 75(1):321–328.

Ogawa, K., Hasegawa, H., Inaba, Y., Kobuke, Y., Inouye, H., Kanemitsu, Y., Kohno, E., Hirano, T., Ogura, S., and Okura, I. (2006). Water-soluble bis(imidazolylporphyrin) self-assemblies with large two-photon absorption cross sections as potential agents for photodynamic therapy. *J. Med. Chem.*, 49(7):2276–2283.

Ohgaki, H. (2009). Epidemiology of brain tumors. *Methods Mol. Biol.*, 472:323–342.

Olzowy, B., Hundt, C. S., Stocker, S., Bise, K., Reulen, H. J., and Stummer, W. (2002). Photoirradiation therapy of experimental malignant glioma with 5-aminolevulinic acid. *Journal of Neurosurgery*, 97(4):970–976.

Origitano, T. C. and Reichman, O. H. (1993). Photodynamic therapy for intracranial neoplasms: development of an image-based computer-assisted protocol for photodynamic therapy of intracranial neoplasms. *Neurosurgery*, 32(4):587–595.

Perria, C., Capuzzo, T., Cavagnaro, G., Datti, R., Francaviglia, N., Rivano, C., and Tercero, V. E. (1980). First attempts at the photodynamic treatment of human gliomas. *J. Neurosurg. Sci.*, 24(3-4):119–129.

Popovic, E. A., Kaye, A. H., and Hill, J. S. (1996). Photodynamic therapy of brain tumors. *J. Clin. Laser Med. Surg.*, 14(5):251–261.

Pottier, R., Krammer, B., Stepp, H., and Baumgartner, R., editors (2006). *Photodynamic Therapy with ALA - A Clinical Handbook*. Comprehensive Series in Photochemistry and Photobiology. The Royal Society of Chemistry.

Powers, S. K., Cush, S. S., Walstad, D. L., and Kwock, L. (1991). Stereotaxic intratumoral photodynamic therapy for recurrent malignant brain-tumors. *Neurosurgery*, 29(5):688–696.

Raab, O. (1898). Über die Wirkung fluoreszierender Stoffe auf Paramaecien. *Z. Biol.*, 524.

Rachinger, W., Goetz, C., Popperl, G., Gildehaus, F. J., Kreth, F. W., Holtmannspotter, M., Herms, J., Koch, W., Tatsch, K., and Tonn, J. C. (2005). Positron emission tomography with O-(2-[18F]fluoroethyl)-l-tyrosine versus magnetic resonance imaging in the diagnosis of recurrent gliomas. *Neurosurgery*, 57(3):505–511.

Rosenthal, M. A., Kavar, B., Hill, J. S., Morgan, D. J., Nation, R. L., Stylli, S. S., Basser, R. L., Uren, S., Geldard, H., Green, M. D., Kahl, S. B., and Kaye, A. H. (2001). Phase I and pharmacokinetic study of photodynamic therapy for high-grade gliomas using a novel boronated porphyrin. *J Clin. Oncol.*, 19(2):519–524.

Samkoe, K. S. and Cramb, D. T. (2003). Application of an ex ovo chicken chorioallantoic membrane model for two-photon excitation photodynamic therapy of age-related macular degeneration. *J. Biomed. Opt.*, 8(3):410–417.

Samkoe, K. S., Fecica, M. S., Goyan, R. L., Buchholz, J. L., Campbell, C., Kelly, N. M., and Cramb, D. T. (2006). Photobleaching kinetics of optically trapped multilamellar vesicles containing verteporfin using two-photon excitation section sign. *Photochem. Photobiol.*, 82(1):152–157.

Sathornsumetee, S., Rich, J. N., and Reardon, D. A. (2007). Diagnosis and treatment of high-grade astrocytoma. *Neurol. Clin.*, 25(4):1111–39, x.

Schmidt, M. H., Meyer, G. A., Reichert, K. W., Cheng, J., Krouwer, H. G., Ozker, K., and Whelan, H. T. (2004). Evaluation of photodynamic therapy near functional brain tissue in patients with recurrent brain tumors. *Journal of Neuro-Oncology*, 67(1-2):201–207.

Shapiro, W. R., Green, S. B., Burger, P. C., M. S. Mahaley, J., Selker, R. G., VanGilder, J. C., Robertson, J. T., Ransohoff, J., J. Mealey, J., and Strike, T. A. (1989). Randomized trial of three chemotherapy regimens and two radiotherapy regimens and two radiotherapy regimens in postoperative treatment of malignant glioma. Brain Tumor Cooperative Group Trial 8001. *J. Neurosurg.*, 71(1):1–9.

Sneed, P. K., McDermott, M. W., and Gutin, P. H. (1997). Interstitial brachytherapy procedures for brain tumors. *Semin. Surg. Oncol.*, 13(3):157–166.

Star, W. M., Marijnissen, H. P., Jansen, H., Keijzer, M., and van Gemert, M. J. (1987). Light dosimetry for photodynamic therapy by whole bladder wall irradiation. *Photochem. Photobiol.*, 46(5):619–624.

Stepp, H., Beck, T., Pongratz, T., Meinel, T., Kreth, F. W., Tonn, J. C., and Stummer, W. (2007). ALA and malignant glioma: fluorescence-guided resection and photodynamic treatment. *J. Environ. Pathol. Toxicol. Oncol.*, 26(2):157–164.

Stummer, W., Beck, T., Beyer, W., Mehrkens, J. H., Obermeier, A., Etminan, N., Stepp, H., Tonn, J. C., Baumgartner, R., Herms, J., and Kreth, F. W. (2008). Long-sustaining response in a patient with non-resectable, distant recurrence of glioblastoma multiforme treated by interstitial photodynamic therapy using 5-ALA: case report. *J. Neurooncol.*, 87(1):103–109.

Stummer, W., Gotz, C., Hassan, A., Heimann, A., and Kempski, O. (1993). Kinetics of Photofrin II in perifocal brain edema. *Neurosurgery*, 33(6):1075–1081.

Stummer, W., Hassan, A., Kempski, O., and Goetz, C. (1996). Photodynamic therapy within edematous brain tissue: considerations on sensitizer dose and time point of laser irradiation. *J. Photochem. Photobiol. B*, 36(2):179–181.

Stummer, W., Novotny, A., Stepp, H., Goetz, C., Bise, K., and Reulen, H. J. (2000). Fluorescence-guided resection of glioblastoma multiforme by using 5- aminolevulinic acid-induced porphyrins: a prospective study in 52 consecutive patients. *J. Neurosurg.*, 93(6):1003–1013.

Stummer, W., Pichlmeier, U., Meinel, T., Wiestler, O. D., Zanella, F., and Reulen, H. J. (2006). Fluorescence-guided surgery with 5-aminolevulinic acid for resection of malignant glioma: a randomised controlled multicentre phase III trial. *Lancet Oncol.*, 7(5):392–401.

Stummer, W., Reulen, H. J., Novotny, A., Stepp, H., and Tonn, J. C. (2003). Fluorescence-guided resections of malignant gliomas–an overview. *Acta Neurochir. Suppl*, 88:9–12.

Stummer, W., Stepp, H., Moller, G., Ehrhardt, A., Leonhard, M., and Reulen, H. J. (1998a). Technical principles for protoporphyrin-IX-fluorescence guided microsurgical resection of malignant glioma tissue. *Acta Neurochir. (Wien.)*, 140(10):995–1000.

Stummer, W., Stocker, S., Novotny, A., Heimann, A., Sauer, O., Kempski, O., Plesnila, N., Wietzorrek, J., and Reulen, H. J. (1998b). In vitro and in vivo porphyrin accumulation by C6 glioma cells after exposure to 5-aminolevulinic acid. *J. Photochem. Photobiol. B: Biol.*, 45(2-3):160–169.

Stummer, W., Stocker, S., Wagner, S., Stepp, H., Fritsch, C., Goetz, C., Goetz, A. E., Kiefmann, R., and Reulen, H. J. (1998c). Intraoperative detection of malignant gliomas by 5-aminolevulinic acid- induced porphyrin fluorescence. *Neurosurgery*, 42(3):518–525.

Stupp, R., Hegi, M. E., Mason, W. P., den Bent, M. J. V., Taphoorn, M. J., Janzer, R. C., Ludwin, S. K., Allgeier, A., Fisher, B., Belanger, K., Hau, P., Brandes, A. A., Gijtenbeek, J., Marosi, C., Vecht, C. J., Mokhtari, K., Wesseling, P., Villa, S., Eisenhauer, E., Gorlia, T., Weller, M., Lacombe, D., Cairncross, J. G., and Mirimanoff, R. O. (2009). Effects of radiotherapy with concomitant and adjuvant temozolomide versus radiotherapy alone on survival in glioblastoma in a randomised phase III study: 5-year analysis of the EORTC-NCIC trial. *Lancet Oncol.*, 10(5):459–466.

Stupp, R., Mason, W. P., den Bent, M. J. V., Weller, M., Fisher, B., Taphoorn, M. J., Belanger, K., Brandes, A. A., Marosi, C., Bogdahn, U., Curschmann, J., Janzer, R. C., Ludwin, S. K., Gorlia, T., Allgeier, A., Lacombe, D., Cairncross, J. G., Eisenhauer, E., and Mirimanoff, R. O. (2005). Radiotherapy plus concomitant and adjuvant temozolomide for glioblastoma. *N. Engl. J. Med.*, 352(10):987–996.

Stylli, S. S. and Kaye, A. H. (2006). Photodynamic therapy of cerebral glioma - a review. Part II - clinical studies. *J. Clin. Neurosci.*, 13(7):709–717.

Stylli, S. S., Kaye, A. H., Macgregor, L., Howes, M., and Rajendra, P. (2005). Photodynamic therapy of high grade glioma - long term survival. *J. Clin. Neurosci.*, 12(4):389–398.

Tsai, J. C., Hsiao, Y. Y., Teng, L. J., Chen, C. T., and Kao, M. C. (1999). Comparative study on the ALA photodynamic effects of human glioma and meningioma cells. *Lasers Surg. Med.*, 24(4):296–305.

v. Tappeiner, H. and Jesionek, A. (1903). Therapeutische Versuche mit fluoreszierenden Stoffen. *Muench. Med. Wochenschr.*, 47:2042–2044.

van Duijnhoven, F. H., Aalbers, R. I., Rovers, J. P., Terpstra, O. T., and Kuppen, P. J. (2003). The immunological consequences of photodynamic treatment of cancer, a literature review. *Immunobiology*, 207(2):105–113.

Veninga, T., Langendijk, H. A., Slotman, B. J., Rutten, E. H., van der Kogel, A. J., Prick, M. J., Keyser, A., and van der Maazen, R. W. (2001). Reirradiation of primary brain tumours: survival, clinical response and prognostic factors. *Radiother. Oncol.*, 59(2):127–137.

Voynov, G., Kaufman, S., Hong, T., Pinkerton, A., Simon, R., and Dowsett, R. (2002). Treatment of recurrent malignant gliomas with stereotactic intensity modulated radiation therapy. *Am. J. Clin. Oncol.*, 25(6):606–611.

Wilson, B. C., Muller, P. J., and Yanch, J. C. (1986). Instrumentation and light dosimetry for intra-operative photodynamic therapy (PDT) of malignant brain tumours. *Phys. Med. Biol.*, 31(2):125–133.

Zelenkov, P., Baumgartner, R., Bise, K., Heide, M., Meier, R., Stocker, S., Sroka, R., Goldbrunner, R., and Stummer, W. (2007). Acute morphological sequelae of photodynamic therapy with 5-aminolevulinic acid in the C6 spheroid model. *J. Neurooncol.*, 82(1):49–60.

Chapter 2

Original Manuscripts

ALA and Malignant Glioma: Fluorescence-Guided Resection and Photodynamic Treatment

Herbert Stepp, Tobias Beck, Thomas Pongratz, Thomas Meinel, Friedrich W. Kreth, Jörg-Christian Tonn, and Walter Stummer

J. Environ. Pathol. Toxicol. Oncol. 26(2):157-164 (2007)

Journal of Environmental Pathology, Toxicology, and Oncology, 26(2)157–164 (2007)

ALA and Malignant Glioma: Fluorescence-Guided Resection and Photodynamic Treatment

Herbert Stepp,[1,] Tobias Beck,[1] Thomas Pongratz,[1] Thomas Meinel,[2] Friedrich-Wilhelm Kreth,[3] Jörg Ch. Tonn,[3] & Walter Stummer[4]*

[1]Laser-Forschungslabor, LIFE-Center, University Clinic Munich–Großhadern, Marchioninistr. 23, 81377 Munich, Germany, [2]Clinstud, Clinical Research Institute Hamburg, Beim Alten Gaswerk 1, 22761 Hamburg, and Institut für Neuroradiologie, Klinikum der J.-W. Goethe Universität Frankfurt, Germany, [3]Dept. of Neurosurgery, University Clinic Munich–Großhadern, Marchioninistr. 15, 81377 Munich, Germany, [4]Department of Neurosurgery, University Clinic Düsseldorf, Moorenstr. 5, 40225 Düsseldorf, Germany

* ***Corresponding author***. E-mail: Herbert.Stepp@med.uni-muenchen.de

Background: Oral application of 20 mg/kg body weight of 5-aminolevulinic acid (ALA) leads to a highly specific accumulation of fluorescent Protoporphyrin IX (PPIX) in malignant glioma tissue. In the past few years, we have participated in several clinical studies designed to investigate fluorescence guided resection (FGR) and photodynamic therapy (PDT). **Methods**: PPIX selectivity and PPIX bleaching during PDT were assessed with spectroscopic measurements. FGR was performed in 18 clinics in Germany (ALA-Glioma Study Group, participants see end of paper) in a phase III trial comprising an ALA group and a white-light group. PDT was performed with microlens fibers or cylindrical diffusers postsurgically to the resection bed. Additionally, a protocol for the interstitial stereotactic placement of cylindrical diffusers was established and applied on patients with recurrent, inoperable glioblastoma. **Results**: Compared to normal cortex, mean PPIX fluorescence in vital tumor was found more than 100-fold increased. During PDT, the PPIX fluorescence bleached to 8%, 16%, and 1% of the initial intensity for the 100, 150, and 200 J/cm² groups (median values). FGR: Contrast-enhancing tumor was completely resected in 65% of patients in the ALA group compared to 36% in the white-light group ($p < 0.0001$). Progression-free survival was superior in the ALA group compared to white-light patients with cumulative 6 months progression-free survival rates of 41% and 21% ($p = 0.0003$), respectively. Interstitial PDT can be performed with multiple radial diffusers approximately 10 mm apart, 200 mW/cm, and an irradiation time of one hour.

KEY WORDS: 5-aminolevulinic acid, fluorescence-guided resection, photodynamic therapy, glioma, brain tumor, interstitial PDT

Introduction

Complete surgical removal of malignant glioma is not possible due to its locally invasive growth. However, maximal cytoreductive surgery is generally performed, aiming at removing at least that part of the tumor that accumulates a contrast agent for magnetic resonance imaging (contrast-enhanced MRI).[1,2] Complete resection of contrast-enhancing tumor regions as judged by postoperative MRI is only achieved in a minority of patients,[3] one of the reasons for this being the difficulty in detecting contrast-enhancing tumor margins intraoperatively.[3]

Intraoperative optical identification of glioma tissue is suggested to be possible by fluorescence imaging of ALA-induced PPIX.[4,5] ALA is a natural biochemical precursor of hemoglobin. Exogenous administration of ALA elicits the synthesis and accumulation of fluorescent porphyrins in various epithelia and cancerous tissues.[6] Malignant glioma tissue has also been demonstrated to specifically synthesize and accumulate porphyrins, mainly PPIX in response to ALA administration. PPIX shows red fluorescence when excited with violet-blue light and can be visualized after appropriate modifications to a standard neurosurgical microscope.[7]

PPIX is also a potent photosensitizer, causing tissue destruction following irradiation with visible light by the action of reactive oxygen species. The conditions for a tumor-selective PDT have been established in a C6-rat-glioma model,[8] showing effective destruction of the tumor and negligible damage to normal or perifocal edematous tissue with the same irradiation parameters applied. In the context of a treatment for malignant glioma, PDT could be beneficial at two points, namely, immediately postsurgery as a selectively acting treatment of microinvasion or on inoperable recurrent tumor by performing the necessary irradiation with cylindrical diffusers that are inserted into the tumor by stereotactic means. In this report we summarize spectral measurements on glioma tissue in order to study the selectivity of PPIX accumulation, spectral measurements to assess PPIX-fluorescence bleaching during PDT, show the basic results of an interim analysis of a multicentric phase III study on FGR, and, finally, present the concept and results of a stereotactic interstitial PDT approach.

Materials and methods

ALA Application

ALA was obtained from medac GmbH, Wedel, Germany, as a sterile powder, dissolved in 100 ml of tap water and delivered orally at a dose of 20 mg/kg body weight three hours before induction of anesthesia.

Fluorescence Spectroscopy

Fluorescence spectra were measured with a multifiber applicator, comprising seven excitation fibers placed around a central detection fiber connected to a spectrometer (Ocean Optics S2000, Mikropack, Ostfildern, Germany). The fiber probe was used in contact with the tissue, cleaned and normalized to a fluorescence reference after each measurement. For evaluation, the spectra obtained were fitted with a pure PPIX spectrum, a gaussian peak at around 660 nm to account for photoproducts, a pure autofluorescence spectrum, and a gaussian peak centered at 455 nm to fit the remission peak. Statistical testing was performed with the Mann-Whitney test using SPSS-software (SPSS 12.0, SPSS, Chicago, IL).

Selectivity of PPIX accumulation was assessed as follows: From 19 patients with glioma grade III or IV, spectra were obtained from the vital part of the tumor at its border (three sites per patient), from the assumed diffuse infiltration zone where the impression of the fluorescence intensity changed to a fainter color contrast (three sites), from the brain adjacent to that zone and considered normal both by white light and fluorescence (two sites), and from a distant control area with no tumor suspicion (two sites). Dose-dependent photobleaching of PPIX fluorescence during PDT was measured as follows: From 20 patients with glioma grade III or IV, spectra were obtained after fluorescence-guided resection (FGR) from the tumor remnant and adjacent normal cortex. Spectra were taken prior to PDT, at certain intervals during PDT with 100 J/cm² (five patients), 150 J/cm² (eight pa-

tients), and 200 J/cm² (seven patients). A monoexponential decay was fitted to the PPIX intensities in order to obtain the bleaching rates. PDT irradiation was performed with light from a 633 nm diode laser (CeraLas, BioLitec, Jena, Germany) delivered with a microlens fiber (Frontal light distributor FD, Medlight, Ecublens, Switzerland) with 200 mW/cm².

Multicenter Study on FGR

This prospective, parallel, randomized, balanced, group-sequential, rater-blinded, two-arm, controlled multicenter phase III study of an intraoperative diagnostic procedure was conducted under the sponsorship of Medac Company (Wedel, Germany). All centers were equipped with identical surgical microscopes modified for intraoperative fluorescence visualization (OPMI NC4 Neuro FL, Zeiss, Oberkochen, Germany).

Two primary efficacy variables were defined: First, the percentage of patients with histologically confirmed malignant gliomas without residual contrast-enhancing tumor on early, postoperative MRI, and second, progression-free survival at six months, defined strictly by the presence of contrast-enhancing tumor on MRI.

In the FL group, the tumor was resected using fluorescence guidance after ALA application. In the control arm (WL group), the tumor was resected as thoroughly as possible using the same microscope and conventional white, xenon illumination. Surgical treatment was followed by radiotherapy. No restrictions were imposed on therapy after documentation of radiological progression.

Stereotactic PDT

For the treatment of recurrent malignant glioma, a concept for stereotactic interstitial PDT with radial diffusers was developed. According to previous measurements,[9] a penetration depth of 2.8 mm for GBM tissue was assumed and the appropriate inter-fiber distance was calculated with a Monte Carlo algorithm. Temperature distribution was calculated using LITCIT-Software (LITCIT 1.5, LMTB, Berlin, Germany). To adapt the irradiated tissue volume to the patient's individual three-dimensional shape of the recurrent tumor, the necessary fiber tip lengths and positions had been determined using a treatment-planning software originally designed for the placement of radioactive seeds (Brainlab Target 1.19, Heimstetten, Germany). Irradiation was then performed with 200 mW/cm fiber length for 1 hr.

Results

Selectivity of PPIX Accumulation

Figure 1 displays the curve-fitting results obtained from the spectroscopic measurements in a logarithmic scaling. Per definition, tissue samples taken

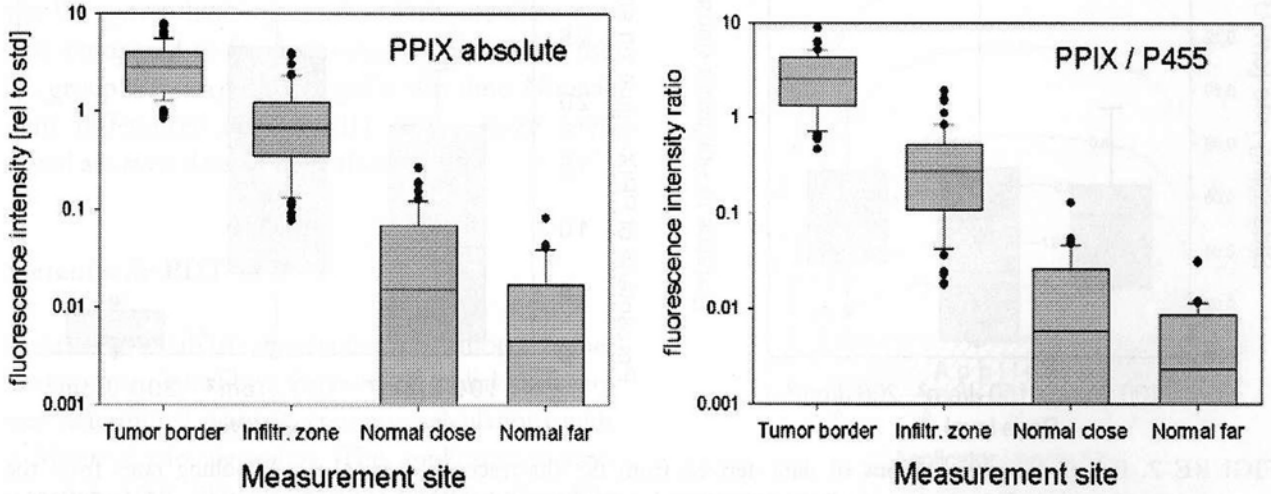

FIGURE 1. PPIX peak intensities in spectra of 19 patients measured at the different sites indicated. In the right graph, PPIX intensities were normalized to the remission peak at 455 nm. Differences between groups were statistically significant with exception of "normal close" and "normal far" in the right graph ($p = 0.09$, Mann-Whitney).

from the tumor border were strongly fluorescent, while samples from the infiltration zone are subjectively weaker. Measurements made on tissue that was considered normal showed no fluorescence as judged from fluorescence imaging, that is, appeared negative (blue only) in fluorescence color contrast. Spectroscopy could clearly show the presence of a PPIX-fluorescence peak with some of these spectra, but the difference to weakly or strongly fluorescent tissue was highly significant ($p < 0.001$).

Dose-dependent Photobleaching of PPIX Fluorescence During PDT

Spectroscopic measurements taken prior to PDT revealed significant amounts of PPIX in the tumor remnant with considerable differences between patients (data not shown). In the majority of cases (13/20), the contrast of PPIX fluorescence from the tumor remnant to adjacent normal cortex was greater than 10:1 (data not shown).

During PDT, PPIX fluorescence bleached considerably in all cases. The mean bleaching rates were quite similar in the three dose-level groups, although there was a high variability at least within the 150 J/cm² group (Fig. 2, left). The mean bleaching rate of 0.05 cm²/J indicates a PPIX bleaching to 50% of the initial intensity after exposure to about 14 J/cm². The residual fluorescence after PDT as compared to pre PDT is depicted in Fig. 2, right. With the high-dose group at 200 J/cm², less than 5% of the initial PPIX fluorescence was measured in all cases. This means that, at least at the tissue surface, the entire phototoxic potential of PPIX had been elicited.

Multicenter Study on FGR

The following is a summary of the original paper by Stummer et al.[10] Glioblastoma multiforme grade IV had been diagnosed in 88% of cases in the FL group and in 89% of cases in the WL group; at least 97% were grade IV tumors in both groups.

Primary efficacy variables. In the FLgroup, 64.7% of patients did not show residual, contrast-enhancing tumor on early postoperative MRI, compared to 35.9% in the WL group ($p < 0.0001$). With respect to the second primary efficacy variable, Kaplan-Meier estimates for progression-free survival at six months were 41% for patients in the FL group and 21.1% for patients in the WL group (log rank test, $p = 0.0003$).

Secondary efficacy variables. The volume of residual tumor was small in both treatment arms. However, patients in the FL group had less residual tumor on early postoperative MRI than patients in

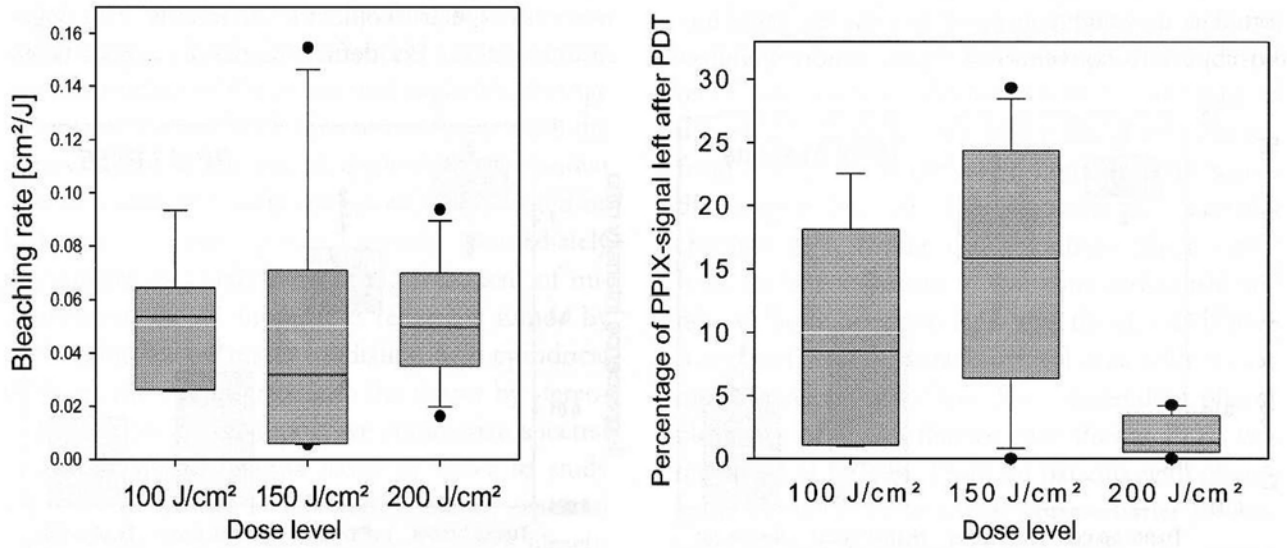

FIGURE 2. Box-plot representations of data derived from the fluorescence decay. Left: Bleaching rates from the monoexponential curve-fitting corresponding to Fig. 3 (right) for the indicated dose levels. Right: Ratios of the PPIX intensities determined at the end of PDT and prior to PDT (normalized to the remission peak at 455 nm). (White line, mean; black line, median.).

the white-light group, with median volumes of 0.0 cm^3 versus 0.7 ccm^3 ($p < 0.0001$).

The study was not designed for a confirmatory demonstration of statistical differences in overall survival, and treatment after progression was not standardized. Nevertheless, median overall survival in the FL group was 15.2 months, compared to 13.5 months in the WL group, when analyzing the per-protocol population. Although this difference failed to reach statistical significance ($p = 0.1245$), the crude hazards ratio was 0.81, favoring fluorescence-guided resections. Differences in survival were found in the subgroup of $n = 168$ patients older than 55 years (FL group 13.8 months, WL group 11.5 months, $p = 0.0577$). Older patients had significantly less exposure to additional treatments after progression than younger patients. In the subgroup of younger patients (≤ 55 years), repeated surgery was performed more frequently in the WL group (62.5%) than in the FL group (41.8%).

Safety. No significant pattern of change was detected between the FL and the WL groups regarding laboratory parameters, except at 24 hours after surgery, when Gamma-GT, ALT/GPT, and AST/GOT values were higher in the FL Group ($p = 0.047$, $p = 0.003$, and $p < 0.001$, respectively), but no longer after seven days or six weeks. Median KPS six weeks after surgery was 90% for both treatment groups, and this remained unchanged three and six months after surgery. No significant differences were noted in the distributions of NIH stroke scores, although the median of patients in the WL group had improved at 48 hours after surgery compared to baseline, whereas patients in the FL group remained unchanged at this time. No evident differences in the NIH stroke score were noted at seven days or thereafter.

Stereotactic PDT

In order to establish an effective irradiation scheme, the optimal interfiber distance of radial diffusers was determined from fluence rate calculations with a Monte Carlo algorithm. The applicator is supposed to emit 200 mW per cm fiber length, while the tissue absorption was assumed to be 0.2 cm^{-1} and effective scattering 20 cm^{-1}. With these parameters, a fluence rate distribution as shown in Fig. 3 is calculated. One penetration depth (~ 3 mm)[9] from the applicator surface, a fluence rate of 520 mW/cm^2 is obtained. If we place two applicators a distance d apart, the corresponding fluence rate profiles overlap and d is determined as the double distance from the applicator surface to a fluence rate of 260 mW/cm^2, which is 4.5 mm according to Fig. 3. Thus, the appropriate interfiber distance is 9 mm. Taking the diameter of the applicator into account, the applicators can be placed 10.6 mm apart. To avoid thermal effects, temperature rise was also calculated for an arrangement with four fibers positioned in the edges of a square, resulting in a tolerable increase to a maximum of 41°C (assuming the following optical and thermal tissue parameters: μ_a, 0.2 cm^{-1}; μ_s', 20 cm^{-1}; initial tissue temp, 37°C; blood perfusion, 0.5 ml/(g·min); water content, 75%; heat conductivity, 0.0048 W/(cm·K); heat capacity, 3.488 J/(g·K); density, 1.075 g/cm^3).

The first patient irradiated this way was a 31-year-old female with a recurrent GBM 12 months after initial surgery. The tumor had progressed despite stereotactic radiotherapy, PCV, and temozolamide chemotherapy. At the time of PDT (7 Oct. 2002), the patient suffered no neurological deficits; KPS was 100. Interstitial PDT with four fibers of 2

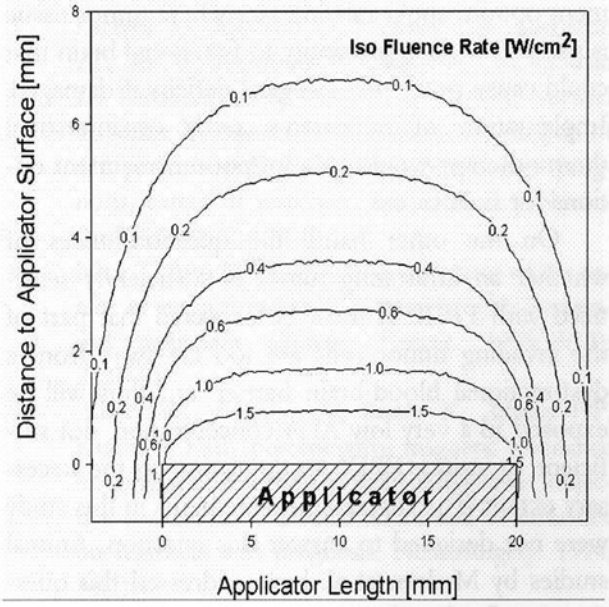

FIGURE 3. Monte Carlo calculation of fluence rates around a single applicator of 2 cm length emitting 200 mW/cm^2 in tissue with $\mu_a = 0.2$ cm^{-1} and $\mu_s' = 20$ cm^{-1}.

cm diffuser length each placed into the tumor with a volume of 6.9 cm^3 was well tolerated; 24 hr postoperative MRI showed no contrast enhancement. Later MRI scans showed transient enhancement in the periphery of the original tumor, but there was no recurrence evident in further follow-up MRI scans. The patient is still (March 2006) free of recurrence. Edema formation was also not observed.

Discussion

Selectivity of PPIX Accumulation and Dose-Dependent Photobleaching of PPIX Fluorescence During PDT

The most important implication of the spectral measurements performed close to the tumor border and more distant on normal brain is probably the conclusion that normal brain is practically free of any detectable PPIX accumulation, even very close to brightly fluorescent malignant tissue. Thus, it is demonstrated that photosensitization is limited to the vital part of the tumor. Considering additionally the pronounced bleaching of PPIX, any small amounts of PPIX present in nonmalignant tissue would bleach on irradiation prior to being able to produce lethal cell damage. It can thus be expected that 5-ALA-PDT could be a very selective treatment option, applicable in cases where tumor tissue is present in close proximity to functional brain that could cause severe neurological deficits if damaged. Implantation of radioactive seeds or interstitial thermotherapy would be a lot poorer treatment options for such cases.

On the other hand, the question arises of whether an infiltrating tumor is sufficiently sensitized with PPIX. It must be expected that part of the invading tumor cells are too far away from a dysfunctional blood-brain barrier and thus will be exposed to a very low ALA concentration, not sufficient to induce PPIX accumulation to the necessary extent. The spectral measurements in this study were not designed to answer this question. Animal studies by Madsen et al. have addressed this question, confirming the concerns of insufficient sensitization.[11] However, it might not be necessary to eradicate every single invading tumor cell by PDT to achieve a curative treatment. It is well known that PDT can induce a significant immune response,[12] which might eliminate tumor cells that initially escape PDT.

Multicenter Study on FGR

This study addresses the basic controversy in neurosurgery on whether maximal cytoreductive therapy of malignant gliomas is of benefit to patients. In this context, the results demonstrate that FGR enhances resections of malignant gliomas and that enhanced resections are beneficial by translating into longer progression-free survival. Furthermore, even though the present study was not powered for demonstrating an increase in overall survival, patients in the FL group had a median survival exceeding patients in the WL arm of 15.2 versus 13.5 months. The difference failed to reach statistical significance, yet the crude hazards ratio of 0.81 clearly favored FGR. The benefit was more evident in older patients (> 55 years) and other predefined subgroups, but not in younger patients (< 55 years). However, these patients were exposed to a significantly higher number of additional therapies (repeat surgery, chemotherapy), more so if they were in the WL group. In this subgroup of patients, therefore, the imbalance in augmental therapies obviously diluted survival effects derived from initial surgery using 5-ALA. Viewed differently, young patients in the WL group were exposed to more therapy, yet their survival was comparable to FL patients.

When data of patients with versus without complete resections—irrespective of study arm—were grouped, superior survival of patients was demonstrated by these data if early postoperative MRI was devoid of residual enhancing tumor. An additional potential benefit of a maximal cytoreductive surgery was pointed out by a retrospective analysis of EORTC study 26981 on the use of radiochemotherapy with temozolomide versus radiotherapy alone.[13,14] The additional benefit of temozolomide in this study was most pronounced in patients with extensive resection (median survival advantage was 4.1 months after complete resection versus 1.8 months after partial resection).

Stereotactic PDT

From all our experience with 5-ALA-PDT gained so far in animal experiments and clinical trials, the risk of the induction of severe side effects by direct or indirect damage to healthy brain is minimal. Not even the formation of problematic edema has been observed clinically, although animal experiments had shown a measurable edema formation that only partly responded to steroid treatment.[15]

The selected light application parameters lead to a very high fluence within the tumor volume, comparable with a surface irradiation with 940 J/cm² (200 mW/cm² plane wave irradiance approximate yield 400 mW/cm² fluence rate at 3 mm depth). Because of the line source geometry instead of a plane wave irradiation, however, the effective fluence rate toward the tumor border and into the infiltration zone decreases more rapidly. Since we placed the applicators a penetration depth away from the contrast-enhancing tumor border, but intended to penetrate the infiltration zone at least one penetration depth deep, the high fluence used is necessary. The surface equivalent of 200 J/cm² is thus achieved at about 7 mm from the applicator surface, a bit more than one penetration depth inside the infiltration zone.

Conclusion

Fluorescence-guided resection of malignant glioma increases the completeness of tumor removal. Combined with PDT to the surgical cavity, a still very safe but ultimately complete destruction of tumor cells may be achieved. This treatment may prolong patient survival either by itself or by providing optimized conditions for adjuvant treatments. Interstitial 5-ALA-PDT may serve as a safe and effective treatment option for recurrent or even primary but otherwise inoperable glioblastoma.

Acknowledgments

We gratefully acknowledge the funding of part of the experimental work by the Deutsche Krebshilfe (70-2864-St), and financial support by the Medac Company in Wedel, Germany.

ALA-Glioma Study Group: F. Oppel, A. Brune (Krankenanstalten Gilead gGmbH, Bielefeld), W. Lanksch, C. Woiciechowsky (Virchow-Klinikum der HU Berlin), M. Brock, J. Vesper (Universitätsklinikum Benjamin Franklin, Berlin), J.-C. Tonn, C. Goetz (Universitätsklinikum München), J.M. Gilsbach, L. Mayfrank (Med. Einrichtungen der RWTH, Aachen), V. Seifert, K. Franz, A. Bink (J.W. Goethe Universitätsklinikum, Frankfurt a. M.), G. Schackert, T. Pinzer (Universitätsklinikum Carl Gustav Carus an der TU, Dresden), W. Hassler, A. Bani (Klinikum Duisburg gGmbH, Duisburg), H.-J. Meisel, B.C. Kern (Bergmannstrost Krankenhaus, Halle), H.M. Mehdorn, A. Nabavi (Universitätsklinikum Kiel), A. Brawanski, O.W. Ullrich (Klinikum der Universität –), D.K. Böker, M. Winking (Universitätsklinikum Giessen), F. Weber, U. Langenbach (Klinikum Saarbrücken), M. Westphal, U. Kähler (Universitätsklinikum Hamburg-Eppendorf), H. Arnold, U. Knopp (Med. Universität zu Lübeck), T. Grumme, T. Stretz (Zentralklinikum Augsburg), D. Stolke, H. Wiedemayer (Universitätsklinikum Essen), B. Turowski (Universitätsklinikum Düsseldorf), T. Pietsch (Universitätsklinikum Bonn).

References

1. Lacroix M, Abi-Said D, Fourney DR, Gokaslan ZL, Shi W, DeMonte F, Lang FF, McCutcheon IE, Hassenbusch SJ, Holland E, Hess K, Michael C, Miller D, Sawaya R. A multivariate analysis of 416 patients with glioblastoma multiforme: prognosis, extent of resection, and survival. J Neurosurg. 2001;95(2):190–8.
2. Nitta T, Sato K. Prognostic implications of the extent of surgical resection in patients with intracranial malignant gliomas. Cancer. 1995;75(11): 2727–31.
3. Albert FK, Forsting M, Sartor K, Adams HP, Kunze S. Early postoperative magnetic resonance imaging after resection of malignant glioma: objective evaluation of residual tumor and its influence on regrowth and prognosis. Neurosurgery. 1994; 34(1):45–60.
4. Stummer W, Novotny A, Stepp H, Goetz C, Bise K, Reulen HJ. Fluorescence-guided resection of glioblastoma multiforme by using 5-aminolevulinic

acid-induced porphyrins: a prospective study in 52 consecutive patients. J Neurosurg. 2000;93(6): 1003–13.

5. Friesen SA, Hjortland GO, Madsen SJ, Hirschberg H, Engebraten O, Nesland JM, Peng Q. 5-Aminolevulinic acid-based photodynamic detection and therapy of brain tumors (review). Int J Oncol. 2002;21(3):577–82.
6. Regula J, MacRobert AJ, Gorchein A, Buonaccorsi GA, Thorpe SM, Spencer GM, Hatfield AR, Bown SG. Photosensitisation and photodynamic therapy of oesophageal, duodenal, and colorectal tumours using 5 aminolaevulinic acid induced protoporphyrin IX--a pilot study. Gut 1995;36(1):67–75.
7. Stummer W, Stepp H, Moller G, Ehrhardt A, Leonhard M, Reulen HJ. Technical principles for protoporphyrin-IX-fluorescence guided microsurgical resection of malignant glioma tissue. Acta Neurochir (Wien). 1998;140(10):995–1000.
8. Olzowy B, Hundt CS, Stocker S, Bise K, Reulen HJ, Stummer W. Photoirradiation therapy of experimental malignant glioma with 5-aminolevulinic acid. J Neurosurg. 2002;97(4):970–6.
9. Beck TJ, Beyer W, Pongratz T, Stummer W, Waidelich R, Stepp H, Wagner S, Baumgartner R. Clinical determination of tissue optical properties in vivo by spatially resolved reflectance measurements. Proc.SPIE. 2003;5138:96–105.
10. Stummer W, Pichlmeier U, Meinel T, Wiestler OD, Zanella F, Reulen HJ. Fluorescence-guided surgery with 5-aminolevulinic acid for resection of malignant glioma: a randomised controlled multicentre phase III trial. Lancet Oncol. 2006; 7(5):392–401.
11. Madsen SJ, Angell-Petersen E, Spetalen S, Carper SW, Ziegler SA, Hirschberg H. Photodynamic therapy of newly implanted glioma cells in the rat brain. Lasers Surg Med. 2006;38(5):540–8.
12. Jalili A, Makowski M, Switaj T, Nowis D, Wilczynski GM, Wilczek E, Chorazy-Massalska M, Radzikowska A, Maslinski W, Bialy L, Sienko J, Sieron A, Adamek M, Basak G, Mroz P, Krasnodebski IW, Jakobisiak M, Golab J. Effective photoimmunotherapy of murine colon carcinoma induced by the combination of photodynamic therapy and dendritic cells. Clin Cancer Res. 2004;10(13):4498–508.
13. Mirimanoff RO, Gorlia T, Mason W, Van den Bent MJ, Kortmann RD, Fisher B, Reni M, Brandes AA, Curschmann J, Villa S, Cairncross G, Allgeier A, Lacombe D, Stupp R. Radiotherapy and temozolomide for newly diagnosed glioblastoma: recursive partitioning analysis of the EORTC 26981/22981-NCIC CE3 phase III randomized trial. J Clin Oncol. 2006;24(16):2563–9.
14. Van den Bent MJ, Stupp R, Mason W, Mirimanoff RO, Lacombe D, Gorlia T. Impact of extent of resection on overall survival in newly-diagnosed glioblastoma after chemo-irradiation with temozolomide: further analysis of EORTC study 26981. Eur J Cancer Suppl. 2005;3:134.
15. Ito S, Rachinger W, Stepp H, Reulen HJ, Stummer W. Oedema formation in experimental photoirradiation therapy of brain tumours using 5-ALA. Acta Neurochir (Wien). 2005;147(1):57–65.

Interstitial Photodynamic Therapy of Nonresectable Malignant Glioma Recurrences Using 5-Aminolevulinic Acid Induced Protoporphyrin IX

Tobias J. Beck, Friedrich W. Kreth, Wolfgang Beyer, Jan H. Mehrkens, Andreas Obermeier, Herbert Stepp, Walter Stummer, and Reinhold Baumgartner

Lasers Surg. Med. 39:386–393 (2007)

Lasers in Surgery and Medicine 39:386–393 (2007)

Interstitial Photodynamic Therapy of Nonresectable Malignant Glioma Recurrences Using 5-Aminolevulinic Acid Induced Protoporphyrin IX

Tobias J. Beck,[1]* Friedrich W. Kreth, MD,[2] Wolfgang Beyer, PhD,[1] Jan H. Mehrkens, MD,[2] Andreas Obermeier,[1] Herbert Stepp, PhD,[1] Walter Stummer, MD,[3] and Reinhold Baumgartner, PhD[1]

[1]*Laser Research Laboratory, Ludwig-Maximilians-University, Marchioninistr. 23, 81377 Munich, Germany*

[2]*Department of Neurosurgery, Ludwig-Maximilians-University, Marchioninistr. 15, 81377 Munich, Germany*

[3]*Department of Neurosurgery, Heinrich-Heine-University, Moorenstr. 5, 40225 Duesseldorf, Germany*

Background and Objective: Limited knowledge of the light and temperature distribution within the target volume in combination with non-selective accumulation of the applied photosensitizers (PS) has hampered the clinical relevance of interstitial photodynamic therapy (iPDT) for treatment of malignant glioma patients. The current pilot study focused on the development and the clinical implementation of an accurate and reproducible irradiation scheme for iPDT using 5-aminolevulinic acid (5-ALA) induced protoporphyrin IX (PPIX) as a selectively working PS.

Study Design/Materials and Methods: Monte Carlo simulations of fluence rate and heat transport simulations were performed using the optical properties of normal brain tissue infiltrated by tumor cells (absorption coefficient $\mu_a = 0.2\ cm^{-1}$, reduced scattering coefficient: $\mu'_s = 20\ cm^{-1}$). A modified 3-D treatment-planning software was used to calculate both, the treatment-volume and the exact position of the light diffusers within the lesion. The feasibility and the risk of iPDT were tested in 10 patients with small and circumscribed recurrent malignant gliomas.

Results: The optimum distance between the implanted light diffusers was determined to be 9 mm with regard to both fluence rate and temperature distribution. For this distance a temperature increase above 42°C was not expected to occur. Up to six cylindrical light diffusers were stereotactically implanted to achieve a complete irradiation of the tumor volume, which was possible in every single patient (mean tumor volume: 5.9 cm^3). The total applied light fluence was between 4,320 J and 11,520 J. Side effectsof iPDT were not observed. Median survival was 15 months.

Conclusion: 5-ALA iPDT in combination with a 3-D treatment-planning (which was based on optical and thermal simulations) is a safe and feasible treatment modality. The clinical impact of these findings deserves further prospective evaluation. Lasers Surg. Med. 39:386–393, 2007. © 2007 Wiley-Liss, Inc.

Key words: neurosurgery; photodynamic therapy; stereotactic; interstitial; intratumoral; light application; brain tumor; glioblastoma; 5-aminolevulinic acid; protoporphyrin IX; cylindrical diffuser; dosimetry

INTRODUCTION

Glioblastoma multiforme is the most common and most malignant primary brain tumor in humans and the overall prognosis for patients continues to be dismal. The median survival after tumor resection, external beam irradiation, and various forms of chemotherapy still lies in the range of 12 months [1,2]. Taken into account that tumor recurrences usually occur locally at the margin of previously treated tumor volumes [3,4], the improvement and further development of local treatment concepts such as photodynamic therapy (PDT) remains a matter of utmost importance [5–10].

Treatment effects of PDT are based on the accumulation of photosensitizing drugs (PS) in malignant tissue, which exert tumor-toxic properties after activation by light of an appropriate wavelength. A possibly minimally invasive way to apply the light to the sensitized tumor is to place light guiding fibers directly within the treatment volume. This treatment modality is referred to as interstitial photodynamic therapy (iPDT). Its feasibility and effectiveness has been investigated in brain tumor models [11,12] and in first clinical applications with Photofrin [13–16]. Unfortunately, prolonged skin sensitization and damage to normal brain tissue due to the limited selectivity of the applied PS (Photofrin or Photofrin II) have obstructed the broad application of this potentially minimal invasive treatment concept.

5-aminolevulinic acid (5-ALA) induced protoporphyrin IX (PPIX) has proven its high potential as a PS for PDT in several experimental studies [17–20] and has recently gained interest in neurosurgery [21,22] due to a selective tumor uptake and only minimal skin sensitization [23–25].

The current pilot study focused on the development of an accurate and reproducible irradiation scheme for the

Tobias J. Beck and Friedrich W. Kreth contributed equally to this work.

Contract grant sponsor: Deutsche Krebshilfe; Contract grant number: 70-2864.

*Correspondence to: Tobias J. Beck, Laser Research Laboratory, Ludwig-Maximilians-University, Marchioninistr. 23, 81377 Munich, Germany. E-mail: tbeck@med.uni-muenchen.de

Accepted 28 February 2007
Published online 18 June 2007 in Wiley InterScience (www.interscience.wiley.com).
DOI 10.1002/lsm.20507

5-ALA iPDT approach (e.g. optimal intratumoral fiber positioning and interfiber distance, applied fluence, fluence rate, and temperature distribution) and the feasibility of its clinical implementation. It was hypothesized that state of the art stereotactic techniques enabling both a 3-D-dosimetry and the optimal placement of the light guiding fibers in combination with a highly tumor selective PS such as 5-ALA induced PPIX would lead to controlled treatment effects and a significant reduction of the risk of the therapy. The feasibility and the risk of iPDT was analyzed in 10 patients with a circumscribed recurrence of a malignant glioma with a maximum diameter of 3 cm. The study protocol was approved by the institutional review board of the Ludwig-Maximilians-University, Klinikum Grosshadern, Munich.

MATERIALS AND METHODS

Technical Setup

The illumination was performed using a laser, a beam splitter, and light diffusers. The light source was a diode laser emitting light at a wavelength of $\lambda = 633$ nm with a maximum output power of 4 W (Ceralas PDT Diode Laser, biolitec AG, Jena, Germany). The laser light was coupled via a 400 μm fiber and a lens into a beam splitter with a variable number of output ports and variable output powers for each port. Up to six diffusers with variable diffuser lengths could be illuminated simultaneously with a constant power of 200 mW/cm.

Fiber-based cylindrical light diffusers were used as treatment fibers (CD403, CeramOptec GmbH, Bonn, Germany). The diffuser tips had an outer diameter of $d = 1.6$ mm and a radiation length of $l = 20$ mm or $l = 30$ mm (CD403-20 and CD403-30, respectively, Fig. 1). Depending on the tumor geometry, the 20 mm or 30 mm diffusers were used. The spatial light distribution of both diffuser lengths used is given in Figure 1. The light intensity distribution measured along the radiating zone was nearly homogeneous. X-ray markers on both ends of the radiating zone enable an X-ray controlled positioning.

Determination of the Irradiation Scheme

Pre-operatively, the temperature distribution was calculated with a commercial Monte Carlo-based simulation program using interfiber distances between 7 and 9 mm (LITCIT 32, LMTB GmbH, Berlin, Germany) [26]. In the LITCIT simulations, four cylindrical light diffusers were positioned at the edges of a square. The light power emitted from the diffusers was set to 200 mW/cm diffuser length, which had been already used for iPDT of malignant glioma by Powers et al. [13]. Optical tissue parameters for glioblastoma recurrences were not available. Instead, the optical properties of normal brain tissue infiltrated by tumor cells (BAT) were used [27], as a model for a multimodally treated malignant glioma. These parameters are similar to in-vivo measurements performed by Muller and Wilson [28,29]. The absorption coefficient μ_a was set to 0.2 cm^{-1} and the reduced scattering coefficient μ'_s to 20 cm^{-1}, resulting in an optical penetration depth (δ_{eff}) of

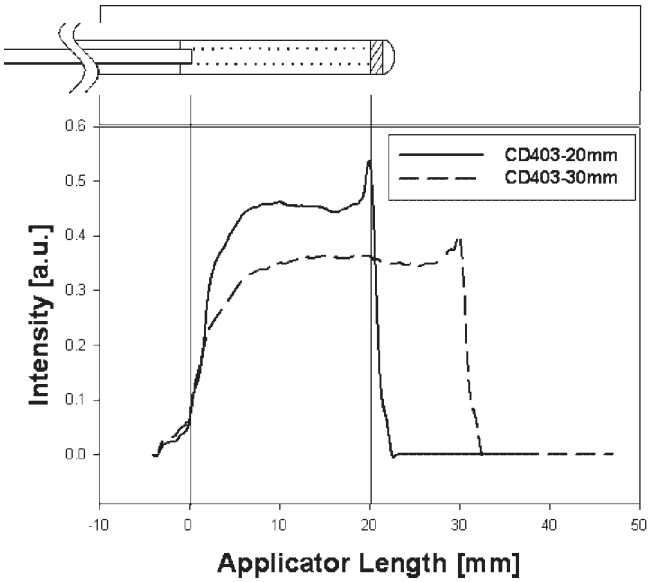

Fig. 1. Top: Cross section of the applicator CD403-20 including X-ray marker at the distal end. Bottom: Radiation profile of the two applicator types, l = 20 mm (—) and l = 30 mm (- - -).

3 mm ($\delta_{eff} = (3\mu_a(\mu_a+\mu'_s))^{-1/2}$). The relevant heat transport parameters were set as follows: initial tissue temperature: 37C, blood perfusion: 0.5 ml/(g · minute), water content: 75%, heat conductivity: 0.0048 W/(cm · K), heat capacity: 3.4882 J/(g · K), density: 1.075 g/cm^3 [26].

The fluence rate distribution was calculated with Monte Carlo simulations based on the algorithm of Prahl [30], using the optical parameters of BAT. Results were obtained by simulating 1,000,000 histories with a running time of some 30 minutes on an Intel Pentium M at 1400 MHz with 512 MB RAM. The fluence rate levels were simulated for one single diffuser. The fluence rate distribution in between two or more fibers could be deduced from these results by summing up the contributions of each single fiber.

Light Fluence

The threshold light fluence necessary to induce a significant phototoxic effect in malignant glioma tissue has still not been defined for the 5-ALA-iPDT approach. Clinical protocols for surface irradiation with 5-ALA-PDT usually operate with fluences in the range of 100 J/cm^2. Excessive photobleaching of the PS occurs at this fluence, and further irradiation should not be associated with a significant increase of phototoxicity. Therefore, the irradiation time was only limited with respect to the duration and invasiveness of the surgical procedure; side effects due to an excessive fluence were not expected. One hour was considered an appropriate irradiation time. The resulting total fluence and the fluence per tumor volume were calculated with the light power of 200 mW/cm diffuser length.

Patient Selection

Adult patients with a circumscribed recurrence of a malignant glioma with a maximum diameter of 3 cm (as defined by gadolinium enhanced T1 weighted magnetic

resonance imaging (MRI)) and a Karnofsky Score (KPS) of at least 70 were considered eligible for the study. A confirmatory stereotactic biopsy was required for all patients.

Stereotactic Treatment Planning

Treatment planning was based on multimodal imaging data: image fusion of the stereotactically localized computerized tomography (CT) scans (contrast enhanced scans, 2 mm slices), with additional MRI (T1 weighted gadolinium enhanced scans, 1 mm slices, T2-weighted scans, 2 mm slices), and FET-PET (*O*-(2-[18F]fluoroethyl)-L-tyrosine—positron emission tomography) scans were done for optimal visualization of the tumor and exact definition of the treatment volume (Image Fusion Software, BrainLAB AG, Heimstetten, Germany).

Irradiation planning was performed with the @target 1.19 software (BrainLAB AG). This program was originally designed for the planning of stereotactic biopsy trajectories and Iodine-125 seed implantation. An additional feature is the 3-D tumor demarcation and calculation of the tumor volume. It supports also the placement of treatment catheters within the tumor under full 3-D control of their position within the brain.

Stereotactic Surgery

One hour prior to surgery, patients received 20 mg/kg body weight 5-ALA (medac GmbH, Wedel, Germany) dissolved in 100 ml water orally. This dose is well tolerated and associated with strong fluorescence in malignant glioma [24]. All patients were treated under general anesthesia. Intraoperatively, the oxygen saturation was set to 100% in order to prevent a possible lack of cellular oxygen due to oxygen consumption during the treatment [31,32].

The output power of each diffuser was controlled with an integrating sphere. All fibers had an X-ray marker and the accuracy of the stereotactic implantation procedure was checked online during the operation with an orthogonal X-ray technique using a C-arm. The inserted fibers were fixed at the entry point with a fiber clip to avoid displacement.

Patient Evaluation

The first postoperative MRI investigation (T1/T2, with/without gadolinium) was done at day one after surgery for assessment of early treatment effects. Further clinical and neuroradiological follow-up was performed 1 month postoperatively and from then on at 3-month intervals at the outpatient clinic. Length of survival was calculated with the Kaplan–Meier-method.

RESULTS

Irradiation Scheme

Heat transport simulations were performed using interfiber distances between 7 and 9 mm. At an interfiber distance of 7 mm the temperature in the vicinity of a diffuser increased up to 42°C, whereas an interfiber distance of 9 mm resulted in a maximum temperature in the range of 41°C (Fig. 2). For this distance, further simulations with unfavorable parameter combinations (variations of absorption and scattering coefficients and heat transport parameters of up to 20%) were performed and did not result in a temperature increase above 42°C. Therefore, a distance of 9 mm seems to be sufficient in order to prevent unfavorable temperature increase within the irradiated tissue. Thus, further treatment planning was based on this interfiber distance.

The fluence rate levels around a single diffuser were calculated with a Monte Carlo program. Figure 3 shows the resulting iso-fluence rates when the applicator has a diffuser length of 2 cm and emits 200 mW/cm. The fluence rate at a distance of 4.5 mm from the applicator's surface is 260 mW/cm^2. Thus, in between two diffusers at an interfiber distance

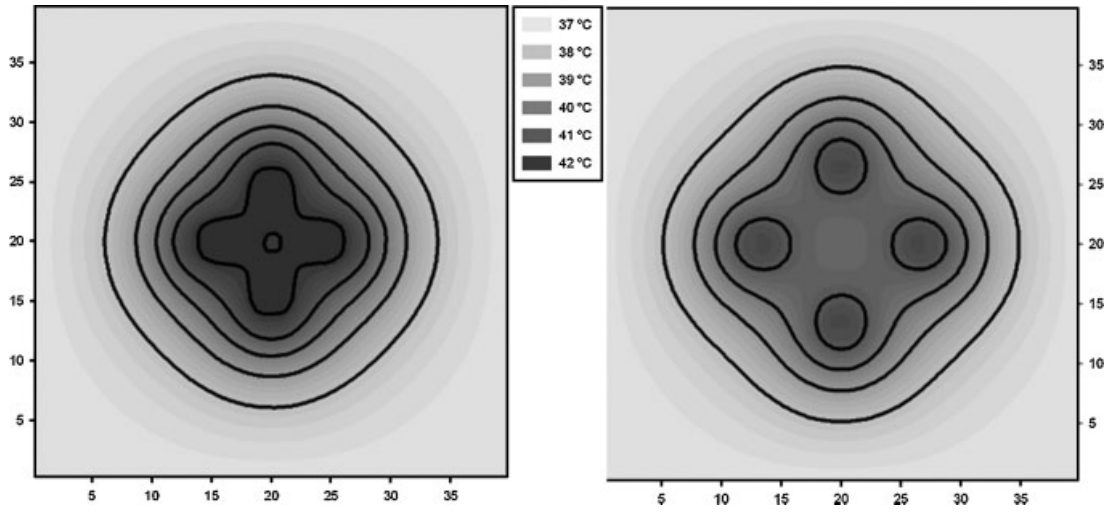

Fig. 2. Temperature distribution within the irradiated tissue according to LITCIT simulations at an interfiber distance of 7 mm (left) and 9 mm (right).

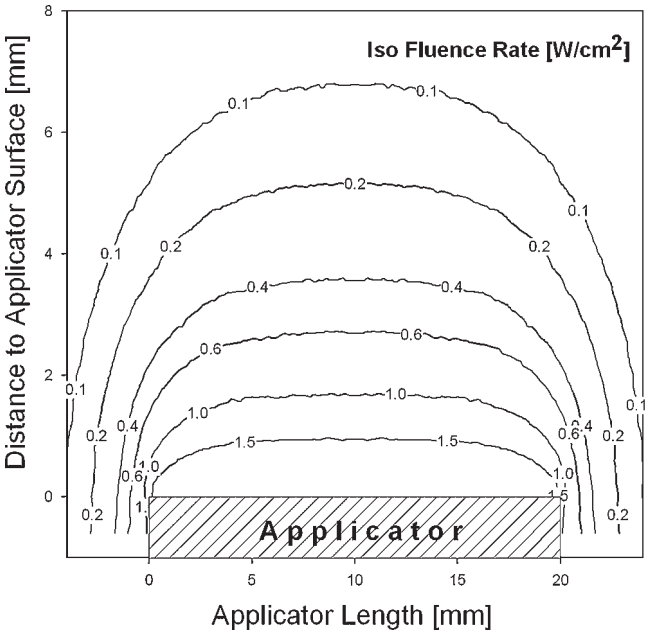

Fig. 3. Iso-fluence rates of a cylindrical light diffuser calculated by Monte-Carlo simulations.

of 9 mm, the fluence rates of both diffusers add to a total fluence rate of 520 mW/cm^2. This value was set to be the threshold value, which should also be obtained at the tumor margin, where, to a first approximation, only one light diffuser illuminates the tissue. As can be seen in Figure 3, 520 mW/cm^2 is obtained at a distance of about 3 mm from the applicator's surface. Accordingly, 3-D treatment planning is based on the maximum distance between the applicator's surface and the tumor margin. Due to the fast decrease of the fluence rate with increasing distance from the light diffuser (Fig. 3), an approximately 1.5 mm increased distance from the tumor border or interfiber distance reduces the available fluence rate by a factor of 2.

As the irradiation time was set to be 1 hour (as described above), a minimum fluence of 1,870 J/cm^2 was obtained at the tumor margin and in between the two diffusers. The light fluence per diffuser length was 720 J/cm. Irradiation parameters are listed in Table 1. The total applied light fluence depended on the number and length of the inserted light diffusers and was between 4,320 J and 11,520 J (mean: 7,212 J).

Treatment Implementation

The irradiation volume was estimated and visualized using the @target 1.19 software: A cylindrical irradiation volume with a diameter of 7.6 mm (radial distance from diffuser surface: 3 mm; diffuser diameter: 1.6 mm) was generated around each diffuser used and the corresponding iso-fluence was displayed in axial, sagittal, and coronar projections. It was aimed to overlap the entire treatment volume with these treatment cylinders. Taken into account the calculated optimal inter-fiber distance of 9 mm, only a minimal overlapping of the cylindrical irradiation volumes was allowed. Special care was taken that the stereotactically defined trajectories for fiber implantation run parallel to each other. In case of a complete irradiation of the treatment volume it could be expected that the fluence rate exceeded 520 mW/cm^2. A typical screen shot of the 3-D planning program is shown in Figure 4.

Feasibility and Risk of iPDT

During a 1-year period (October 2002–2003) 10 patients were included in the current pilot study. The median age was 54 years (range 31–72 years). Tumor volumes ranged between 2.1 and 10.2 cm^3 (mean: 5.9 cm^3) and the total volume light fluence ranged between 939 and 2,304 J/cm^3 (mean: 1,405 J/cm^3) (Table 1). A complete irradiation of the tumor volume was possible in all of these patients using four to six fibers per patient. The accuracy of the final fiber position (as compared to the original treatment plan) was in the range of 2 mm, as judged by X-ray control. Perioperative morbidity was not observed. A symptomatic early or delayed treatment induced edema did not occur during the follow-up period and steroid medication was only applied perioperatively (during the first 3 days after surgery).

TABLE 1. Patient Characteristics, Treatment Parameters, and Survival of the 10 Patients Included in the Pilot Study

Patient ID	Age	KPS pre-Op	Tumorlocation	Side	Tumor volume (ccm)	Total light fluence (J)	Volume light fluence (J/ccm)	Survival time (months)
1	31	100	Frontal	Left	6.9	7,200	1043	49
2	69	80	Parietal	Right	4.8	5,700	1188	4
3	72	90	Temporal	Right	4.5	7,500	1667	11
4	42	90	Fronto-temporal	Left	2.1	4,320	2057	32
5	54	90	Parietal	Right	6.3	6,600	1048	7
6	54	100	Frontal	Left	10.2	11,520	1129	5
7	56	80	Fronto-temporal	Left	9.9	10,080	1018	39
8	57	90	Parietal	Left	2.9	4,800	1655	27
9	32	80	Frontal	Left	9.2	8,640	939	17
10	50	90	Temporal	Right	2.5	5,760	2304	13

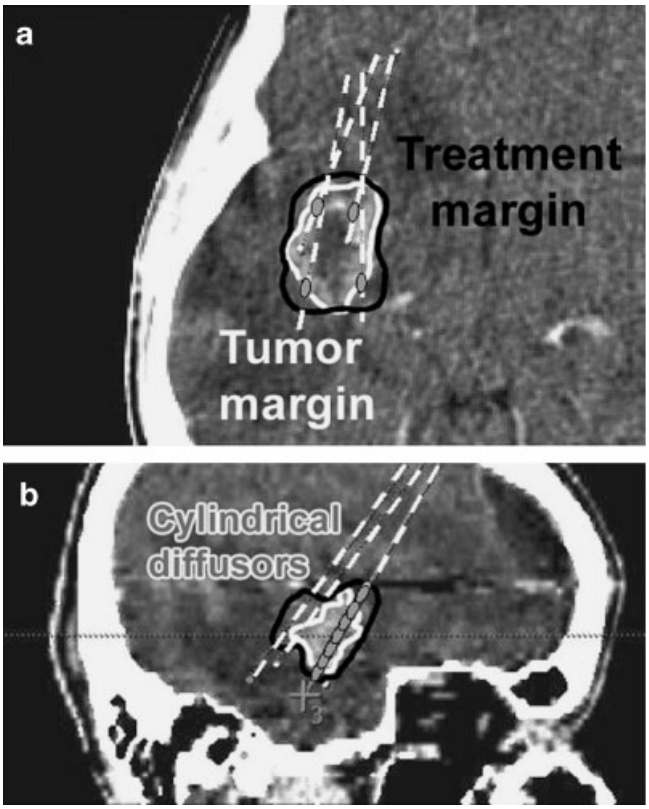

Fig. 4. Screen shot of the 3-D-planning showing excellent agreement between the estimated treatment margin (black line) and the tumor margin (white line). Axial plane (**a**) and sagittal plane (**b**).

MRI Follow-Up After iPDT

Early postoperative MRI (at day 1 after surgery) showed a complete resolution of the contrast enhancement of the treated lesion in seven patients and a partial resolution in the other three. Typically, transient contrast enhancement was seen again at day 7 after treatment at the boundary of the treatment volume. It was accompanied by a moderate increase of the peri-lesional edema, which slowly resolved spontaneously during the first 3 months after surgery. A representative example is given in Figure 5.

Survival

The 1-year-survival rate was 60% (median survival: 15 months). Four patients lived longer than 24 months and two of them are still alive (Fig. 6). Last follow-up evaluation revealed a high KPS of the survivors ($\geq$80).

DISCUSSION

A prerequisite for iPDT as a possible minimal invasive treatment option for selected patients with a circumscribed malignant glioma recurrence (after previously applied standard therapy) is the application of a PS with a selective tumor uptake and the availability of an accurate and reproducible irradiation scheme. In the current study an irradiation scheme was developed on the basis of theoretical models and the feasibility of its clinical implementation was tested thereafter. It was hypothesized that the combination of a new and selectively working PS (5-ALA induced PPIX) with stereotactic techniques enabling both a 3-D-dosimetry and optimal placement of the laser fibers thereafter would lead to controlled treatment effects.

Photosensitizer

Inefficient tumor control and severe side effects of the therapy have been described for iPDT if it is based on

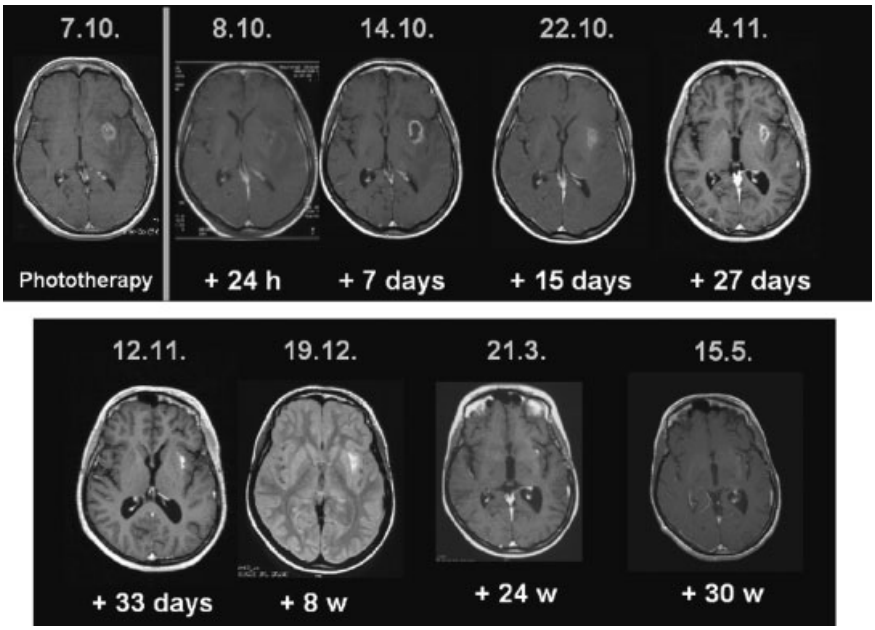

Fig. 5. Series of contrast-enhanced MRI-scans (T1 weighted) of a patient treated with iPDT.

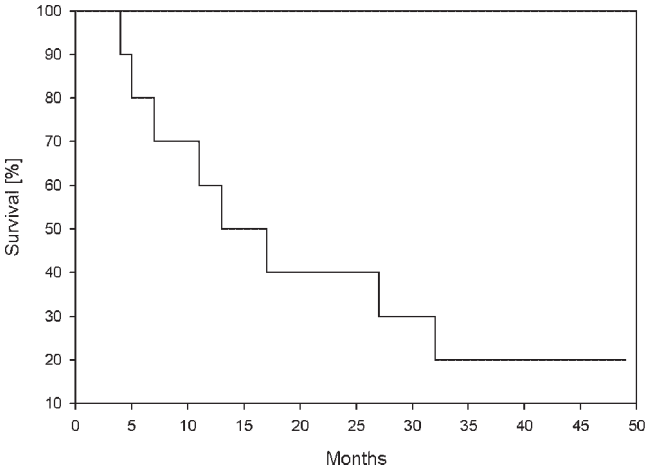

Fig. 6. Kaplan–Meier survival curve for survival post-iPDT calculated from date of surgery of the 10 patients included in the pilot-study.

synthetic porphyrins such as hematoporphyrin derivative (HpD) or Photofrin®. For example, five out of eight glioblastoma patients treated by Powers et al. [13] had a recurrence within two months after iPDT (using Photofrin®), while at the same time all patients suffered from treatment-induced edema and prolonged skin sensitization. Similar results have been reported by other groups [15,16].

Unselective effects of HpD and Photofrin® were also described in animal studies [12,33–37] and have been related to both the inhomogeneous distribution of the PS within the tumors and extensive leakage of the PS to the surrounding normal tissue (via peritumoral edema bulk flow). PDT by means of 5-ALA induced PPIX is expected to induce less often and less severe side effects for several reasons: (1) The drug applied systemically (5-ALA) is itself not phototoxic, (2) 5-ALA induced PPIX has been shown to accumulate selectively within the tumor, and (3) a significant redistribution of the PS by peritumoral edema bulk flow does not seem to occur. Olzowy et al. [17], for example, who investigated treatment effects of PDT by means of 5-ALA induced PPIX in an experimental glioma model, found selective phototoxic effects within the tumor (coagulative or hemorrhagic necrosis), whereas the damage to the normal or perifocal edematous tissue was negligible. Exactly these favorable characteristics of 5-ALA have led to a re-evaluation of iPDT as a potentially minimal invasive treatment modality and are an important prerequisite for accurate treatment planning.

Irradiation Scheme and Treatment Planning

A reproducible irradiation scheme for iPDT with 5-ALA induced PPIX has not been provided in the literature so far. Thus, uncertainties persist as to the temperature and light distribution within the treatment volume and the appropriate total light fluence.

In a first step, it was aimed to determine an interfiber distance that reliably excludes tissue heating beyond the 42°C level. Light dosimetry—in a second step—was mainly determined by clinical parameters such as the duration and invasiveness of the surgical procedure. A treatment time in the range of 1 hour was considered to be appropriate. Due to the selectivity of the applied PS and its photobleaching with fluences in the range of 100 J/cm^2,side effects due to an excessive fluence were not expected to occur and an upper limit for the applied fluence was therefore not considered necessary to define.

Temperature and light distributions during iPDT were analyzed by Monte-Carlo simulations and then indirectly validated by clinical data. Online measurements were not performed. The significance of such online measurements might be limited due to heterogeneous optical penetration depths within the tumor and the brain/tumor interface [28] and inaccurate position measurements of the implanted sensors. Moreover, the interstitial placements of sensors might be associated with an additional risk for the patient. Therefore, simulations were preferred in the current study. As optical parameters for malignant glioma recurrences are not available, the optical properties of BAT were used, which might be considered an adequate model for a mutimodally treated glioma; based on this model, different sets of input parameters were tested to check for the effects of a possible heterogeneity.

As expected, the LITCIT simulations showed that the degree of temperature increase within the treatment volume depended on the interfiber distance. An inter-fiber distance of 9 mm did not result in a temperature increase above 42°C even in the case of unfavorable input parameters and was therefore judged to be safe. A larger distance between the fibers is not advisable, as the steep decrease of the fluence rate from the fiber surface has to be compensated with much longer irradiation times.

With an interfiber distance of 9 mm, a distance from fibers to tumor margin of 3 mm, a light power of 200 mW/cm diffuser length, and a treatment time of 1 hour, the individually applied total fluence can be calculated depending on the number of diffusers. At the tumor margin, which is one penetration depth away from the light diffusers, a fluence of 1,870 J/cm^2 can be expected. This fluence may appear very high as compared to fluences commonly used in plane wave irradiation [10,38]. However, the fluence in cylindrical light diffuser irradiation decreases more rapidly to the periphery than in plane wave irradiation: The fluence at a distance of 6 mm (one penetration depth outside the treatment volume) from the applicator's surface decreases to a value of 400 J/cm^2 and equals the fluence obtained in 3 mm depth in plane wave irradiation using a fluence rate of 200 mW/cm^2 and a treatment time of 1,000 seconds. These estimations imply that high fluences must be expected to be applied to the adjacent normal brain tissue outside the treatment volume. However, due to the absence of a significant photosensitization of normal brain tissue as a consequence of a selectively working PS [23], significant side effects of the 5-ALA iPDT approach were not expected to occur.

To confirm the results of the Monte-Carlo simulations, online measurements of temperature, fluence rate, PS

concentration, and oxygenation would be helpful. Johansson et al. [39] presented such an online measurement system, which has been validated in animal studies. Thompson et al. [40] lately reported about a novel approach for a therapy system with combined on-line dosimetry, being able to monitor fluence rate, sensitizer fluorescence, and oxygenation. These combined systems seem to have a high potential for a reliable treatment dosimetry in iPDT. However, the fibers used in these systems were bare fibers and thus, the described computer model cannot be easily adapted to cylindrical diffusers used in the current study.

Clinical Implementation

An image-based computer-assisted protocol for iPDT of intracranial neoplasms has been already described by Origitano and Reichman [14]. Photoactivation was done intracavitarily or interstitially by inserting multiple fibers using the PS Photofrin-II. Even though the authors demonstrated the successful clinical implementation of their system within the framework of a phase I study, they did not provide data concerning the optimal interfiber distance, the corresponding temperature and light distributions, and the side effects of the applied therapy. In the present study, the customized 3-D planning software proved to be very useful for the determination of the exact fiber positions within the tumor volume. The accuracy of the final fiber position was always in the range of 2 mm and the treatment volume matched accurately the tumor volume in every single patient of this series. However, both the treatment-planning and stereotactic implantation procedure turned out to be complex and rather time consuming. The development of a computer-based optimization algorithm is therefore desirable and would help to simplify and standardize the planning procedure.

Imaging Changes After iPDT

The radiographic changes observed in the 10 treated patients were impressive with early MRI (within 24 hour) follow-up showing a complete resolution of the contrast-enhanced lesion in seven patients (a representative example is given in Fig. 5) and a partial response in the other three. This very early response might be explained by a treatment induced swelling of endothelial cells leading to a temporary "sealing" of the blood-brain-barrier (BBB). However, later MRI-scans (approximately after 1 week) showed a recurrent contrast enhancement at the boundary of the treatment volume indicating a transient leakage in the BBB, which was accompanied by moderate increase of the peri-lesional edema.

Median survival was 15 months in the current series and four patients lived longer than 24 months. Generally, a median survival in the range of 6–8 months is expected for patients with malignant glioma recurrences. Whether the encouraging survival data of this series should be related to effects of patient selection, treatment efficacy or both could not be resolved at this moment. Beyond direct phototoxic effects of iPDT (such as apoptosis and necrosis) activation of the immune response after PDT has been reported (e.g., increased expression of heat shock proteins), which deserves further experimental and clinical evaluation [41–43].

Risk of iPDT

The total applied light fluences in this study (4,320–11,520 J) are very high, yet there was no surgery or treatment-related morbidity or mortality in our patient series, whereas Krishnamurty [15] reported about increased risk of neurologic injury and permanent deficits at a total applied light dose above 4,000 J as compared to light doses between 3,700 and 4,000 J after administration of Photofrin®. In our patient series there was no enhanced treatment-induced brain edema and steroid medication was only applied for 3 days as routinely done in other stereotactic procedures in our institution. The absence of side effects supports the concept of a selectively working PS such as 5-ALA induced PPIX and the postulated implications of the applied irradiation scheme: Significant treatment-induced hyperthermia (42°C or more) and/or unwanted accumulation and activation of 5-ALA outside the tumor tissue apparently did not occur.

SUMMARY AND PERSPECTIVE

The intention of the present study was to establish an implementation concept for iPDT with 5-ALA-induced PPIX for minimally invasive treatment of patients with small malignant glioma recurrences. The development of a 3-D treatment-planning was based on optical and thermal simulations. A modus operandi was established to implant stereotactically up to six cylindrical light diffusers within the tumor in accordance with the created treatment plan. This treatment procedure ensured a minimum threshold light fluence within the entire tumor thereby avoiding significant hyperthermia (42°C or higher). Clinical implementation and outcome support the theoretical assumptions used for the determination of the irradiation and the postulated selective uptake of 5-ALA-induced PPIX: No side effects of the therapy were observed during the follow-up period. A further (prospective) clinical evaluation with a greater patient cohort is needed, which is the subject of an ongoing study at our institution.

REFERENCES

1. Shapiro WR, Green SB, Burger PC, Mahaley MS Jr, Selker RG, VanGilder JC, Robertson JT, Ransohoff J, Mealey J, Jr., Strike TA. Randomized trial of three chemotherapy regimens and two radiotherapy regimens and two radiotherapy regimens in postoperative treatment of malignant glioma. Brain Tumor Cooperative Group Trial 8001. J Neurosurg 1989; 71:1–9.
2. Jemal A, Tiwari RC, Murray T, Ghafoor A, Samuels A, Ward E, Feuer EJ, Thun MJ. Cancer statistics, 2004. CA Cancer J Clin 2004;54:8–29.
3. Bashir R, Hochberg F, Oot R. Regrowth patterns of glioblastoma multiforme related to planning of interstitial brachytherapy radiation fields. Neurosurgery 1988;23:27–30.
4. Albert FK, Forsting M, Sartor K, Adams HP, Kunze S. Early postoperative magnetic resonance imaging after resection of malignant glioma: Objective evaluation of residual tumor and its influence on regrowth and prognosis. Neurosurgery 1994; 34:45–60.

5. Kostron H, Obwegeser A, Jakober R. Photodynamic therapy in neurosurgery: A review. J Photochem Photobiol B 1996; 36:157–168.
6. Popovic EA, Kaye AH, Hill JS. Photodynamic therapy of brain tumors. J Clin Laser Med Surg 1996;14:251–261.
7. Muller PJ, Wilson BC. Photodynamic therapy of malignant brain tumours. Can J Neurol Sci 1990;17:193–198.
8. Muller PJ, Wilson BC. Photodynamic therapy for malignant newly diagnosed supratentorial gliomas. J Clin Laser Med Surg 1996;14:263–270.
9. Origitano TC, Caron MJ, Reichman OH. Photodynamic therapy for intracranial neoplasms. Literature review and institutional experience. Mol Chem Neuropathol 1994;21: 337–352.
10. Stylli SS, Kaye AH, Macgregor L, Howes M, Rajendra P. Photodynamic therapy of high grade glioma—long term survival. J Clin Neurosci 2005;12:389–398.
11. Lilge L, Olivo MC, Schatz SW, MaGuire JA, Patterson MS, Wilson BC. The sensitivity of normal brain and intracranially implanted VX2 tumour to interstitial photodynamic therapy. Br J Cancer 1996;73:332–343.
12. Hebeda KM, Kamphorst W, Sterenborg HJCM, Wolbers JG. Damage to tumour and brain by interstitial photodynamic therapy in the 9L rat tumour model comparing intravenous and intratumoral administration of the photosensitiser. Acta Neurochir 1998;140:495–501.
13. Powers SK, Cush SS, Walstad DL, Kwock L. Stereotaxic intratumoral photodynamic therapy for recurrent malignant brain-tumors. Neurosurgery 1991;29:688–696.
14. Origitano TC, Reichman OH. Photodynamic therapy for intracranial neoplasms: Development of an image-based computer-assisted protocol for photodynamic therapy of intracranial neoplasms. Neurosurgery 1993;32:587–595.
15. Krishnamurthy S, Powers SK, Witmer P, Brown T. Optimal light dose for interstitial photodynamic therapy in treatment for malignant brain tumors. Lasers Surg Med 2000;27:224–234.
16. Schmidt MH, Meyer GA, Reichert KW, Cheng J, Krouwer HG, Ozker K, Whelan HT. Evaluation of photodynamic therapy near functional brain tissue in patients with recurrent brain tumors. J Neurooncol 2004;67:201–207.
17. Olzowy B, Hundt CS, Stocker S, Bise K, Reulen HJ, Stummer W. Photoirradiation therapy of experimental malignant glioma with 5-aminolevulinic acid. J Neurosurg 2002;97: 970–976.
18. Madsen SJ, Sun CH, Tromberg BJ, Wallace VP, Hirschberg H. Photodynamic therapy of human glioma spheroids using 5- aminolevulinic acid. Photochem Photobiol 2000;72:128–134.
19. Hirschberg H, Sun CH, Tromberg BJ, Madsen SJ. ALA- and ALA-ester-mediated photodynamic therapy of human glioma spheroids. J Neurooncol 2002;57:1–7.
20. Madsen SJ, Sun CH, Tromberg BJ, Hirschberg H. Repetitive 5-aminolevulinic acid-mediated photodynamic therapy on human glioma spheroids. J Neurooncol 2003;62:243–250.
21. Friesen SA, Hjortland GO, Madsen SJ, Hirschberg H, Engebraten O, Nesland JM, Peng Q. 5-Aminolevulinic acid-based photodynamic detection and therapy of brain tumors (Review). Int J Oncol 2002;21:577–582.
22. Stepp H, Beck T, Beyer W, Pongratz T, Sroka R, Baumgartner R, Stummer W, Olzowy B, Mehrkens JH, Tonn JC, Reulen HJ. Fluorescence-guided resections and photodynamic therapy for malignant gliomas using 5-aminolevulinic acid. Proc SPIE 2005;5686:547–557.
23. Stummer W, Stocker S, Wagner S, Stepp H, Fritsch C, Goetz C, Goetz AE, Kiefmann R, Reulen HJ. Intraoperative detection of malignant gliomas by 5-aminolevulinic acid-induced porphyrin fluorescence. Neurosurgery 1998;42:518–525.
24. Stummer W, Novotny A, Stepp H, Goetz C, Bise K, Reulen HJ. Fluorescence-guided resection of glioblastoma multiforme by using 5- aminolevulinic acid-induced porphyrins: A prospective study in 52 consecutive patients. J Neurosurg 2000;93:1003–1013.
25. Stummer W, Pichlmeier U, Meinel T, Wiestler OD, Zanella F, Reulen HJ. Fluorescence-guided surgery with 5-aminolevulinic acid for resection of malignant glioma: A randomised controlled multicentre phase III trial. Lancet Oncol 2006;7:392–401.
26. Laser- und Medizin-Technologie gGmbH B. LITCIT: Technical Reference Manual; Version 4.8. LMTB 1998.
27. Beck TJ, Beyer W, Pongratz T, Stummer W, Waidelich R, Stepp H, Wagner S, Baumgartner R, Clinical determination of tissue optical properties in vivo by spatially resolved reflectance measurements. Proc SPIE 2003;5138:96–105.
28. Muller PJ, Wilson BC. An update on the penetration depth of 630 nm light in normal and malignant human brain tissue in vivo. Phys Med Biol 1986;31:1295–1297.
29. Wilson BC, Muller PJ. Instrumentation and light dosimetry for intraoperative photodynamic therapy (PDT) of malignant brain-tumors. Phys Med Biol 1986;31:125–133.
30. Prahl SA, Keijzer M, Jacques SL, Welch AJ. A Monte Carlo model of light propagation in tissue. In: Dosimetry of laser radiation in medicine and biology, Mueller G, Sliney D, Eds., SPIE Institute Series. 1989; IS 5:102–111.
31. Curnow A, Haller JC, Bown SG. Oxygen monitoring during 5-aminolaevulinic acid induced photodynamic therapy in normal rat colon. Comparison of continuous and fractionated light regimes. J Photochem Photobiol B 2000;58:149–155.
32. Pogue BW, O'Hara JA, Goodwin IA, Wilmot CJ, Fournier GP, Akay AR, Swartz H, Tumor PO2 changes during photodynamic therapy depend upon photosensitizer type and time after injection. Comp Biochem Physiol A Mol Integr Physiol 2002;132:177–184.
33. Chen Q, Chopp M, Madigan L, Dereski MO, Hetzel FW. Damage threshold of normal rat brain in photodynamic therapy. Photochem Photobiol 1996;64:163–167.
34. Dereski MO, Chopp M, Chen Q, Hetzel FW. Normal brain-tissue response to photodynamic therapy—histology, vascular-permeability and specific-gravity. Photochem Photobiol 1989;50:653–657.
35. Whelan HT, Schmidt MH, Segura AD, McAuliffe TL Bajic DM, Murray KJ, Moulder JE, Strother DR, Thomas JP, Meyer GA. The role of photodynamic therapy in posterior fossa brain tumors. A preclinical study in a canine glioma model. J Neurosurg 1993;79:562–568.
36. Stummer W, Gotz C, Hassan A, Heimann A, Kempski O. Kinetics of Photofrin II in perifocal brain edema. Neurosurgery 1993;33:1075–1081.
37. Stummer W, Hassan A, Kempski O, Goetz C. Photodynamic therapy within edematous brain tissue: Considerations on sensitizer dose and time point of laser irradiation. J Photochem Photobiol B 1996;36:179–181.
38. Ericson MB, Sandberg C, Stenquist B, Gudmundson F, Karlsson M, Ros AM, Rosen A, Larko O, Wennberg AM, Rosdahl I. Photodynamic therapy of actinic keratosis at varying fluence rates: Assessment of photobleaching, pain and primary clinical outcome. Br J Dermatol 2004;151:1204–1212.
39. Johansson T, Thompson MS, Stenberg M, af Klinteberg C, Engels SA, Svanberg S, Svanberg K. Feasibility study of a system for combined light dosimetry and interstitial photodynamic treatment of massive tumors. Applied Optics 2002;41:1462–1468.
40. Thompson MS, Johansson A, Johansson T, Andersson-Engels S, Svanberg S, Bendsoe N, Svanberg K. Clinical system for interstitial photodynamic therapy with combined on-line dosimetry measurements. Appl Opt 2005;44:4023–4031.
41. van Duijnhoven FH, Aalbers RI, Rovers JP, Terpstra OT, Kuppen PJ. The immunological consequences of photodynamic treatment of cancer, a literature review. Immunobiology 2003;207:105–113.
42. Jalili A, Makowski M, Switaj T, Nowis D, Wilczynski GM, Wilczek E, Chorazy-Massalska M, Radzikowska A, Maslinski W, Bialy L, Sienko J, Sieron A, Adamek M, Basak G, Mroz P, Krasnodebski IW, Jakobisiak M, Golab J. Effective photoimmunotherapy of murine colon carcinoma induced by the combination of photodynamic therapy and dendritic cells. Clin Cancer Res 2004;10:4498–4508.
43. Korbelik M, Sun J, Cecic I. Photodynamic therapy-induced cell surface expression and release of heat shock proteins: relevance for tumor response. Cancer Res 2005;65:1018–1026.

Long-sustaining response in a patient with non-resectable, distant recurrence of glioblastoma multiforme treated by interstitial photodynamic therapy using 5-ALA: case report

Walter Stummer, Tobias Beck, Wolfgang Beyer, Jan Hendrik Mehrkens, Andreas Obermeier, Nima Etminan, Herbert Stepp, Jörg-Christian Tonn, Reinhold Baumgartner, Jochen Herms, Friedrich Wilhelm Kreth

J Neurooncol (2008) 87:103–109

J Neurooncol (2008) 87:103–109
DOI 10.1007/s11060-007-9497-x

CLINICAL-PATIENT STUDIES

Long-sustaining response in a patient with non-resectable, distant recurrence of glioblastoma multiforme treated by interstitial photodynamic therapy using 5-ALA: case report

Walter Stummer · Tobias Beck · Wolfgang Beyer · Jan Hendrik Mehrkens · Andreas Obermeier · Nima Etminan · Herbert Stepp · Jörg-Christian Tonn · Reinhold Baumgartner · Jochen Herms · Friedrich Wilhelm Kreth

Received: 5 October 2007 / Accepted: 6 November 2007 / Published online: 23 November 2007

Abstract Glioblastoma multiforme continues to be a devastating disease despite modest improvements in survival achieved at present, and there is an urgent need for innovative treatment concepts. Five-aminolevulinic acid (ALA) is a drug which induces protoporphyrin IX accumulation in malignant gliomas and has been explored for fluorescence-guided resections of these tumors. ALA is also under investigation as a photosensitizer. We report a case of a patient with prior left frontal glioblastoma multiforme treated by surgery, radiation and chemotherapy, who developed a remote lesion in the left insula, which was refractory to secondary treatments. In a compassionate use setting she was treated by oral application of ALA (20 mg/kg bodyweight), and stereotactic phototherapy achieved by positioning four laser diffusors using 3-dimensional irradiation planning, and a 633 nm diode laser. The lesion disappeared 24 h after therapy. Circumferential contrast enhancement was observed at 72 h, which disappeared in the course of subsequential months. Edema resolved completely. The patient is still free of recurrence 56 months after treatment, demonstrating an impressive and long-lasting response to this novel mode of therapy.

Keywords ALA · Local therapy · Malignant glioma · Photodynamic therapy · Porphyrins · Stereotactic surgery · Stereotactic · Interstitial · Glioblastoma · 5-aminolevulinic acid · Protoporphyrin IX

W. Stummer · N. Etminan
Department of Neurosurgery, Heinrich-Heine-University, Moorenstr. 5, 40225 Duesseldorf, Germany

T. Beck · W. Beyer · A. Obermeier · H. Stepp · R. Baumgartner
Laser Research Laboratory, Ludwig-Maximilians-University, Marchioninistr. 23, 81377 Munich, Germany

J. H. Mehrkens · J.-C. Tonn · F. W. Kreth
Department of Neurosurgery, Ludwig-Maximilians-University, Marchioninistr. 15, 81377 Munich, Germany

J. Herms
Center for Neuropathology and Prion Research, Ludwig-Maximilians-University, Marchioninistr. 15, 81377 Munich, Germany

W. Stummer (✉)
Department of Neurosurgery, University of Düsseldorf, Moorenstr. 5, 40225 Düsseldorf, Germany
e-mail: stummer@uni-duesseldorf.de

Introduction

Desptie recent advances in the therapy of patients with glioblastoma multiforme [1] median survival is still restricted to 15 months. In recurrent disease, the best possible established second line-treatments, apart from surgery, are local chemotherapy with BCNU wafers [2] or temozolamide chemotherapy [3], which result in an overall survival of less than 8 months. Novel therapies, such as immunotoxins, administered via convection-enhanced delivery [4], or gene therapy [5] have so far failed phase III evaluations. Therefore, new treatment concepts are desperately needed.

We have explored the endogenous heme precursor 5-aminolevulinic acid (ALA) for fluorescence-guided resections of malignant gliomas because ALA leads to the synthesis and accumulation of highly fluorescent protoporphyrin IX within malignant glioma tissue experimentally [6] and in patients [7, 8]. The usefulness of this approach has been validated in the framework of a prospectively-randomized phase III study [9] and approval has

recently been granted for the European Union (http://www.emea.europa.eu/pdfs/human/opinion/36383007en.pdf).

Apart from its fluorescence, protoporphyrin IX is also a strong photosensitizer. The photosensitizing properties of the compound had been in investigated vitro [10–13] and in vivo [14, 15], and selective destruction of sensitized malignant glioma tissue has been noted. Thus, ALA-induced protoporphyrin IX accumulation in malignant glioma cells appear to render these selectively susceptible to phototherapy, provided they are exposed to sufficient light. To this end, we have recently published an overview of the technical approach to the problem of treating deep-seated tumors [16]. This technique utilizes a software platform for 3-dimensional planning and stereotactic implantation of light diffusors into sensitized malignant glioma tissue. The first patients subjected to this method harbored the distant recurrence of a previously resected glioblastoma multiforme treated by adjuvant radio- and chemotherapy, which was unresponsive to second-line interventions. She responded dramatically to 5-ALA-phototherapy and remains without recurrence more than 56 months after treatment.

Case material and results

In October 2002, a 31-year-old female consulted our neuro-oncology service. In April 2001, she had suffered a grand mal seizure. She was diagnosed with left frontal glioblastoma multiforme and underwent surgery 2 days later. Surgery was followed by conventional external beam, fractionated radiotherapy of 60 Gy to the tumor bed and 2 cm margin, delivered in 30 fraction of 2 Gy. Radiation therapy was followed by two cycles of PCV (procarbacine, CCNU, vincristine) chemotherapy. During the second cycle she developed an allergic reaction to procarbacine, so that chemotherapy was continued with temozolamide, initiated with 150 mg/m^2/day for five consecutive days every 28 days. During the second to fourth cycles the dose was increased to 200 mg/m^2/day on the first 5 days. After four cycles the patient wished to temporarily discontinue treatment. MRI exams obtained in three monthly intervals after surgery were unremarkable and without contrast enhancing lesions. In April 2002 the patient again suffered a grand mal seizure. MRI obtained at this time now demonstrated second, remote lesion in the left insula with a diameter of 5 mm. Since surgery was not considered an option, the lesion was treated by a stereotactic conformal radiotherapy boost of 40 Gy, which was applied to the new lesion and its 2 cm margin. Two additional cycles of chemotherapy with temozolamide were then initiated. Nevertheless, MRI obtained after these therapies revealed progressive disease with a tumor diameter of 2.2 cm.

At the time of her initial consultation at our center, the patient's lesion measured 2.5 cm in its greatest diameter and was accompanied by marked edema, extending into the frontal and occipital lobes (Fig. 1), with mild midline displacement. The patient was without deficits and in good clinical condition, with a Karnofsky Performance Score of 100. She was offered treatment in the setting of a number of experimental protocols, including treatment according to a novel protocol for interstitial, 5-ALA-phototherapy for which a pilot study was in preparation. She was selected to participate in the latter study and expedited permission to perform treatment was obtained via the ethical committee of the Ludwig–Maximilians-University, Munich.

Treatment was performed as previously described [16]. Briefly, the patient was placed on 3 × 8 mg dexamethasone for 2 days prior to therapy. About 20 mg/kg bodyweight 5-ALA (medac, Wedel, Germany) were administered orally 3 h prior to the procedure. Under local anesthesia and mild diazepam sedation, stereotactic biopsy of the lesion was performed, confirming glioblastoma multiforme (Fig. 2). Using @target software version 1.19 (Brainlab AG, Gilching), 3-dimensional irradiation planning was carried out and four glasfiber light guides (diameter 600 μm) were

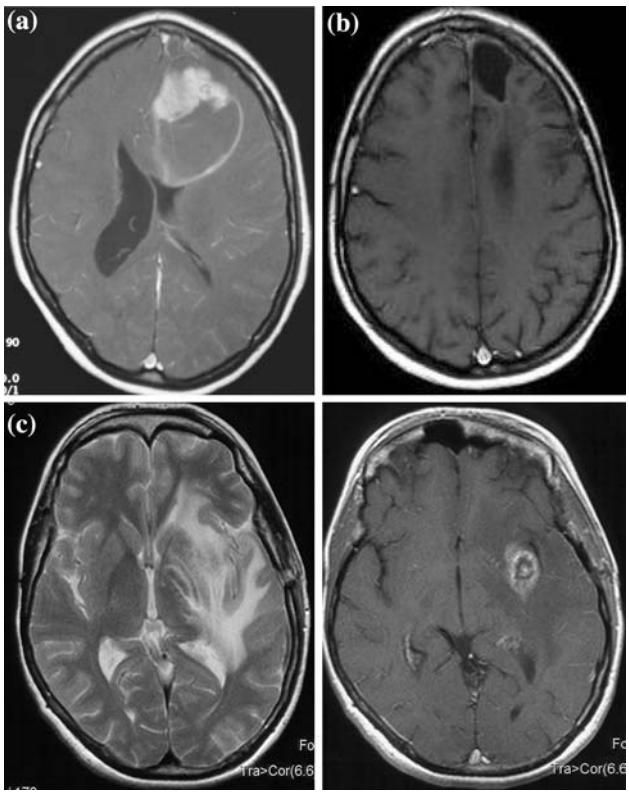

Fig. 1 (**a**) MR prior to initial surgery April 2001; (**b**) left frontal surgical cavity after tumor removal (October 2002); (**c**) remote secondary lesion with hemispheric edema (t1 weighted MR with constrast and t2-weighted MRI)

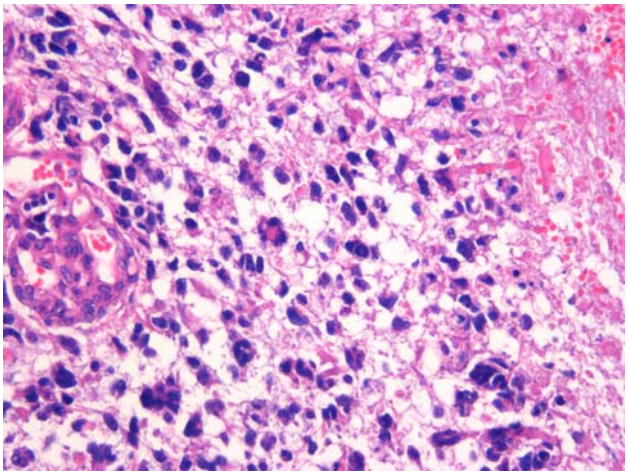

Fig. 2 Photomicrograph of H & E-stained operative specimen from serial stereotactic biopsy of left insular lesion, demonstrating capillary proliferation, cell anaplasia and necrosis consistent with gliolastoma multiforme

implantated into the tumor. These were tipped with diffusors measuring 2 cm in length. During light irradiation f_iO_2 was increased to 100%. For a tumor volume of 7.9 ccm a total energy of 1,200 J/ccm diffuser length was applied using a 633 nm Ceralas PDT Diode Laser (biolitec AG, Jena, Germany) at a power 200 mW/cm of light diffusor. MR images were obtained 24 h later (Fig. 3), then at 7, 15 and 27 days after the procedure. The MRI obtained at 24 h demonstrated almost complete disappearance of contrast-enhancement. At 7 days, a small rim of marginal enhancement had appeared (Figs. 4–6). Thereafter, contrast-enhancement slowly disappeared. On t2-weighted imaging, edema was mildly increased 24 h after the procedure and dissipated within the following weeks. Clinically, the course of the patient was unremarkable and then she retained her fully functional status. She was discharged 5 days after surgery. Throughout the 2 weeks following the procedure, dexamethasone was gradually tapered and stopped. The patient was followed closely thereafter. After 6 months ACNU (90 mg/m^2 iv, day 1) and VM 26 VM26 (60 mg/m^2, days 1–3; both drugs given in six-week intervals) was initiated at an outside center. Over a period of 1 year five cycles were administered with several interruptions due to myelosuppresion. The patient was then enrolled in a protocol with hydroxyurea and imantinib in the beginning of 2004 (400 mg once daily and hydroxyurea 500 mg twice daily). Due to myelosuppression hydroxyurea was administerd at a reduced dose of 500 mg once daily. Anemia was treated by two weekly applications of erythropoietin. This therapy was continued until the end of 2006.

The patient is still free of recurrence at time of last contact (July 2007).

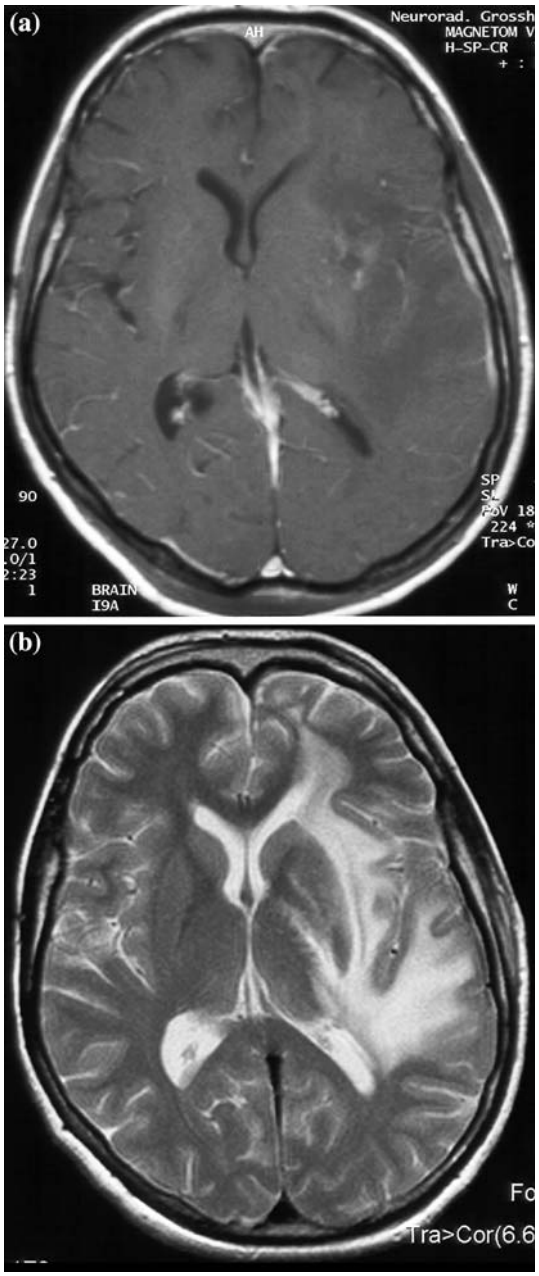

Fig. 3 MR images 24 h after phototherapy. (**a**) t1-weighted sequence with contrast. Note complete loss of contrast-enhancement. (**b**) t2-weighted image. Edema appears mildly increased compared to the preoperative image

Discussion

Photodynamic therapy, that is, the combination of photosensitizer and light for sensitization and destruction of malignant glioma cells has been attempted in the past using synthetic porphyrins such as hematoporphyrin derivative (HpD) or Photofrin® (as reviewed in Madsen and Hirschberg [17]). Stereotactic applications have also been studied, for instance by Powers et al. [18]). However, in

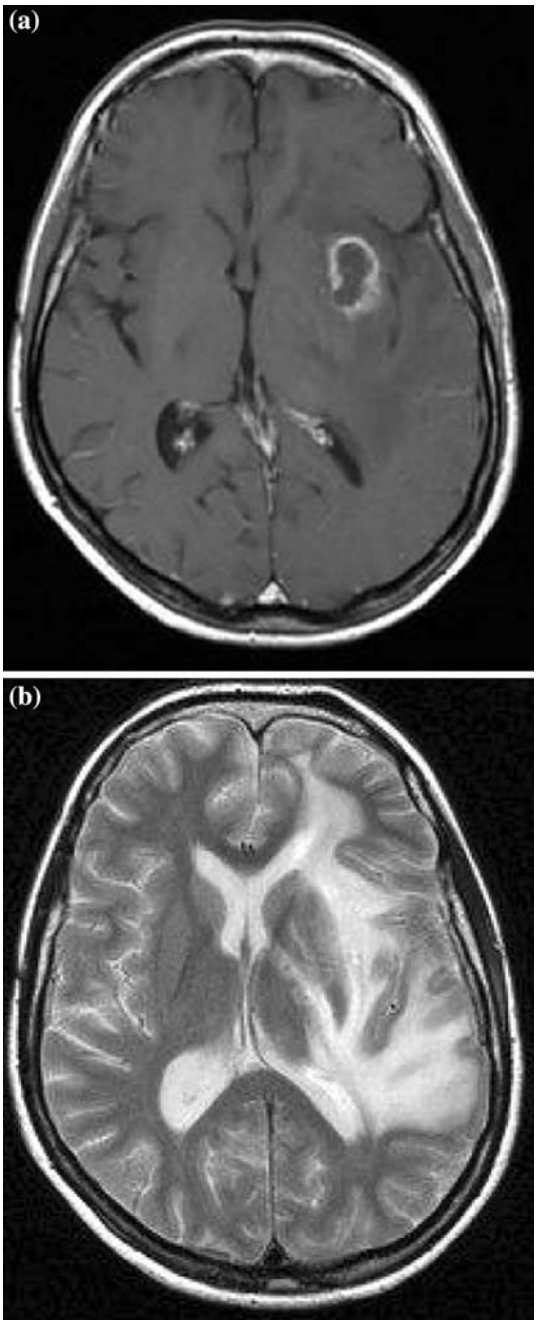

Fig. 4 MR images 7 days after phototherapy. (**a**) t1-weighted sequence with contrast. Note contrast-enhancement circumferential to the intial lesion. (**b**) t2-weighted image

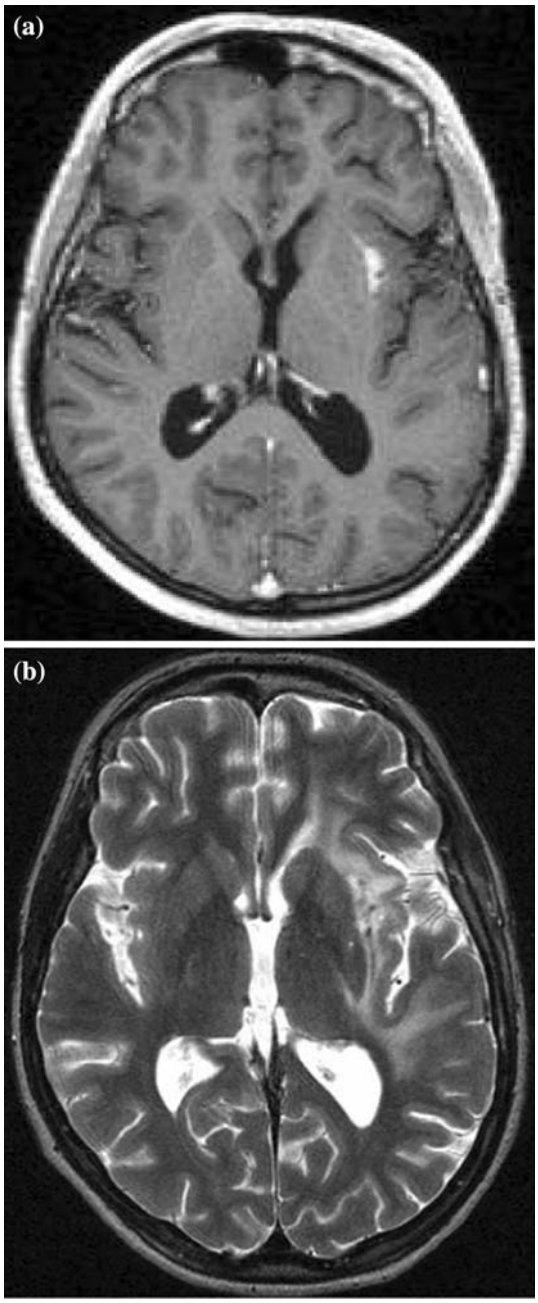

Fig. 5 MR images 33 days after phototherapy. (**a**) t1-weighted sequence with contrast. (**b**) t2-weighted image

that study efficacy was limited, with five out of eight glioblastoma patients suffering a recurrence within 2 months after therapy, with some concern about treatment related side-effects, such as brain edema and prolonged skin sensitization. This experience has been shared by others [19, 20]. In this context, animal experiments suggest that impaired efficacy using synthetic porphyrins may be related to inhomogeneous tumor distribution of sensitizer, whereas enhanced edema may be due to the unspecific sensitization of peritumoral tissue as a consequence of unwanted leakage across the blood–brain barrier within malignant glioma [21–26]. Propagation of sensitizer with edema bulk flow will then render peritumoral tissue sensitive to light, causing unwanted brain damage.

Five-aminolevulinic acid (ALA) is conceptually different compared to the synthetic porphyrins. ALA is a prodrug, which is taken up and metabolized into photoactive protoporphyrin IX *within* malignant glioma cells. The advantages are selective tumor sensitization, lack of

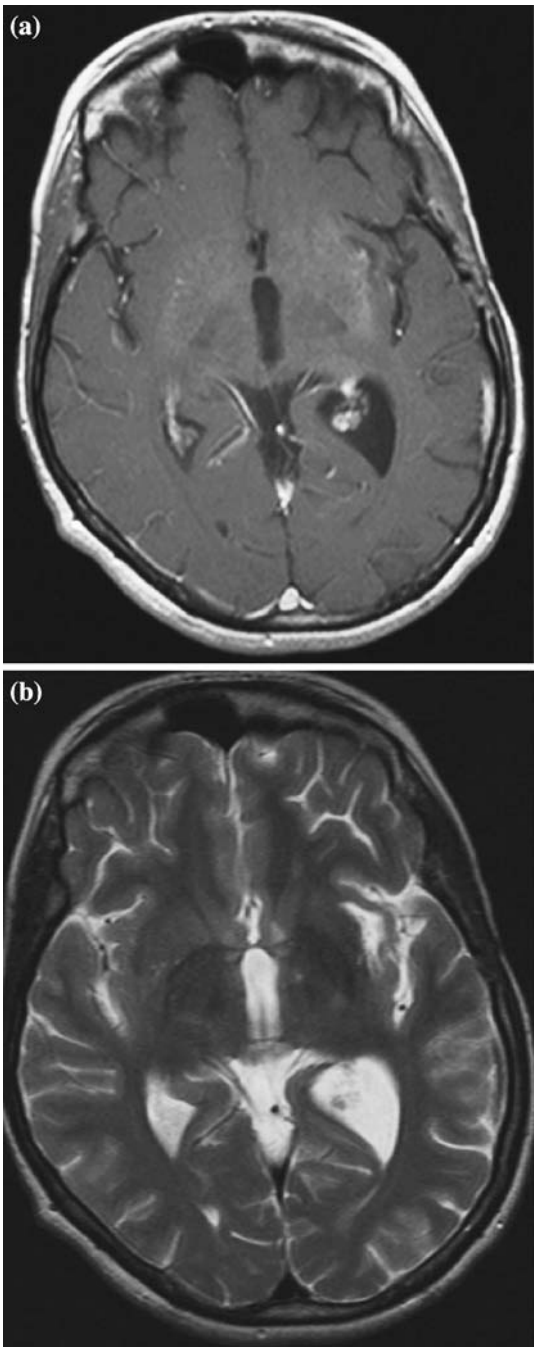

Fig. 6 MR images 38 months after phototherapy. (**a**) t1-weighted sequence with contrast. (**b**) t2-weighted image

unspecific sensitization of adjacent brain [15] and only brief skin sensitization (24 h). Furthermore, very recently approval has been granted within the European Community for the use of ALA for fluorescence-guided resections of malignant gliomas (http://www.emea.europa.eu/pdfs/human/opinion/36383007en.pdf), suggesting a combination fluorescence-guided resection with phototherapy as an attractive treatment option.

The benefits of ALA compared to synthetic porphyrins have now prompted a re-evaluation of stereotactic phototherapy using this drug. Technical details of a first pilot series of patients suffering recurrent malignant gliomas have recently been published, including an overview of their clinical outcomes and safety [16]. Median survival in this series of patients was approximately 15 months.

The patient reported here was the first patient in that series and served as proof of principle for the concept of stereotactic phototherapy using ALA and 3-dimensional planning of laser light delivery using customized software. The low light fluences and geometrical location of diffusors used in our study ruled out thermic effects to be the cause of this efficacy. Experimental modelling using worst case assumptions have demonstrated temperatures to remain under 42° in the irradiated tissue [16].

Remarkably, in this patient as in the other patients of the intial series, contrast-enhancement related to tumor tissue was no longer evident on MR imaging obtained only 24 h after the procedure, which can be taken to represent "complete response". The reason for this phenomenon is unclear. Abolishment of contrast–enhancement might represent an acute interruption of tumor perfusion and one possible explanation could be treatment-induced swelling of tumor and endothelial cells with consecutive vessel occlusion. On the other hand, MR images obtained after 7 days again revealed contrast–enhancement, albeit not within the volume of the original tumor. Rather, enhancement was located outside the original tumor margins and was probably indicative of reactive changes. The resolution of secondary enhancement within successive months supports this assumption.

The most remarkable observation in the present case, however, was the length of disease stabilisation, now lasting 57 months after treatment and approximately 75 months after initial diagnosis in a patient with remote recurrence of glioblastoma and multimodal treatment failures. It cannot be ascertained that ALA-phototherapy was the only factor involved in this stabilisation, because the patient was subsequentially exposed to two further modes of chemotherapy, beginning 6 months later. However, the remarkable initial response strongly encourages the view that ALA-phototherapy was efficacious and durable. Furthermore, assuming phototherapy to be responsible for long-acting stabilisation, mere cytoreduction by drug and laser light interaction may not be the only mechanism playing a role. Beyond direct phototoxic effects, such as necrosis, activation of an immune response (e.g., increased expression of heat shock proteins) has been reported after ALA-mediated phototherapy in other organ systems [27–29]. Furthermore, suppression of survival factors and activation of proteases for apoptosis has also been suggested as a possible mechanism [11].

Although preliminary results of the pilot trial in which the patient reported here participated have been published previously [16], that report provided no details on the clinical history nor the pathologic findings for this particular patient. Therefore, the patient has been presented here separately to allow readers to make independent judgments concerning the long-standing response of her tumor.

Conclusions

Phototherapy using ALA as sensitizer demonstrates biologic activity, as demonstrated by the patient reported here, who suffered remote recurrence of glioblastoma multiforme and had failed augmental radio-and chemotherapy. This response has been associated with a durable clinical and radiographic stabilization. Toxicity was not observed. The observation strongly warrants further investigation into the clinical benefits of this approach, as well as the mechanisms involved.

Acknowledgments This research was funded by Deutsche Krebshilfe; Grant Number: 70-2864

References

1. Stupp R, Mason WP, van den Bent MJ, Weller M, Fisher B, Taphoorn MJ, Belanger K, Brandes AA, Marosi C, Bogdahn U, Curschmann J, Janzer RC, Ludwin SK, Gorlia T, Allgeier A, Lacombe D, Cairncross JG, Eisenhauer E, Mirimanoff RO; European Organisation for Research, Treatment of Cancer Brain Tumor and Radiotherapy Groups; National Cancer Institute of Canada Clinical Trials Group (2005) Radiotherapy plus concomitant and adjuvant temozolomide for glioblastoma. N Engl J Med 352:987–996
2. Brem H, Piantadosi S, Burger PC, Walker M, Selker R, Vick NA, Black K, Sisti M, Brem S, Mohr G et al (1995) Placebo-controlled trial of safety and efficacy of intraoperative controlled delivery by biodegradable polymers of chemotherapy for recurrent gliomas. The polymer-brain tumor treatment group. Lancet 345:1008–1012
3. Yung WK, Albright RE, Olson J, Fredericks R, Fink K, Prados MD, Brada M, Spence A, Hohl RJ, Shapiro W, Glantz M, Greenberg H, Selker RG, Vick NA, Rampling R, Friedman H, Phillips P, Bruner J, Yue N, Osoba D, Zaknoen S, Levin VA (2000) A phase II study of temozolomide vs. procarbazine in patients with glioblastoma multiforme at first relapse. Br J Cancer 83:588–593
4. Kunwar S, Prados MD, Chang SM, Berger MS, Lang FF, Piepmeier JM, Sampson JH, Ram Z, Gutin PH, Gibbons RD, Aldape KD, Croteau DJ, Sherman JW, Puri RK; Cintredekin Besudotox Intraparenchymal Study Group (2007) Direct intracerebral delivery of cintredekin besudotox (IL13-PE38QQR) in recurrent malignant glioma: a report by the cintredekin besudotox intraparenchymal study group. J Clin Oncol 25:837–844
5. Rainov NG (2000) A phase III clinical evaluation of herpes simplex virus type 1 thymidine kinase and ganciclovir gene therapy as an adjuvant to surgical resection and radiation in adults with previously untreated glioblastoma multiforme. Hum Gene Ther 11:2389–2401
6. Stummer W, Stocker S, Novotny A, Heimann A, Sauer O, Kempski O, Plesnila N, Wietzorrek J, Reulen HJ (1998) In vitro and in vivo porphyrin accumulation by C6 glioma cells after exposure to 5-aminolevulinic acid. J Photochem Photobiol B 45:160–169
7. Stummer W, Stocker S, Wagner S, Stepp H, Fritsch C, Goetz C, Goetz AE, Kiefmann R, Reulen HJ (1998) Intraoperative detection of malignant gliomas by 5-aminolevulinic acid induced porphyrin fluorescence. Neurosurgery 42:518–525
8. Stummer W, Novotny A, Stepp H, Goetz C, Bise K, Reulen HJ (2000) Fluorescence guided resection of glioblastoma multiforme by using 5-aminolevulinic acid-induced porphyrins: as prospective study in 52 consecutive patients. J Neurosurg 93:1003–1013
9. Stummer W, Pichlmeier U, Meinel T, Wiestler OD, Zanella F, Reulen HJ (2006) Fluorescence-guided surgery with 5-aminolevulinic acid for resection of malignant glioma: a randomised controlled multicentre phase III trial. Lancet Oncol 7:392–401
10. Zelenkov P, Baumgartner R, Bise K, Heide M, Meier R, Stocker S, Sroka R, Goldbrunner R, Stummer W (2007) Acute morphological sequelae of photodynamic therapy with 5-aminolevulinic acid in the C6 spheroid model. J Neuro Oncol 82:49–60
11. Karmakar S, Banik NL, Patel SJ, Ray SK (2007) 5-Aminolevulinic acid-based photodynamic therapy suppressed survival factors and activated proteases for apoptosis in human glioblastoma U87MG cells. Neurosci Lett 415:242–247
12. Inoue H, Kajimoto Y, Shibata MA, Miyoshi N, Ogawa N, Miyatake S, Otsuki Y, Kuroiwa T (2007) Massive apoptotic cell death of human glioma cells via a mitochondrial pathway following 5-aminolevulinic acid-mediated photodynamic therapy. J Neurooncol 83:223–231
13. Hirschberg H, Sun CH, Krasieva T, Madsen SJ (2006) Effects of ALA-mediated photodynamic therapy on the invasiveness of human glioma cells. Lasers Surg Med 38:939–945
14. Angell-Petersen E, Spetalen S, Madsen SJ, Sun CH, Peng Q, Carper SW, Sioud M, Hirschberg H (2006) Influence of light fluence rate on the effects of photodynamic therapy in an orthotopic rat glioma model. J Neurosurg 104:109–117
15. Olzowy B, Hundt CS, Stocker S, Bise K, Reulen HJ, Stummer W (2002) Photoirradiation therapy of experimental malignant glioma with 5-aminolevulinic acid. J Neurosurg 97:970–976
16. Beck TJ, Kreth FW, Beyer W, Mehrkens JH, Obermeier A, Stepp H, Stummer W, Baumgartner R (2007) Interstitial photodynamic therapy of nonresectable malignant glioma recurrences using 5-aminolevulinic acid induced protoporphyrin IX. Lasers Surg Med 39:386–393
17. Madsen S, Hirschberg H (2006) Photodynamic therapy and detection of high-grade gliomas. J Environ Pathol Toxicol Oncol 25:453–466
18. Powers SK, Cush SS, Walstad DL, Kwock L (1991) Stereotaxic intratumoral photodynamic therapy for recurrent malignant brain tumors. Neurosurgery 29:688–696
19. Krishnamurthy S, Powers SK, Witmer P, Brown T (2000) Optimal light dose for interstitial photodynamic therapy in treatment for malignant brain tumors. Lasers Surg Med 27:224–234
20. Schmidt MH, Meyer GA, Reichert KW, Cheng J, Krouwer HG, Ozker K, Whelan HT (2004) Evaluation of photodynamic therapy near functional brain tissue in patients with recurrent brain tumors. J Neuro Oncol 67:201–207
21. Hebeda KM, Kamphorst W, Sterenborg HJCM, Wolbers JG (1998) Damage to tumour and brain by interstitial photodynamic therapy in the 9L rat tumour model comparing intravenous and intratumoral administration of the photosensitiser. Acta Neurochir 140:495–501

22. Chen Q, Chopp M, Madigan L, Dereski MO, Hetzel FW (1996) Damage threshold of normal rat brain in photodynamic therapy. Photochem Photobiol 64:163–167
23. Dereski MO, Chopp M, Chen Q, Hetzel FW (1989) Normal braintissue response to photodynamic therapy—histology, vascular-permeability and specific-gravity. Photochem Photobiol 50:653–657
24. Whelan HT, Schmidt MH, Segura AD, McAuliffe TL, Bajic DM, Murray KJ, Moulder JE, Strother DR, Thomas JP, Meyer GA (1993) The role of photodynamic therapy in posterior fossa brain tumors. A preclinical study in a canine glioma model. J Neurosurgery 79:562–568
25. Stummer W, Gotz C, Hassan A, Heimann A, Kempski O (1993) Kinetics of Photofrin II in perifocal brain edema. Neurosurgery 33:1075–1081
26. Stummer W, Hassan A, Kempski O, Goetz C (1996) Photodynamic therapy within edematous brain tissue: considerations on sensitizer dose and time point of laser irradiation. J Photochem Photobiol B 36:179–181
27. van Duijnhoven FH, Aalbers RI, Rovers JP, Terpstra OT, Kuppen PJ (2003) The immunological consequences of photodynamic treatment of cancer, a literature review. Immunobiology 207: 105–113
28. Jalili A, Makowski M, Switaj T, Nowis D, Wilczynski GM, Wilczek E, Chorazy-Massalska M, Radzikowska A, Maslinski W, Bialy L, Sienko J, Sieron A, Adamek M, Basak G, Mroz P, Krasnodebski IW, Jakobisiak M, Golab J (2004) Effective photoimmunotherapy of murine colon carcinoma induced by the combination of photodynamic therapy and dendritic cells. Clin Cancer Res 10:4498–4508
29. Korbelik M, Sun J, Cecic I (2005) Photodynamic therapy-induced cell surface expression and release of heat shock proteins: relevance for tumor response. Cancer Res 65:1018–1026

Two-photon photodynamic therapy of C6 cells by means of 5-aminolevulinic acid induced protoporphyrin IX

Tobias J. Beck, Marius Burkanas, Saulius Bagdonas, Zita Krivickiene, Wolfgang Beyer, Ronald Sroka, Reinhold Baumgartner, Ricardas Rotomskis

J. Photochem. Photobiol. B: Biol., 87(3):174-182 (2007)

Available online at www.sciencedirect.com
ScienceDirect
ELSEVIER
Journal of Photochemistry and Photobiology B: Biology 87 (2007) 174–182
Journal of Photochemistry and Photobiology B:Biology
www.elsevier.com/locate/jphotobiol

Two-photon photodynamic therapy of C6 cells by means of 5-aminolevulinic acid induced protoporphyrin IX

Tobias J. Beck [a,*], Marius Burkanas [b], Saulius Bagdonas [b], Zita Krivickiene [c], Wolfgang Beyer [a], Ronald Sroka [a], Reinhold Baumgartner [a], Ricardas Rotomskis [b]

[a] *Laser Research Laboratory, Ludwig-Maximilians-University, Munich, Germany*
[b] *Vilnius University Laser Research Center, Vilnius University, Vilnius, Lithuania*
[c] *Institute of Immunology, Vilnius University, Vilnius, Lithuania*

Received 26 October 2006; received in revised form 20 February 2007; accepted 13 March 2007
Available online 4 April 2007

Abstract

Photodynamic therapy (PDT) has received increased attention as a treatment modality for malignant tumors as well as non-oncologic diseases such as age-related macular degeneration (AMD). An alternative to excite the photosensitizer by the common one-photon absorption is the method of two-photon excitation (TPE). This two-photon photodynamic therapy has the potential of improving the therapeutic outcome due to a highly localized photodynamic effect. The present study investigated the two-photon excited PDT performing in vitro experiments where C6 rat glioma cells were irradiated with a pulsed and focused fs Ti:sapphire laser emitting light at 800 nm. The irradiance distribution of the laser beam was carefully analyzed before the experiment and the applied irradiance was known for each position within the irradiated cell layer. Cells were divided into four groups and one group was incubated with 5-ALA and irradiated 4–5 h later. The survival of this group was tested after irradiation by means of ethidium bromide and acridine orange staining and compared to a control group, which was irradiated under the same conditions, but not incubated with 5-ALA before. Both groups showed necrotic areas depending on the applied irradiance, the value of which at the margin of the necrotic area could be deduced from its size. 5-ALA incubated cells became necrotic after irradiation with a mean irradiance above 6.1×10^{10} W/cm^2, while non-incubated cells remained viable. Cells of both groups became necrotic when treated with an irradiance above 10.9×10^{10} W/cm^2. The observed affected area of the cell layers was between 0.13 mm^2 and 1.10 mm^2. Since the irradiation of non-incubated cells below the mean power density of 10.9×10^{10} W/cm^2 induced no necrosis, apparently no thermal damage was induced in the cells and necrosis of the 5-ALA incubated cells can be ascribed to the photodynamic effect induced by two-photon excitation. The successful photodynamic treatment of a large area of a monolayer cell culture induced by two-photon excitation offers new perspectives for photodynamic treatment modalities.

Keywords: Two-photon; TPE; Photodynamic therapy; 5-Aminolevulinic acid; Protoporphyrin IX; C6 cells

1. Introduction

In recent years, photodynamic therapy (PDT) has received increased attention as a treatment modality for tumors as well as non-oncologic diseases [1]. In PDT a photosensitizer (PS) such as 5-aminolevulinic acid (5-ALA) induced protoporphyrin IX (PPIX) accumulates within the treatment tissue and is activated by light illumination [2]. The interaction with light results in the generation of reactive oxygen species within the treated cells, leading to cell death. Different studies were performed in order to investigate the influence of treatment parameters such as fluence rate [3], light application scheme [4], tissue temperature [5], and tissue oxygenation [6] on the therapeutic outcome.

* Corresponding author. Tel.: +49 089 7095 4884; fax: +49 089 7095 4864.
E-mail address: tobias.beck@med.uni-muenchen.de (T.J. Beck).

1011-1344/$ - see front matter © 2007 Elsevier B.V. All rights reserved.
doi:10.1016/j.jphotobiol.2007.03.008

Usually, a PS exhibits its cell toxicity when it is excited to a higher energetic state by single-photon absorption in the VIS spectra. However, the excited state of the photosensitizer can be reached as well by two-photon excitation (TPE). TPE is the simultaneous absorption of two-photons, where each photon provides half of the energy needed to excite the photosensitizer.

The effect of two-photon or multiphoton excitation has already found diagnostic applications in life sciences: near infrared (NIR) multiphoton microscopy is a novel optical tool for fluorescence imaging based on non-resonant two-photon fluorophore excitation [7]. This technique allows to obtain morphological and functional fluorescence images of endogenous fluorophores. However, also exogenous fluorophores can be imaged with high spatial resolution. Madsen et al. [8] reported about two-photon fluorescence microscopy in human glioma spheroids in order to show the conversion of 5-ALA to PPIX throughout the entire spheroid volume.

Besides fluorescence effects, two-photon excitation can also initiate phototoxic effects in labeled cells via photodynamic action. The further investigation of this mechanism could possibly result in a novel therapeutic application of TPE, which could help to overcome some shortcomings of single-photon excited PDT. The therapeutic outcome of single-photon PDT is mostly, depending on the photosensitizer, not very selective and often healthy tissue adjacent to target tissue is damaged too. In contrast to this, the therapeutic volume of TPE-PDT is very small and localized only within a small spot of a focused laser beam, where high light intensities are obtained. These high light intensities are needed in order to excite a significant amount of PS-molecules via a two-photon absorption path. Thus, the photodynamic effect is highly localized, which is of advantage when treating sensitive tissue. Another benefit of TPE-PDT could be a higher therapeutic penetration depth in tissue compared to VIS-single-photon excitation. Usually near infrared (NIR) light is used for two-photon excitation, which lies within the optical window of tissue (800–1100 nm), a wavelength range with high optical penetration depth.

Two-photon excited PDT has gained interest about 10 years ago [9,10]. Since then, reports have been published investigating basic pathways of TPE [11–15], how to enhance two-photon absorption by using novel effective two-photon phototherapeutic agents [16–18], and about the treatment of cells in vitro [19–21]. Furthermore, the application of TPE-PDT in clinical therapies, such as treatment of age-related macular degeneration (AMD), were investigated in model systems [22].

In the present paper we report about the investigation of TPE induced photodynamic effect in a cell model. C6 rat glioma cells were grown in monolayers and incubated with 5-ALA. Cells were illuminated with a focused 800 nm laser beam and cell viability was controlled before and after the illumination. Incubated cells were compared to non-incubated cells in order to prove the induced photodynamic effect. The applied irradiance was determined.

2. Materials and methods

2.1. C6 cells

The C6 glioma is a model cell line for human malignant glioma. Cells (10^5) were seeded 24 h before the treatment in a 6-well plate on cover glasses and grown to get monolayers in Dulbecco's minimal essential medium (DMEM, Cambrex Corporation, NJ, USA) containing 2 mM L-glutamine, 100 v.v./ml streptomycin, 100 v.v./ml penicillin, 1.5 g/l sodium bicarbonate, 10% FBS-fetal bovine serum at 37 °C in 5% CO_2 atmosphere. Every cell experiment was performed with four groups. Two groups were incubated with 1 mM 5-ALA [23]. Group 1 was irradiated 4 h after incubation, when PPIX-level reaches a maximum [24]. Group 2 underwent incubation, but was not irradiated. Group 3 was irradiated without incubation of photosensitizer and group 4 was neither incubated nor irradiated.

Cell viability of all four groups was controlled after the irradiation of groups 1 and 3. Cell staining was performed with ethidium bromide/acridine orange (4 μg/ml, BD Biosciences, Mississauga, Canada) and cells were investigated with a fluorescence microscope [25]. Living cells were stained green (Fig. 1a) and necrotic cells red (Fig. 1b).

2.2. Fluorescence measurement

Protoporphyrin IX (PPIX) content in the cells was controlled by fluorescence intensity measurements under excitation at 380–450 nm. The fluorescence spectra of 5-ALA incubated C6 cells were recorded using a bifurcated fiber (Somta Ltd., Riga, Latvia) and a spectrophotometer (PC2000, Ocean Optics, Dunedin, USA). A cut-off filter was used to suppress the major part of the backscattered excitation light in order to avoid saturation of the spectrophotometer.

2.3. Experimental set-up and irradiation

To irradiate samples under two-photon absorbance conditions a Ti:sapphire laser (chirped pulse amplification

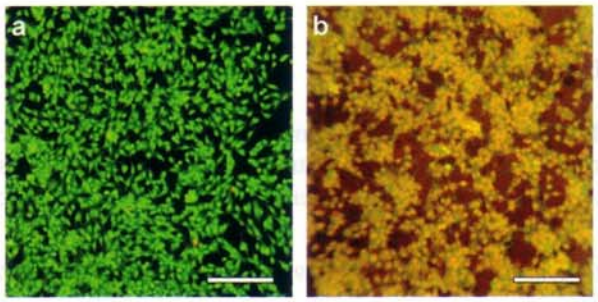

Fig. 1. Fluorescence microscope image of C6 cells after ethidium bromide/acridine orange staining. Living cells before treatment are stained green (a) and cells killed by one-photon PDT ($\lambda = 635$ nm) are stained red (b). Scale bar: 0.1 mm.

system consisting of Tsunami (Spectra Physics) oscillator and super spitfire amplifier (Spectra Physics)) was used to generate pulses of 130 fs duration at a wavelength of 800 nm. The repetition rate of the laser pulse was 1 kHz. The average optical power entering the plate with cells was adjusted to approximately $P_{ave} = 150$ mW (pulse energy = 150 μJ; total pulse power $P_{tot} = 1.15 \times 10^9$ W). The average laser power was measured with a power meter (model 407ATC, Spectra Physics, USA).

The set-up used for the two-photon irradiation is shown in Fig. 2a. Two lenses (L1: −4D and L2: +25D) were used to focus the laser beam. The 6-well plates were placed on a micrometric table between the second lens and the focus spot (F) of the laser beam. The accurate positioning of the sample was performed in all three directions during exposure. Varying the vertical position of the 6-well plates the distance z between plate and focus spot (F) and thus the intensity distribution of the laser beam was changed. Irradiation time was set to 20 min. One well in every plate was reserved for control (group 2).

As a control, some samples were irradiated under one-photon absorbance conditions with a high power light diode ($\lambda = 630$ nm; LED630-66-60, Roithner Lasertechnik, Austria). The experimental set-up for this experiment can be seen in Fig. 2b. The cells were exposed to 40 mW/cm^2 for 8 min through the diaphragm of 1.5 mm in diameter. The applied light dose was 20 J/cm^2.

2.4. Determination of irradiance and irradiation at necrosis margin

In order to determine the irradiance, which is needed to induce thermal or photodynamic effects, the irradiance at the necrosis margin of the cell layer has to be known. The beam profile had to be measured and analyzed for all positions z. The geometry of a standard Gaussian beam is shown in Fig. 3. The local distribution of the power density transversal to its optical axis z (propagation axis) is given in cylindrical coordinates by [26,27]:

$$I(\rho,z) = I_0(z) \cdot \exp\left[\frac{-2\rho^2}{w(z)^2}\right], \quad (1)$$

where $I_0(z) = I_0 \cdot (\frac{w_0}{w(z)})^2$ is the irradiance along the optical axis ($\rho = 0$), $w(z) = w_0 \cdot [1 + (\frac{\lambda z}{\pi w_0^2})^2]^{1/2}$ is the beam radius or spot size at a distance z from the beam waist ($z = 0$; beam diameter $= 2w_0$). The laser beam used in this experiment has a non-rotational symmetric power distribution along its optical axis and thus is described by:

$$I(x,y,z) = I_0(z) \cdot \exp\left[\frac{-2x^2}{w_x(z)^2}\right] \cdot \exp\left[\frac{-2y^2}{w_y(z)^2}\right], \quad (2)$$

where $w_x(z)$ and $w_y(z)$ is the beam radius along the x-axes and the y-axes, respectively. When $I_0(z)$, $w_x(z)$, and $w_y(z)$ are determined for all positions z, then Eq. (2) can be used to calculate the power density at every point in space x, y, z within the laser beam.

The beam radii along both axes, $w_x(z)$ and $w_y(z)$, could be determined for all positions z by measuring the spatial intensity distribution of the Gaussian beam at each position z with a CCD camera and analyzing the resulting image.

The irradiance along the optical axis, $I_0(z)$, can be determined by a two-dimensional integration of the Gaussian beam $I(x,y,z)$, resulting in the total pulse power, P_{tot}:

$$\begin{aligned} P_{tot} &= \int_{x=-\infty}^{x=+\infty} \int_{y=-\infty}^{y=+\infty} I(x,y,z)\,dx\,dy \\ &= \int_{x=-\infty}^{x=+\infty} \int_{y=-\infty}^{y=+\infty} I_0(z) \cdot \exp\left[\frac{-2x^2}{w_x(z)^2}\right] \cdot \exp\left[\frac{-2y^2}{w_y(z)^2}\right] \\ &= I_0(z) \cdot \frac{\pi}{2} \cdot w_x(z) \cdot w_y(z) \end{aligned} \quad (3)$$

The total pulse power, P_{tot}, could be deduced from the measured average power and is constant for each position z. Thus, the irradiance along the optical axes, $I_0(z)$, can be deduced for each position z.

The irradiation, D, is calculated as follows:

$$D(x,y,z) = I(x,y,z) \cdot \Delta t \cdot f_{rep} \cdot T \quad (4)$$

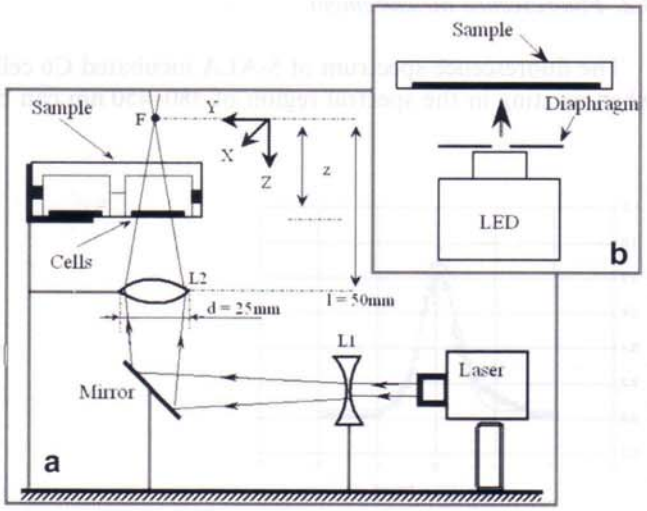

Fig. 2. Experimental set-up to focus the laser beam and to illuminate the cell layer. Set-up for TPE (a) and SPE (b).

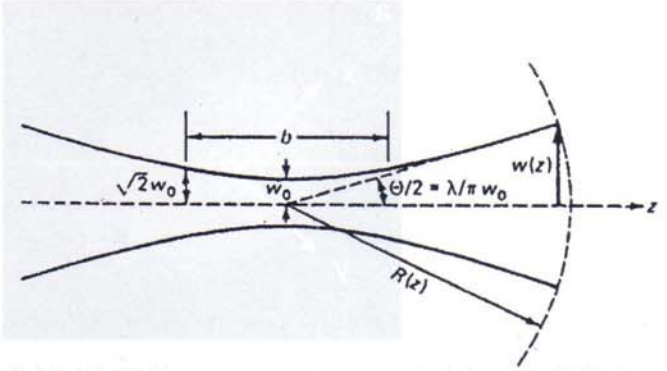

Fig. 3. Schematic of a Gaussian beam geometry.

where Δt is the pulse duration, f_{rep} is the repetition rate, and T is the treatment time.

3. Results

3.1. Irradiance distribution of 800 nm laser beam

The beam radii along both axes, $w_x(z)$ and $w_y(z)$, were determined for all positions z. This was done by imaging the beam profile with a CCD-camera at all positions z and analyzing the results. The CCD-image of the laser beam at position $z = 10$ mm can be seen in Fig. 4a. A non-rotational symmetric power distribution can be observed. The beam intensity along the y-axes ($x = 0$ mm) is plotted in Fig. 4b. The beam radius $w_x(z = 10\text{ mm})$ can be deduced by fitting a Gaussian function to this intensity profile, resulting in a beam radius of $w_x(z = 10\text{ mm}) = 1.00$ mm. The beam radius $w_y(z = 10\text{ mm})$ can be obtained correspondingly, resulting in a beam radius of $w_y(z = 10\text{ mm}) = 0.66$ mm. Inserting these values and the total pulse power $P_{tot} = 1.15 \times 10^9$ W in Eq. (3) results in the irradiance of $I_0(z = 10\text{ mm}) = 1.1 \times 10^{11}$ W/cm^2.

Thus, the irradiance distribution in x- and y-axes is given for the focused laser beam:

$$I_x(x, y = 0, z) = I_0(z) \cdot \exp\left[\frac{-2x^2}{w_x(z)^2}\right] \quad (5)$$

$$I_y(x = 0, y, z) = I_0(z) \cdot \exp\left[\frac{-2y^2}{w_y(z)^2}\right] \quad (6)$$

This procedure was performed for values of z between $z = 6.5$ mm and $z = 11.5$ mm with an increment of 0.5 mm. The beam radii in both directions are plotted versus the position z in Fig. 5, left ordinate. The asymmetric power distribution profile of the beam was very similar for all z-positions and the ratio of w_x to w_y is 1.46 ± 0.03 (mean $\pm$ standard deviation). In Fig. 5, right ordinate, the calculated irradiance along the optical axes $I_0(x = 0, y = 0, z)$ is plotted versus the position z.

The irradiance distribution of the laser beam along the y-axes, $I_y(x = 0, y, z)$, was calculated with Eq. (6) and is plotted for positions $z = 6.5$ mm to $z = 11$ mm in Fig. 6.

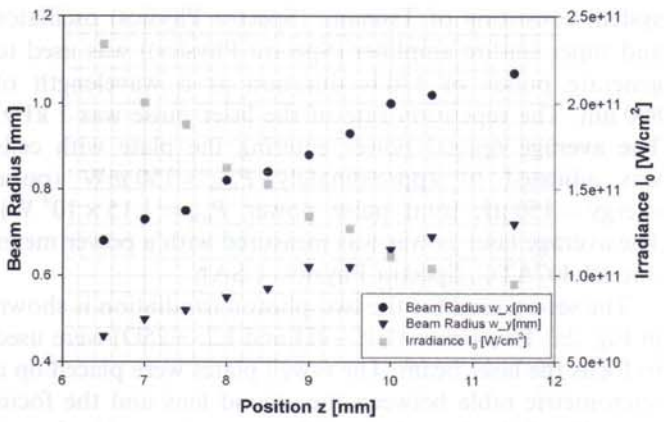

Fig. 5. Beam radius w_x (●, left ordinate), beam radius w_y (▼, left ordinate), and irradiance along the optical axes $I_0(x = 0, y = 0, z)$ derived from beam radii (■, right ordinate) are plotted versus position z.

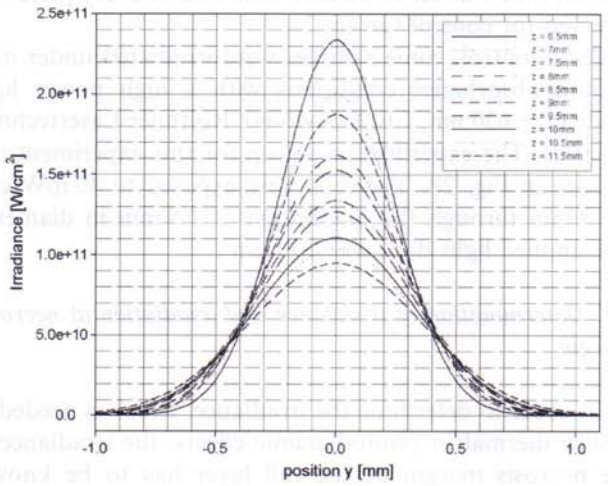

Fig. 6. Irradiance distributions of the focused laser beam along the y-axes, $I_y(x = 0, y, z)$, for positions $z = 6.5$ mm to $z = 11$ mm.

3.2. Fluorescence measurement

The fluorescence spectrum of 5-ALA incubated C6 cells when exciting in the spectral region of 380–450 nm can be

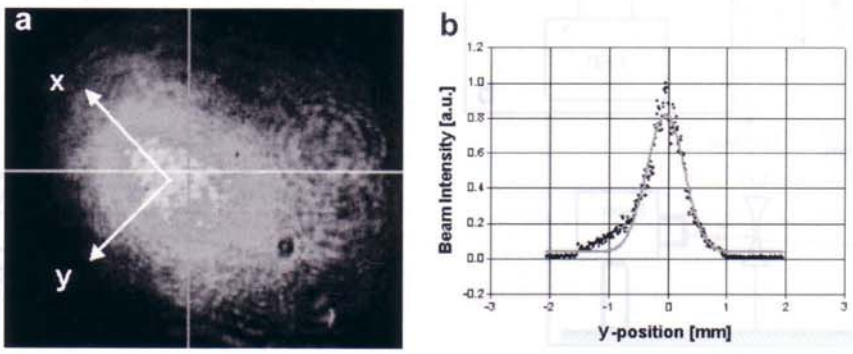

Fig. 4. CCD-image of the laser beam at position $z = 10$ mm (a) and the deduced beam intensity versus position y (black dots) including a Gaussian function fit (grey line) (b).

seen in Fig. 7. The peaks at 635 nm and at 705 nm are the characteristic fluorescence peaks of PPIX.

3.3. One-photon excitation induced PDT

Some cells were treated with one-photon excited photodynamic therapy to prove the reliability of the experimental set-up. Cells were treated as described before. An image of the cells observed after the treatment can be seen in Fig. 8a. Parts of the cell layer were located outside the light spot. These cells remained alive and stained green. Cells located inside the light spot were inactivated by the induced photodynamic effect and thus stained red. Within this region an area can be observed where the cell layer, which was uniform before the treatment, ends abruptly due to detached cells.

A group of non-incubated cells treated under the same conditions was not affected by the light and all cells survived (data not shown).

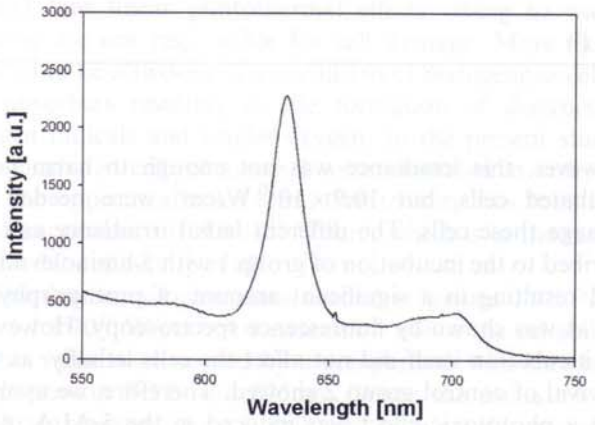

Fig. 7. Fluorescence spectrum of 5-ALA incubated C6 cells when exciting with a spectral region of 380–450 nm. The spectrum has been measured 4 h after incubation.

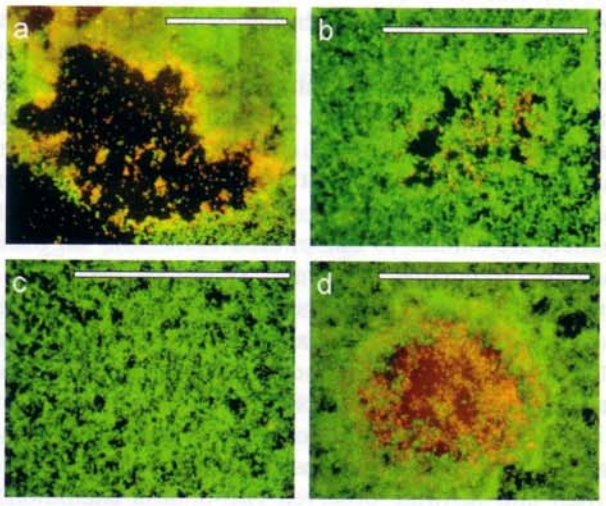

Fig. 8. Images of treated cells after ethidium bromide/acridine orange staining: (a) cells treated with one-photon excitation; (b) cells treated with two-photon excitation without incubation of 5-ALA at position $z = 8$ mm; (c) cells treated with two-photon excitation without incubation of 5-ALA at position $z = 10$ mm; (d) cells treated with two-photon excitation with incubation of 5-ALA at position $z = 10$ mm. Scale bar in all images is 1 mm.

3.4. Two-photon irradiation

Cells were divided in four groups. Group 1 was incubated with 5-ALA and irradiated, group 2 was only incubated and not irradiated, group 3 was only irradiated without incubation, and group 4 was neither incubated nor irradiated. Group 2 and group 4 served as control and did not show necrotic regions after the treatment procedure. Non-incubated cells of group 3 as well as 5-ALA-incubated cells of group 1 showed necrotic areas after irradiation, depending on the treatment position z within the convergent laser beam. The geometry of the necrotic area within the cell layer was observed after staining under fluorescence microscopy. In all experiments the area had an elliptical shape, very similar to the asymmetric laser profile. The elliptic semi axis a and b were measured and inserted in Eq. (5) and in Eq. (6), respectively, in order to obtain the irradiances I_x and I_y. Additionally, the size of the necrotic area was calculated by $A = a \cdot b \cdot \pi$.

Necrotic areas of non-incubated cells of group 3 were observed for positions $z \leqslant 9$ mm. The size of the necrotic area varied between 0.13 mm^2 and 0.34 mm^2 (see Table 1). The mean size ± standard deviation was 0.24 ± 0.09 mm^2. As an example, cells illuminated at position $z = 8$ mm can be seen in Fig. 8b after staining. Irradiation of the non-incubated cells at positions $z > 9$ mm did not cause any damage to the cells. As an example, cells illuminated at position $z = 10$ mm can be seen in Fig. 8c after staining. The irradiance at the margins of the necrotic region varied between 8.8×10^{10} W/cm^2 and 14×10^{10} W/cm^2 (mean ± standard deviation: $(10.9 \pm 1.8) \times 10^{10}$ W/cm^2). No cell destruction was observed for non-incubated cells at intensities below 8.8×10^{10} W/cm^2. Mean irradiation was calculated with Eq. (4) to be $D = 17$ kJ/cm^2. Deducing the time-averaged irradiance results in I(time-averaged) = 14 W/cm^2.

The 5-ALA-incubated cells of group 1 also showed necrotic cell areas when the cells were treated at positions $z \leqslant 9$ mm. However, in difference to the non-incubated cells, the ALA-incubated cells showed necrotic regions also at positions $z > 9$ mm. The size of the necrotic area varied between 0.25 mm^2 and 1.10 mm^2 (see Table 1). The mean size ± standard deviation was 0.68 ± 0.26 mm^2. As an example, 5-ALA incubated cells illuminated at position $z = 10$ mm can be seen in Fig. 8d after staining. The irradiance at the margins of the necrotic region varied between 3.5×10^{10} W/cm^2 and 9.8×10^{10} W/cm^2 (mean ± standard deviation: $(6.1 \pm 1.7) \times 10^{10}$ W/cm^2). No cell destruction was observed for 5-ALA-incubated cells at intensities below 3.5×10^{10} W/cm^2. Mean irradiation was $D = 9.5$ kJ/cm^2. Time-averaged irradiance was 8 W/cm^2.

Table 1
Necrotic area and irradiance at necrosis margin of non-incubated cells (group 3) and of 5-ALA incubated cells (group 1)

Non-incubated cells (group 3)					5-ALA incubated cells (group 1)				
Exp. no.	Position z (mm)	Area (mm^2)	I_x (10^{10} W/cm^2)	I_y (10^{10} W/cm^2)	Exp. no.	Position z (mm)	Area (mm^2)	I_x (10^{10} W/cm^2)	I_y (10^{10} W/cm^2)
1	8.0	0.13	13.0	14.0	14	8.0	0.41	9.8	8.4
2	8.0	0.29	10.4	11.1	15	8.9	0.76	5.0	6.1
3	8.9	0.34	8.8	9.2	16	9.0	0.68	6.5	5.6
4	9.0	0.21	10.3	10.7	17	9.0	0.52	8.0	6.6
5	9.4	–			18	9.4	0.86	5.3	4.5
6	9.5	–			19	9.5	0.96	5.8	3.1
7	9.8	–			20	9.8	0.71	6.7	4.4
8	9.8	–			21	9.8	0.38	8.5	6.7
9	9.9	–			22	9.9	0.97	4.6	4.1
10	10.0	–			23	10.0	0.51	7.3	6.2
11	10.0	–			24	10.0	0.71	6.6	4.5
12	10.0	–			25	10.4	1.10	3.5	4.2
13	10.0	–			26	11.0	0.25	7.8	7.6
Mean irradiance at necrosis margin ± standard deviation (10^{10} W/cm^2)									
10.9 ± 1.8					6.1 ± 1.7				

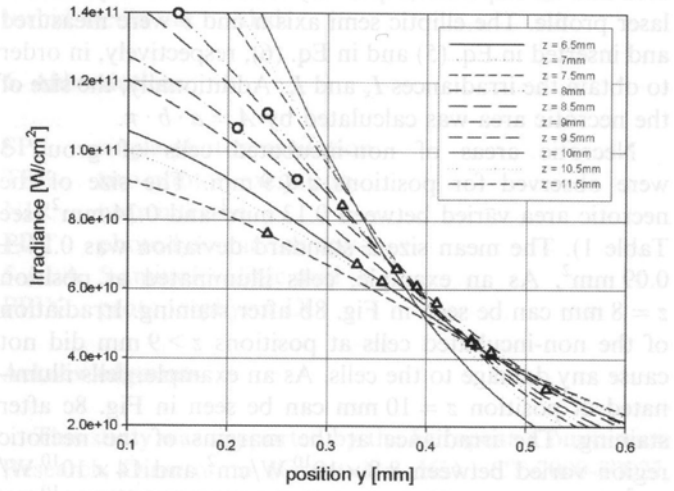

Fig. 9. Margins of necrotic areas in y-direction and corresponding irradiances of the cell experiments are plotted for 5-ALA incubated cells (△) and non-incubated cells (○). Irradiance distribution of the focused laser beam along the y-axes, $I_y(x = 0, y, z)$ is included.

For better illustration, the obtained irradiance I_y is plotted for all necrotic areas versus position y (elliptic semi axis b) in Fig. 9. Additionally, the irradiance distribution of the laser beam is plotted for the various z-positions. It can be seen that the elliptic semi axes for the margins of the necrotic areas of 5-ALA cells are larger than of non-incubated cells.

4. Discussion

Comparison between the survival of 5-ALA incubated (group 1) and non-incubated cells (group 3) after NIR-irradiation showed that differences occurred depending on the applied irradiance. 5-ALA incubated cells showed cell destruction at a mean irradiance above 6.1×10^{10} W/cm^2. However, this irradiance was not enough to harm non-incubated cells, but 10.9×10^{10} W/cm^2 were needed to damage these cells. The different lethal irradiance can be ascribed to the incubation of group 1 with 5-aminolevulinic acid resulting in a significant amount of protoporphyrin IX, as was shown by fluorescence spectroscopy. However, the incubation itself did not affect the cells lethally, as the survival of control group 2 showed. Therefore, we assume that a phototoxic effect was induced in the 5-ALA incubated cells by TPE.

The potential of PPIX to serve as a photosensitizer for TPE-PDT was investigated by Goyan and Cramb [11]. They confirmed a two-photon excitation of PPIX under 790 nm-irradiation by measuring the fluorescence intensity dependence on the laser power and estimated the two-photon absorption cross-section. The measured fluorescence spectra were equivalent for single-photon and two-photon excitation. Therefrom they deduced that the resulting excited state after TPE does not have different electronic characteristics compared to the excitation with one-photon. The observed bleaching effects and resulting photoproducts are similar to one-photon excitation, suggesting similar photodynamic pathways. Singlet oxygen plays an important role in single-photon PDT mechanism and Frederiksen et al. have showed that this reactive species is generated also after two-photon excitation [12,14]. They have demonstrated that singlet oxygen can be produced and optically detected in time-resolved experiments upon two-photon excitation of a photosensitizer dissolved in water. Dittrich and Schwille observed two-photon excitation to use in confocal fluorescence correlation spectroscopy (FCS) [13]. They found signal limitations apparently caused by photobleaching pathways via the formation of radicals.

The aim of the present study was not only to induce TPE-PDT, but also to understand, in which irradiance

window this effect occurs. The upper limit of this window is determined by the onset of damage of non-incubated cells and the lower limit is determined by the minimum amount of photons necessary to produce enough radicals to harm the cells lethally. König et al. investigated the upper power limit for multiphoton microscopy and found cell destructive effects at extremely high fields without applying exogenous PS [28,29]. At irradiances of the order of 10^{12} W/cm^2 (10 mW mean power, 730 nm, 760 nm, 800 nm) they observed complete cell destruction, including cell fragmentation, possibly induced by destructive intracellular plasma formation. But also at lower laser powers (7 mW @ 780 nm), a loss of cell viability was observed. Changing the wavelength to 920 nm resulted in fewer destructive effects, although water has a 7 times greater absorption coefficient at 920 nm than at 780 nm. The authors concluded that linear photothermal effects owing to water heating are not responsible for cell damage. More likely seemed to be a two-photon excitation of endogenous cellular absorbers resulting in the formation of destructive oxygen radicals and singlet oxygen. In the present study, non-incubated cells of group 3 were irradiated in order to find the upper irradiance limit. Cell toxicity was found at irradiances above 10.9×10^{10} W/cm^2, which is in the range of the data of König et al.

The determined irradiance needed to induce TPE-PDT was 6.1×10^{10} W/cm^2. An estimation about the reliability of this value is attempted by a comparison with standard single-photon PDT with 635 nm. When the excitation of PPIX with two-photons is followed by a similar pathway compared to single-photon excitation, then a similar amount of excited PPIX-molecules should result in a similar PDT-effect, assuming identical starting conditions in cells, such as PPIX content, oxygen saturation, et cetera. The amount of generated reactive radicals is then proportional to the amount of excited PPIX-molecules. The probability of molecular excitation due to light absorption, β, is given by $\beta = 1 - e^{-kt}$, where k is the absorption rate and t is the time of irradiation [30]. Single-photon and two-photon absorption rates, given in photons per second, are $k_{SPE} = \sigma_{SPE} \cdot \phi_{SPE}$ and $k_{TPE} = \sigma_{TPE} \cdot \phi_{TPE}^2/2$, respectively [13,20]. ϕ is given in (photons/(cm^{2}s)) and is taking into account the relative photon energies ($\phi = I \cdot \lambda/(hc)$, where I is the irradiance). σ_{SPE} (cm^2) and σ_{TPE} (cm^4 s/photon) are the absorption cross-sections for single-photon and two-photon excitation, respectively. The absorption cross-section for SPE of PPIX at 635 nm is $\sigma_{SPE} = 0.37 \times 10^{-15}$ cm^2 as determined by Theodossiou and MacRobert [31]. The absorption cross-section for TPE of PPIX at 790 nm is $\sigma_{TPE} = 2.0 \times 10^{-50}$ cm^4 s/photon as determined by Goyan and Cramb [11].

With $I_{SPE} = 0.04$ W/cm^2 (1.3×10^{17} photons/(cm^2 s)) and $I_{TPE} = 6.1 \times 10^{10}$ W/cm^2 (2.5×10^{29} photons/(cm^2 s)) this results in absorption rates of $k_{SPE} = 50$ photons/s and $k_{TPE} = 6 \times 10^8$ photons/s. The irradiation time of SPE-PDT was $t = 480$ s. This results in an excitation probability of $\beta_{SPE} = 1$, since the exponent in the calculation of β is very small. The same result is obtained under TPE. The effective irradiation time for TPE-PDT was $t = t_p \cdot f_{rep} \cdot 1200\,\text{s} = 1.56 \times 10^{-7}$ s, yielding also an excitation probability of $\beta_{TPE} = 1$. However, since one molecule can be excited several times, it seems to be reasonable to compare the exponent kt for SPE and TPE, which is $(kt)_{SPE} = 2.4 \times 10^4$ and $(kt)_{TPE} = 94$, respectively. The value $(kt)_{TPE}$ is three orders of magnitude lower than compared to $(kt)_{SPE}$. The same ratio was estimated by Karotki et al. comparing the probability of TPE and SPE [20]. As could be shown, the determined value of $(kt)_{TPE}$ seems to be still large enough for TPE-PDT effects. Moreover, the applied irradiation in SPE-PDT should be probably well above the threshold irradiation for PDT and lower irradiances or shorter irradiation times should result in cell toxicity as well.

Furthermore, comparing SPE-PDT and TPE-PDT it has to be noted that the photodynamic dose in SPE-PDT and TPE-PD is applied in cw-mode and in pulsed mode, respectively. Several authors have compared phototoxicity mechanism between pulsed and continuous wave irradiation in photodynamic therapy [32–34]. They found cw-irradiation to be more effective compared to pulsed irradiation due to slower oxygen consumption. However, the difference is only about a factor of two in oxygen consumption, and therefore not relevant in the present considerations.

In the present study, cells were irradiated at various positions z within a focused laser beam. With the beam waist at position $z = 0$ (beam diameter $= 2w_0$), the spot size increases when increasing the distance from the focus and going to higher z values, thus the irradiance should decrease at higher distances z. A closer look to the measured irradiance distribution along the y-axes is taken in Figs. 6 and 9 for various positions z. It can be seen that the irradiance distribution broadens going to higher z values and that there is an overlap of all curves around y-position 0.4 mm. This means that no matter which position z is chosen between $z = 6.5$ mm and $z = 11$ mm, the irradiances at y-position 0.4 mm are very similar for every z-position (around 6×10^{10} W/cm^2). Since the semi axes in y-direction of 5-ALA cells was around 0.4 mm (see Fig. 9), this could explain, why the size of the observed necrotic area for experiments at various positions z did not depend significantly on the position z. However, the semi axes in y-direction and thus the mean size of the observed necrotic area was different for incubated cells (mean $\pm$ std. dev. $= 0.68 \pm 0.26$ mm^2) and non-incubated cells (mean $\pm$ std. dev. $= 0.24 \pm 0.09$ mm^2), as can been seen in Fig. 9 and in Table 1.

The irradiance distribution along the y-axes is given in Fig. 6 for positions $z = 6.5$ mm to $z = 11$ mm. It can be seen that the determined threshold value for damaging non-incubated cells (10.9×10^{10} W/cm^2) cannot be obtained for positions $z > 9.5$ mm, even not at position $y = 0$ mm, where the maximum irradiance occurs. This is in good accordance with the obtained results. At position $z = 9.5$ mm the irradiance in the beam center ($y = 0$ mm)

should be high enough to damage non-incubated cells (see Fig. 6). However, at this position no cell damage was observed, which may be explained by the small size of the affected area.

5. Conclusions

Concluding the present results, it can be asserted, that two-photon excited photodynamic therapy could be induced in 5-aminolevulinic acid incubated cells. Our focus was to investigate the therapeutic irradiance window, where incubated cells are damaged and non-incubated cells remain viable. This window was determined to be quite narrow but still realizable in practice. Since only cell monolayers were irradiated in the present study, it is difficult to transfer the obtained results to tissue. On one hand, cells react differently to stress when they are surrounded by other cells. Moreover, it seems to be more difficult to reach the necessary irradiances in turbid media as was investigated by Ying et al. [35] Thus, further studies on the formation of the two-photon induced photodamage zone in turbid media are needed.

6. Abbreviations

SPE	single-photon excitation
TPE	two-photon excitation
NIR	near infrared
PDT	photodynamic therapy
5-ALA	5-aminolevulinic acid
PPIX	protoporphyrin IX

Acknowledgments

This study was supported by the European Commission Research Directorate (Grant Nr. ICA1-CT-2000-70027, project CEBIOLA ("Cell biology and lasers: towards new technologies")).

References

[1] Z. Huang, A review of progress in clinical photodynamic therapy, Technol. Cancer Res. Treat. 4 (3) (2005) 283–293.
[2] J.C. Kennedy, R.H. Pottier, Endogenous protoporphyrin IX, a clinically useful photosensitizer for photodynamic therapy, J. Photochem. Photobiol. B: Biol. 14 (4) (1992) 275–292.
[3] B.W. Henderson, T.M. Busch, J.W. Snyder, Fluence rate as a modulator of PDT mechanisms, Lasers Surg. Med. 38 (5) (2006) 489–493.
[4] H.S. de Bruijn, A. van der Ploeg-van den Heuvel, H.J. Sterenborg, D.J. Robinson, Fractionated illumination after topical application of 5-aminolevulinic acid on normal skin of hairless mice: the influence of the dark interval, J. Photochem. Photobiol. B: Biol. 85 (3) (2006) 184–190.
[5] A. Juzeniene, P. Juzenas, I. Bronshtein, A. Vorobey, J. Moan, The influence of temperature on photodynamic cell killing in vitro with 5-aminolevulinic acid, J. Photochem. Photobiol. B: Biol. 84 (2) (2006) 161–166.
[6] A. Curnow, J.C. Haller, S.G. Bown, Oxygen monitoring during 5-aminolaevulinic acid induced photodynamic therapy in normal rat colon. Comparison of continuous and fractionated light regimes, J. Photochem. Photobiol. B: Biol. 58 (2–3) (2000) 149–155.
[7] K. König, Invited review: multiphoton microscopy in life sciences, J. Microsc. 200 (2000) 83–104.
[8] S.J. Madsen, C.H. Sun, B.J. Tromberg, V.P. Wallace, H. Hirschberg, Photodynamic therapy of human glioma spheroids using 5-aminolevulinic acid, Photochem. Photobiol. 72 (1) (2000) 128–134.
[9] W.G. Fisher, W.P. Partridge, C. Dees, E.A. Wachter, Simultaneous two-photon activation of type-I photodynamic therapy agents, Photochem. Photobiol. 66 (2) (1997) 141–155.
[10] J.D. Bhawalkar, N.D. Kumar, C.F. Zhao, P.N. Prasad, Two-photon photodynamic therapy, J. Clin. Laser Med. Surg. 15 (5) (1997) 201–204.
[11] R.L. Goyan, D.T. Cramb, Near-infrared two-photon excitation of protoporphyrin IX: photodynamics and photoproduct generation, Photochem. Photobiol. 72 (6) (2000) 821–827.
[12] P.K. Frederiksen, M. Jorgensen, P.R. Ogilby, Two-photon photosensitized production of singlet oxygen, J. Am. Chem. Soc. 123 (6) (2001) 1215–1221.
[13] P.S. Dittrich, P. Schwille, Photobleaching and stabilization of fluorophores used for single-molecule analysis with one- and two-photon excitation, Appl. Phys. B 73 (8) (2001) 829–837.
[14] P.K. Frederiksen, S.P. McIlroy, C.B. Nielsen, L. Nikolajsen, E. Skovsen, M. Jorgensen, K.V. Mikkelsen, P.R. Ogilby, Two-photon photosensitized production of singlet oxygen in water, J. Am. Chem. Soc. 127 (1) (2005) 255–269.
[15] K.S. Samkoe, M.S. Fecica, R.L. Goyan, J.L. Buchholz, C. Campbell, N.M. Kelly, D.T. Cramb, Photobleaching kinetics of optically trapped multilamellar vesicles containing verteporfin using two-photon excitation section sign, Photochem. Photobiol. 82 (1) (2006) 152–157.
[16] M. Drobizhev, A. Karotki, M. Kruk, N.Z. Mamardashvili, A. Rebane, Drastic enhancement of two-photon absorption in porphyrins associated with symmetrical electron-accepting substitution, Chem. Phys. Lett. 361 (5–6) (2002) 504–512.
[17] J. Liu, Y.W. Zhao, J.Q. Zhao, A.D. Xia, L.J. Jiang, S. Wu, L. Ma, Y.Q. Dong, Two-photon excitation studies of hypocrellins for photodynamic therapy, J. Photochem. Photobiol. B: Biol. 68 (2–3) (2002) 156–164.
[18] K. Ogawa, H. Hasegawa, Y. Inaba, Y. Kobuke, H. Inouye, Y. Kanemitsu, E. Kohno, T. Hirano, S. Ogura, I. Okura, Water-soluble bis(imidazolylporphyrin) self-assemblies with large two-photon absorption cross sections as potential agents for photodynamic therapy, J. Med. Chem. 49 (7) (2006) 2276–2283.
[19] K. König, I. Riemann, P. Fischer, Photodynamic therapy by nonresonant two-photon excitation, in: Thomas J. Dougherty (Ed.), Proc. SPIE, Optical Methods for Tumor Treatment and Detection: Mechanisms and Techniques in Photodynamic Therapy VIII, 3592 (1999) 43–49.
[20] A. Karotki, M. Khurana, J.R. Lepock, B.C. Wilson, Simultaneous two-photon excitation of photofrin in relation to photodynamic therapy, Photochem. Photobiol. 82 (2) (2006) 443–452.
[21] Y. Mir, D. Houde, J.E. van Lier, Two-photon absorption of copper tetrasulfophthalocyanine induces phototoxicity towards jurkat cells in vitro, Photochem. Photobiol. Sci. 5 (11) (2006) 1024–1030.
[22] K.S. Samkoe, D.T. Cramb, Application of an ex ovo chicken chorioallantoic membrane model for two-photon excitation photodynamic therapy of age-related macular degeneration, J. Biomed. Opt. 8 (3) (2003) 410–417.
[23] W. Stummer, S. Stocker, A. Novotny, A. Heimann, O. Sauer, O. Kempski, N. Plesnila, J. Wietzorrek, H.J. Reulen, In vitro and in vivo porphyrin accumulation by c6 glioma cells after exposure to 5-aminolevulinic acid, J. Photochem. Photobiol. B: Biol. 45 (2–3) (1998) 160–169.
[24] C. af Klinteberg, A.M. Enejder, I. Wang, S. Andersson-Engels, S. Svanberg, K. Svanberg, Kinetic fluorescence studies of 5-aminolaevulinic acid-induced protoporphyrin IX accumulation in basal cell

carcinomas, J. Photochem. Photobiol. B: Biol. 49 (2–3) (1999) 120–128.
[25] D.R. Parks, V.M. Bryan, V.T. Oi, L.A. Herzenberg, Antigen-specific identification and cloning of hybridomas with a fluorescence-activated cell sorter, Proc. Natl. Acad. Sci. USA 76 (4) (1979) 1962–1966.
[26] H. Kogelnik, T. Li, Laser beams and resonators, Appl. Opt. 5 (10) (1966) 1550–1567.
[27] W. Koechner, 4th ed.Solid-State Laser Engineering, vol. 1, Springer Verlag, Berlin, Heidelberg, New York, 1996.
[28] K. König, P.T.C. So, W.W. Mantulin, E. Gratton, Cellular response to near-infrared femtosecond laser pulses in two-photon microscopes, Opt. Lett. 22 (2) (1997) 135–136.
[29] K. König, T.W. Becker, P. Fischer, I. Riemann, K.-J. Halbhuber, Pulse-length dependence of cellular response to intense near-infrared laser pulses in multiphoton microscopes, Opt. Lett. 24 (2) (1999) 113–115.
[30] G.J. Brakenhoff, M. Muller, R.I. Ghauharali, Analysis of efficiency of two-photon versus single-photon absorption of fluorescence generation in biological objects, J. Microsc. 183 (2) (1996) 140–144.
[31] T. Theodossiou, A.J. MacRobert, Comparison of the photodynamic effect of exogenous photoprotoporphyrin and protoporphyrin IX on PAM 212 murine keratinocytes, Photochem. Photobiol. 76 (5) (2002) 530–537.
[32] K. Seguchi, S. Kawauchi, Y. Morimoto, T. Arai, H. Asanuma, M. Hayakawa, M. Kikuchi, Critical parameters in the cytotoxicity of photodynamic therapy using a pulsed laser, Lasers Med. Sci. 17 (4) (2002) 265–271.
[33] S. Kawauchi, Y. Morimoto, S. Sato, T. Arai, K. Seguchi, H. Asanuma, M. Kikuchi, Differences between cytotoxicity in photodynamic therapy using a pulsed laser and a continuous wave laser: study of oxygen consumption and photobleaching, Lasers Med. Sci. 18 (4) (2004) 179–183.
[34] Y. Miyamoto, Y. Umebayashi, T. Nishisaka, Comparison of phototoxicity mechanism between pulsed and continuous wave irradiation in photodynamic therapy, J. Photochem. Photobiol. B: Biol. 53 (1–3) (1999) 53–59.
[35] J.P. Ying, F. Liu, R.R. Alfano, Spatial distribution of two-photon-excited fluorescence in scattering media, Appl. Opt. 38 (1) (1999) 224–229.

Acknowledgements

First of all I would like to thank Prof. Dr. med. Jörg-Christian Tonn for my admission at the Department of Neurosurgery of Ludwigs-Maximilians-University Munich and for giving me the chance to work on this interesting topic.

Then I want to thank Dr. Reinhold Baumgartner for giving me the possibility to work at the Laser Research Laboratory of Ludwigs-Maximilians-University Munich and for supervising and supporting this work.

"Labai jums aèiû" to Prof. Dr. Ricardas Rotomskis for his generous hospitality at Vilnius University in Lithuania. His organization of a fund provided by the European Union allowed me to work on an exciting project and to get to know a great city with great people.

I am grateful for the fruitful and interesting cooperation with the neurosurgeons of the Department of Neurosurgery of Ludwigs-Maximilians-University Munich and the Department of Neurosurgery of University Clinic Düsseldorf. Especially the close teamwork with Prof. Dr. Friedrich W. Kreth and Prof. Dr. Walter Stummer was a great experience for me.

I would like to give my special thanks to the staff of the Laser Research Laboratory, in particular to Dr. Herbert Stepp, Dr. Wolfgang Beyer, Dr. Ronald Sroka, Dipl.Ing.(FH) Thomas Pongratz, and Dipl.Phys. Richard Meier. They always shared their technical and scientific knowledge and competence and were there whenever I needed consulting. The excellent working atmosphere made it hard for me to leave the LFL.

Thanks also to Dr. Saulius Bagdonas and Marius Burkanas of Vilnius University, who introduced me to the experimental apparatus in the laboratory and who always found the time to answer my questions.

Thanks also to Dr. Jan H. Mehrkens and Dr. Ann Johansson for their helpful discussions and for proof-reading this work.

I am grateful to Deutsche Krebshilfe for funding this research project (Grant number: 70-2864).

Finally I want to thank my beloved family Valerie, Leander, and Bine for their love and patience during the last months of this work.